Chapter 10
Cosmogenic Radioisotopes for Study of the Genesis and Dynamics of Water

Abstract The Earth's atmosphere is penetrated by a continuous flux of charged particles, consisting of protons and nuclei of various elements of cosmic origin. Consequently, a great variety of radioisotopes, referred to as cosmogenic, are produced due to the interaction of these particles with the atomic nuclei of elements that constitute the atmosphere. Transported by air masses, radioisotopes are abundant over the whole gaseous sphere of the Earth. Being mixed with atmospheric moisture, a proportion falls over the Earth's surface, to enter the hydrological cycle as components of surface waters, soil-ground moisture and groundwaters. Another proportion becomes a component of ocean and inland basin waters through exchange at the surface of water reservoirs. Finally, the Earth's biosphere plays an active role in exchange processes, which are of great importance for some cosmogenic isotopes. Cosmic dust is another source of cosmogenic isotopes, as are meteorites that are continually falling onto the Earth's surface. Being in cosmic space these meteorites have been subjected to a bombardment of cosmic radiation. Nuclear reactions accompanying the process produce many radioisotopes. The origin and distribution of cosmogenic radioisotopes, global circulation of tritium, radiocarbon and other cosmogenic radionuclides are discussed in this chapter.

10.1 Origin and Distribution of Cosmogenic Radioisotopes

Cosmic radiation plays the main role in the origin of cosmogenic radioisotopes. Understanding the nature of cosmic radiation has been important for the development of the Earth sciences. In particular, the solution of a number of hydrological and hydrogeological problems, related to natural water dynamics, their genesis and age, has become possible due to investigations of abundances of cosmogenic radioisotopes in the hydrosphere, i.e., isotopes, produced by cosmic radiation.

Cosmic rays of solar and galactic origin are distinguishable. The nature of the nuclear particle flux of solar origin is related to fusion and decay reactions in the solar interior. The origin of galactic and metagalactic cosmic radiation bombarding the Earth's atmosphere is still uncertain.

V. I. Ferronsky, *Nuclear Geophysics,* Springer Geophysics,
DOI 10.1007/978-3-319-12451-3_10

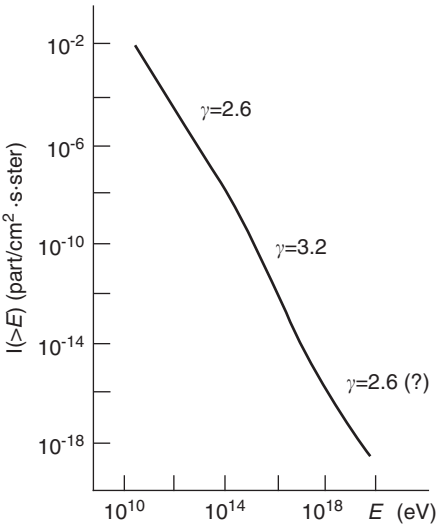

Fig. 10.1 Energy spectrum of primary cosmic radiation. (Ferronsky and Polyakov 2012)

In practical studies of cosmic radiation there have been cases when particles of galactic origin with energies of $10^{19}-10^{20}$ eV have been detected. Some idea of the spectrum of cosmic radiation with energy greater than $E=10^{10}$ eV is given by Fig. 10.1.

Cosmic radiation is made up of about 90% protons, about 9% helium nuclei (α-particles) and about 1% other nuclei. Table 10.1 shows specific abundances of nuclei in the solar system, cosmic space and in cosmic radiation (Webber 1967).

Except for hydrogen and helium, the composition of primary cosmic radiation is poorly understood. The estimations of specific abundances of carbon isotopes show

Table 10.1 Nuclei abundances in the solar system, cosmic space and in primary cosmic rays relative to carbon

Element	Abundances			Element	Abundances		
	Solar system	Cosmic space	Primary cosmic rays		Solar system	Cosmic space	Primary cosmic rays
He	?	400	38	Al	0.004	0.005	0.03
Li	<<0.001	<<0.001	0.27	Si	0.063	0.13	0.11
Be	<<0.001	<<0.001	0.19	P	–	0.002	0.01
B	<<0.001	<<0.001	0.43	16≤Z≤19	0.050	0.02	0.02 – 0.05
C	1.0	1.0	1.0	Ca	–	<<0.001	0.026
N	0.16	0.27	0.46	Ti	–	0.006	0.017
O	1.7	2.3	0.61	Ci	–	0.06	0.030
F	<<0.001	<<0.001	0.09	Fe	–	0.06	0.080
Ne	?	0.80	0.18	Ni	–	0.008	0.015
Na	0.004	0.006	0.08	Z>20	–	<<0.001	0.01
Mg	0.005	0.12	0.15	Z>30	–	~0.001	< 0.004

that in primary cosmic radiation $^{13}C/^{12}C \approx 1$. Measuring this ratio with the help of photo-emulsion techniques, a value close to unity is obtained.

As for deuterium, no sufficiently reliable measurements of its content in primary cosmic radiation have been carried out so far. Those measurements that were carried out in the upper atmosphere (for atmospheric depths 2–4 g/cm^2) gave values of $^2H/^1H = 0.05–0.12$. The large discrepancy in these data results from the fact that the measurements correspond to different energy intervals and latitudes. But on the whole, the data are in agreement with satellite data ($^2H/^1H \leq 0.06$ or $\varepsilon =$ 25–80 MeV/nucleon), where the effect of the Earth's magnetism and atmosphere are excluded (MeV = 10^6 eV).

The ratio of deuterium abundance to proton abundance in the universe is of the order of $1.4 \cdot 10^{-4}$ (Webber 1967), which may be accounted for by its disintegration. According to spectroscopic measurements, the ratio $^2H/^1H$ is also small in the solar atmosphere, amounting to $4 \cdot 10^{-5}$ (Kinman 1956). Only in the atmosphere of magnetic stars does the ratio increase up to 10^{-2}. The ratio of $^2H/^1H = 10^{-5}\,\rho$, where ρ (particle/cm^3) is the average density of substance through which cosmic radiation has passed (Singer 1958).

While studying the helium isotope composition in cosmic radiation (Appa Rao 1962) the ratio $^3He/(^3He + ^4He) = 0.20–0.30$ was obtained in the energy range $\varepsilon = 160–360$ MeV/nucleon. Attempts to measure this ratio for higher energies have failed.

Besides nuclei, α-particles and nuclides of various elements and their isotopes, primary cosmic radiation also contains gamma-ray protons, neutrons, electrons and positrons. The source of gamma-ray protons and neutrons in primary cosmic radiation is supposed to be related to supernova.

Primary cosmic radiation interacts with the Earth's magnetic field, which results in a relationship between the intensity of radiation and geomagnetic latitude. All available data concerning geomagnetic effects of cosmic radiation are in good agreement with the idea that the isotropic flow of charged particles coming from the universe is deviated by the terrestrial magnetic field. Analysing the effect of the Earth's magnetic field on the motion of charged particles, favoured and unfavoured directions of charged particle motion to a given point of the Earth's surface have been found.

The interaction of the Earth's magnetic field with primary cosmic radiation results in latitude variations of its intensity I (Fig. 10.2). This effect, referred to as the latitude effect, is quantitatively expressed by the ratio $[I(90°) - I(0°)]/I(90°)$.

It has been found that the intensity of cosmic radiation coming to the Earth varies with time. Four different types of these time-dependant variations are known (Fireman 1967):

1. Variations related to the 11-year cycle of solar activity. With increasing intensity of the solar particle flux the galactic radiation intensity decreases.
2. Heliocentric variations of galactic radiation, the radial gradient of which is in the range of 1.0–1.5 astronomical units of length (1 a.u. $\approx 1.5 \cdot 10^8$ km), are about +9.6% per 1 a.u.

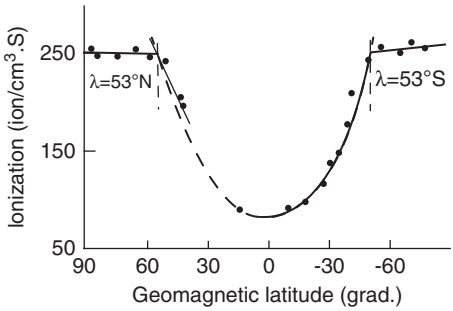

Fig. 10.2 Latitude effect of cosmic radiation for the depth of atmosphere at 50 g/cm^2. (Ferronsky and Polyakov 2012)

3. The secular variations of radiation detected with the help of ^{14}C content vary in the atmosphere in different centuries. They were measured by ^{14}C content variations recorded in the year-rings of trees from various ages.
4. The sporadic flows of nuclear particles of low energies emitted during solar flares.

The intensity of the flux of protons of solar origin, with energies greater than 10 MeV near to the Earth, is equal to 100 protons/cm$^2 \cdot$ sec during a typical solar cycle (relative to the Earth's surface) (Lal et al. 1967). This value was obtained using experimental data at the rate of ^{26}Al production during a time interval of about 10^5 year. The intensity of protons in the solar flux is higher than the galactic intensity by about one order of magnitude, i.e., the latter is characterised by a value of about 10 protons/cm$^2 \cdot$ sec. But while the solar protons have energies of about several dozens of MeV, the protons of galactic origin have energies two orders greater on average. The intensity of α-particle flux, both of solar and galactic origin, is lower than of protons by one order of magnitude. The velocity of nuclear particles of solar origin near the Earth is about 300 km/sec.

In the course of the interaction of high-energy cosmic radiation with the atmosphere the major part of its energy is absorbed and scattered by the Earth's atmosphere. This leads to the production of secondary low-energy radiation composed of mesons, gamma-ray photons, positrons and other particles of various energies. This secondary radiation is mainly composed of less energetic protons and neutrons, which play the main role in nuclear reactions, resulting in the production of cosmogenic radioisotopes in the Earth's atmosphere. The energy threshold of these reactions ranges between 10 and 40 MeV.

The distribution of secondary neutrons and protons in the atmosphere varies both in latitude and altitude. Figure 10.3a shows the experimental data of energy distribution in the neutron flux, characterised by energies lower than 20 MeV, obtained in 1966 during an experiment in Sicily during a quiet Sun period (Boella et al. 1968). A similar thermal neutron distribution was obtained by Korff using a thermal neutron counter in the Princeton region (USA). The data from these measurements are shown in Fig. 10.3b. One can see from the figure that a total flux of neutrons at first increases with altitude and then decreases with atmospheric density due to their escaping from high atmospheric layers. With the transition in latitude from the

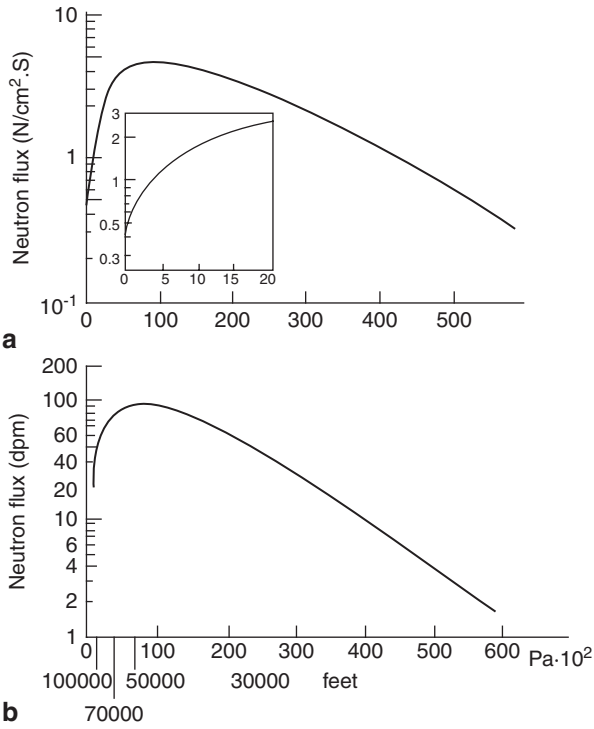

Fig. 10.3 Relation of integrated neutron flux from an atmospheric depth of 0–600 mbar in Sicily for neutron energy lower than 20 MeV (**a**), and for thermal neutrons in the Princeton region (**b**). (Ferronsky and Polyakov 2012)

equator to the poles the density of neutron flux increases. Figure 10.4 shows the experimental data of latitude dependency of neutron flux at an altitude of 1000 m, obtained by Simpson (Libby 1967).

The effect of the production of cosmogenic isotopes in the Earth's crust is negligible even in the upper layers. Nuclear transformations occur here mainly due to the penetration of primary nucleons of light energies, thermal neutrons and $\overline{\mu}$-mesons. The dominating component of this flux varies with depth. At a depth of several metres most nuclear transformations are provided by quick $\overline{\mu}$-mesons and at depths where pressure is greater than 400 kg/cm^2, by the interaction with neutrino flux of both primary and secondary origin (Lal and Peters 1967).

According to Lal and Peters, at depths characterised by pressures greater than 0.7 kg/cm^2, the majority of nuclear transformations occur due to interaction with $\overline{\mu}$ -mesons and 10 % of them are the effect of negative meson capture.

The main proportion of cosmogenic radionuclides is formed in the atmosphere. The main components of atmospheric air are: nitrogen (78.09 %), oxygen (20.95 %), argon (0.93 %), carbon dioxide (0.03 %) and neon (0.0018 %). In the course of interaction between cosmic radiation and atmospheric elements nuclear transformation occurs with the nuclei of neon, oxygen and argon, which plays a major role in the production of cosmogenic radioisotopes. The most typical reactions are: (n, p), (n, 2n), (n, α), (n, γ), (p, n), (p, 2n), (p, pn), (p, 2p).

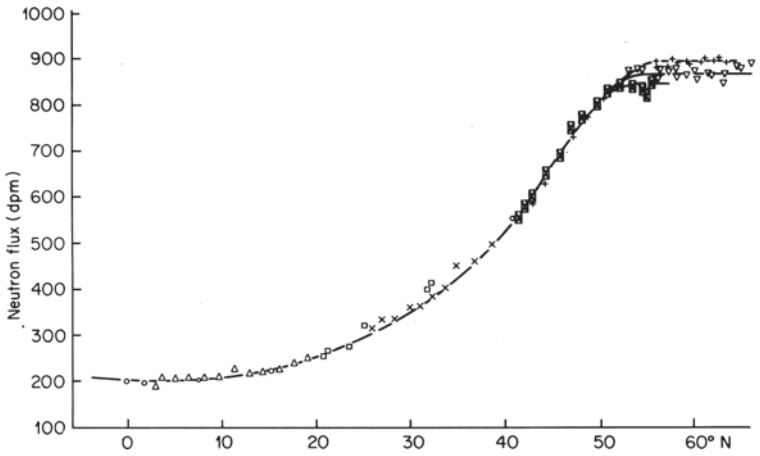

Fig. 10.4 Latitude effect in distribution of neutron flux at an altitude of 1000 m for the North American continent. (Libby 1967; Ferronsky and Polyakov 2012)

Isotopes of cosmogenic origin, which are of interest for the investigations of water circulation patterns in the hydrosphere, are: ^{3}H, ^{3}He (stable), ^{7}Be, ^{10}Be, ^{14}C, ^{22}Na, ^{24}Na, ^{26}Al, ^{32}Si, ^{32}P, ^{33}P, ^{36}Cl, ^{37}Ar, ^{39}Ar, ^{81}Kr. The irradiation of cosmic dust, falling down in amounts of about 10^{9} kg/year on the Earth's surface, by cosmic radiation results in the production of radioisotopes of great importance such as ^{10}B, ^{14}C, ^{22}Na, ^{26}Al, ^{36}Cl, ^{39}Ar, ^{53}Mn, ^{59}Ni.

The rate of production of cosmogenic isotopes varies with altitude and latitude and depends on the intensity of secondary neutron and proton flux in the atmosphere. At the same time the rate of their formation remains constant over time. As a first approximation the ratio of various isotopes produced may be considered to be independent of altitude and time. According to estimations by Lal and Peters (1962) and Young et al. (1970) the rate of isotope production per gram of air, e.g., at 46° N, increases exponentially at an altitude of about 21 km by three orders of magnitude higher than at the surface of the Earth. Further on, it decreases with altitude due to escaping neutrons from the upper atmospheric layers. The isotope production rate increases by about one order of magnitude with transition from the equator to the poles.

Estimations of the production rate of cosmogenic radioisotopes in the atmosphere and in cosmic dust, carried out by a number of authors (Bhaudari et al. 1969; Lal et al. 1967; Lal and Venkatavaradan 1967; Schell 1970), used a value of average density of proton flux with energy $E > 10$ MeV at the upper boundary of the Earth's atmosphere, equal to 100 protons/cm$^2 \cdot$ sec. The latitude and altitude effects of nuclear reactions were taken into account in the course of the calculations.

In order to carry out estimations of steady-state amounts of individual isotopes on the Earth, it was assumed that the flux of cosmic radiation remained constant over a long period of time (being not less than the half-life of a given radioisotope). With a constant cosmic flux and a certain atmospheric composition the production rate of isotopes will also be independent of time.

The steady-state amount of an individual isotope on the Earth follows from the equation:

$$nS = q\lambda,$$

where n is the production rate of a radioisotope relative to the Earth's surface (atom/$cm^2 \cdot sec$); S is the area of the Earth's surface, cm^2; q is the steady-state amount of isotopes or atoms; λ is the decay constant of a given nucleus.

The results of estimations carried out by the above-mentioned authors and clarified by experimental research, related to the production rates and steady-state abundances of various cosmogenic radioisotopes and also their main physical properties, are presented in Table 10.2.

The total steady-state amount of cosmogenic isotopes on the Earth depends on the balance between their production rate in the atmosphere, accumulation over their life and reduction due to radioactive decay.

The main proportion of isotopes (except of the noble gases) is oxidised immediately after production. Among these oxides only carbon dioxide and tritium occur in the atmosphere in a free form. The other isotopes are absorbed by aerosols a short time after their formation. Radioisotopes, contained in aerosols, are removed from the atmosphere fairly quickly by condensation of moisture in low tropospheric layers, whereas those isotopes that remain constant gaseous components of the atmosphere (CO_2, Ar, Kr) are removed from it far more slowly by molecular exchange at the boundary between the atmosphere and oceans.

The ability of cosmogenic isotopes to aid the study of hydrological and hydrogeological processes is restricted by the condition of correspondence between their lifetimes and the duration of a considered process and also by the principles of their displacement in geospheres. The major proportion of cosmogenic isotopes (~70%) is formed in the upper atmospheric layers, about 30% of them in the troposphere. There sequential redistribution is caused by large-scale processes involving the motion of air masses in the troposphere and the precipitation of atmospheric moisture on the Earth's surface, together with cosmic dust or in the form of aerosols.

The absolute amount of an individual isotope, or its ratio relative to another radioactive or stable isotope within a natural reservoir, is used for dating or reconstructing events that have taken place in the past and also for elucidating the nature of prevailing physical, chemical and biological processes. Resolution of the investigation of these processes depends largely on the information available concerning the source and rate of production of a radionuclide.

As pointed out earlier, the production rate of a cosmogenic isotope in the atmosphere depends on latitude and altitude. Comparison of the expected production rate with those amounts actually observed in the air for isotopes with adequate lifetimes provides a basis for studying the principles of large-scale circulations and tropospheric fallout. The abundance of an isotope in the hydrosphere depends on its lifetime, its biochemical role and, finally, on the nature of oceanic circulations. Investigations of abundance of isotopes, characterised by different lifetimes and chemical properties, provide an opportunity for understanding the principles of mass-transfer of substance and, in some cases, helps in understanding the geochemistry of an

Table 10.2 Physical parameters and steady-state amounts of cosmogenic radioisotopes on the Earth

Isotope	Production reaction	Half-life	Radiation type and energy (MeV)	Decay product	Production rate (atom/cm^2 · sec	Steady-state amount on the Earth (g)
^{3}H	^{14}N(n, ^{14}C)^{3}H	12.32 year	β$^-$; 0.018	^{3}He	0.25	3500
	^{16}O(p, ^{14}C) ^{3}H					
^{3}He	N, O(^{3}He)	Stable		–	0.2	$3.2 \cdot 10^{9}$
^{7}Be	^{14}N(n, 3p5n)^{7}Be	53 days	χ; 0.48	^{7}Li	$8.1 \cdot 10^{-3}$	3.2
	^{14}N(p, 4p4n)^{7}B					
	^{16}O(n, 5p5n)^{7}Be					
^{10}Be	^{14}N(p, 4pn)^{10}Be	$1.6 \cdot 10^{6}$ year	β$^-$; 0.55	^{10}B	$4.5 \cdot 10^{-2}$	$4.8 \cdot 10^{8}$
	^{16}O(p, 5p2n)^{10}Be					
^{14}C	^{14}N(n, p)^{14}C	5730 year	β$^-$; 0.156	^{14}N	2.5	$7.5 \cdot 10^{7}$
	^{16}O(p, 3p)^{14}C					
^{22}Na	^{40}Ar(split)^{22}N	2.6 year	β$^+$; 0.54	^{22}Ne	$8.6 \cdot 10^{-5}$	1.9
			γ; 1.28			
^{24}Na	^{40}Ar(split.)^{24}N	15 h	γ; 2.75	^{24}Mg	$1.2 \cdot 10^{-4}$	–
			β$^-$; 1.4			
^{26}Al	^{26}Mg(p, n)^{26}Al	$7.4 \cdot 10^{5}$ year	β$^+$; 2.77	^{26}Mg	$1.4 \cdot 10^{-4}$	$1.2 \cdot 10^{6}$
	^{26}Si(p, 2p)^{26}Al					
^{28}Mg	^{40}Ar (split.)^{28}Mg	21.3 h	β$^-$; 0.42	^{28}Al	$5.2 \cdot 10^{-5}$	–
^{32}Si	^{40}Ar (split ^{32}Si	~450 year	β$^-$; 0.1	^{32}P	$1.6 \cdot 10^{-4}$	1400
^{32}P	^{40}Ar (split)^{32}P	14.3 days	β$^-$; 1.7	^{32}S	$8.1 \cdot 10^{-4}$	0.4
^{33}P	^{40}Ar (split)^{33}P	25 days	β$^-$; 0.25	^{33}S	$6.8 \cdot 10^{-4}$	0.6
^{35}S	^{40}Ar (split)^{35}S	87.4 days	β$^-$; 1.67	^{35}Cl	$1.4 \cdot 10^{-3}$	4.5
^{36}Cl	^{40}Ar (split)^{36}Cl	$3.0 \cdot 10^{5}$ year	β$^-$; 0.714	^{36}Ar	$1.1 \cdot 10^{-3}$	$1.5 \cdot 10^{6}$
^{37}Ar	^{37}Cl (p, 2p)^{37}Ar	35 days	K−capture	^{37}Cl	$8.3 \cdot 10^{-4}$	–
	^{40}Ca (n, α)^{37}Ar					
	^{36}Ar (n, γ)^{37}Ar					
^{39}Ar	^{40}Ar (n, 2n)^{39}Ar	270 year	β$^-$; 0.565	^{39}K	$5.6 \cdot 10^{-3}$	–
	^{39}K (n, p)^{39}Ar					
	^{38}Ar (n, γ)^{39}Ar					
^{53}Mn	^{53}Fe (p, 2p)^{53}Mn	$3.7 \cdot 10^{6}$ year	K-capture	^{53}Cr	$<10^{-7}$	–

Table 10.2 (continued)

Isotope	Production reaction	Half-life	Radiation type and energy (MeV)	Decay product	Production rate (atom/cm^2 · sec	Steady-state amount on the Earth (g)
	^{56}Fe (p, α) ^{53}Mn					
^{59}Ni	^{59}Co (p, n)^{59}Ni	$7.5 \cdot 10^4$ year	K-capture	^{9}Co	$<10^{-7}$	–
	^{60}Ni (p, pn)^{59}Ni					
^{81}Kr	^{82}Kr (p, n)^{81}Kr	$8.1 \cdot 10^{5r}$ year	K-capture	^{81}Br	$1.5 \cdot 10^{-7} - 10^{-5}$	–

element's behaviour. Isotopes that have entered into the biosphere, into oceanic floor sediments and into some other objects, thus becoming isolated from the transitional dynamics in the cycle (which is characterised by a continuous process of mixing of substance), can be used to determine the time elapsed since the moment they escaped from the cycle.

In studying the nature of geophysical and geochemical processes it is convenient to divide the atmosphere and upper layers of the Earth into a number of zones or reservoirs characterised by homogeneous pressure, temperature and character of mass-transfer. A schematic description of isotope migration in natural reservoirs is presented in Fig. 10.5 (Lal and Peters 1962).

The rate of isotope production caused by cosmic radiation in ocean waters is negligible. The detectable concentrations of all the isotopes found in these waters

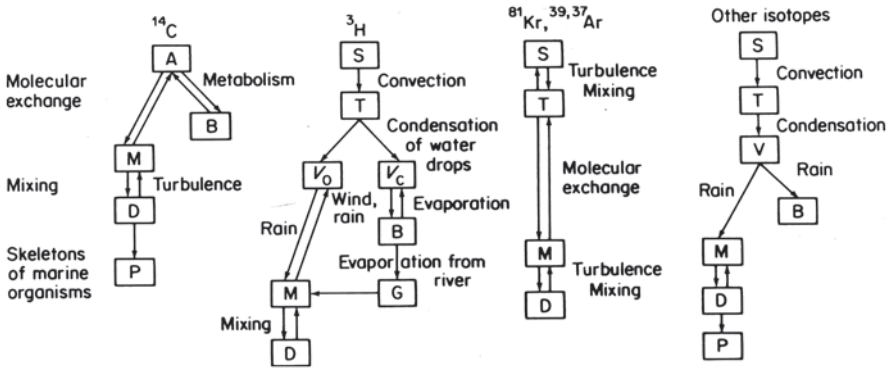

Fig. 10.5 Schematic description and migration of cosmogenic isotopes in the geospheres: (*A*) atmosphere; *(B)* biosphere; (*S*) stratosphere (90–340 g air per 1 cm^2, 1–8 year exchange time); (*T*) troposphere (720–940 g air per 1 cm^2, 30–90 d exchange time); (*V*) water vapour (3–7 g water per 1 cm^2, 4–14 d exchange time); (*M*) mixing layer (75–100 m, 20 year exchange time); (*D*) deep layer (3500 м, 500–3000 year exchange time); (*P*) marine sediments; (*G*) soil water . (Ferronsky and Polyakov 2012)

are the result of exchange between the atmosphere and the oceans. The upper layer of the ocean, receiving cosmogenic isotopes from the atmosphere, is characterised by vigorous movement and quick mixing. It is due to these processes that the geographical inhomogeneity of cosmic radiation is markedly smoothed. Therefore, as a first approximation, the source function of the ocean is equal to zero at depth and constant at the surface. This approximation is accurate for ^{14}C dissolved in water and mixed together with water masses. But there are some other isotopes, such as ^{32}Si and $^{32, 33}P$ that are not displaced by water masses.

The use of cosmogenic isotopes for the solution of practical problems is more easily realised if the theoretical data related to their abundances and decay rates in the major reservoirs of the Earth, where their migration occurs, are available. For the calculations that were carried out by Lal (1963), the oversimplified box-model (see Fig. 10.5) was assumed. The model consists in a six reservoir exchange system: stratosphere (170 g/cm^2), troposphere (860 g/cm^2), continental reservoir (biosphere + surface waters), the upper mixed ocean layer (75 m), deep oceanic layer (3500 m) and ocean sediments. The calculations were carried out using the following simplified constants: the average time of air exchange in the stratosphere equals 2 years and the average time of water exchange in the deep oceanic layer equals 1000 years (Table 10.3).

The distribution of an isotope in individual geospheres depends both on its half-life and chemical behaviour. The usefulness of an isotope in hydrological and hydrogeological process studies depends on its half-life, distribution in exchange

Table 10.3 Steady-state inventories and decay rates of cosmogenic radioisotopes in the exchange reservoirs relative to 1 cm^2 of the Earth's surface. (Lal 1963)

Radioisotope	Exchange reservoir				
	Stratosphere	Troposphere	Mixed oceanic layer	Deep oceanic layer	Ocean sediments
^{3}H	$6.8 \cdot 10^{-2}$	$4 \cdot 10^{-3}$	0.50[a]	0.43	0
^{7}Be	0.60	0.11	0.28	$3 \cdot 10^{-3}$	0
^{10}Be	$3.7 \cdot 10^{-7}$	$2.3 \cdot 10^{-8}$	$8 \cdot 10^{-6}$	$1.4 \cdot 10^{-4}$	0.999
^{14}C	$3 \cdot 10^{-3}$	$6 \cdot 10^{-2}$ [b]	$2.3 \cdot 10^{-2}$	0.91	10^{-2}
^{22}Na	0.25	$1.7 \cdot 10^{-2}$	0.62	0.11	0
^{26}Al	$1.3 \cdot 10^{-6}$	$7.7 \cdot 10^{-8}$	$5 \cdot 10^{-5}$	10^{-4}	0.999
^{32}Si	$1.9 \cdot 10^{-3}$	$1.1 \cdot 10^{-4}$	$5 \cdot 10^{-3}$	0.96	$4 \cdot 10^{-2}$
^{32}P	0.60	0.24	0.16	$1.5 \cdot 10^{-4}$	0
^{33}P	0.64	0.16	0.19	10^{-3}	0
^{35}S	0.57	$8 \cdot 10^{-2}$	0.34	$6 \cdot 10^{-3}$	0
^{36}Cl	10^{-6}	$6 \cdot 10^{-8}$	$2 \cdot 10^{-2}$	0.98	0
^{37}Ar	0.63	0.37	0	0	0
^{39}Ar	0.16	0.83	$2 \cdot 10^{-4}$	$3 \cdot 10^{-3}$	0

[a] The value includes amounts present in the biosphere and humus
[b] Includes amount present in the continental waters

Table 10.4 Specific activities of cosmogenic radioisotopes in oceans and the atmosphere. (Lal 1963)

Radioisotope	Average specific activity in oceans		Radioisotope	Average specific activity in atmosphere, disintegrations min^{-1} kg^{-1} air	
	Disintegrations min^{-1} t^{-1} water	Disintegrations min^{-1} t^{-1} element		Stratosphere	Troposphere
^{3}H	36	$3.3 \cdot 10^{-4}$	^{3}H	6	$7 \cdot 10^{-2}$
^{10}Be	10^{-3}	$1.6 \cdot 10^{-3}$	^{7}Be	17	0.63
^{14}C	260	10	^{22}Na	$5 \cdot 10^{-3}$	$6.7 \cdot 10^{-5}$
^{26}Al	$2 \cdot 10^{-5}$	$2 \cdot 10^{-3}$	^{32}P	0.17	$1.4 \cdot 10^{-2}$
^{32}Si	$2.4 \cdot 10^{-2}$	$8 \cdot 10^{-3}$	^{33}P	0.15	$7.6 \cdot 10^{-3}$
^{36}Cl	0.55	$3 \cdot 10^{-5}$	^{35}S	0.28	$7.8 \cdot 10^{-3}$
^{39}Ar	$2.9 \cdot 10^{-3}$	$5 \cdot 10^{-3}$	^{37}Ar	0.19	$2.1 \cdot 10^{-2}$

reservoirs and the technical ability required to measure the expected activity. The specific activities of a number of cosmogenic radioisotopes in the two principal exchange reservoirs, those of the ocean and atmosphere, were evaluated by Lal (1963) and are presented in Table 10.4.

It follows from Tables 10.3 and 10.4 that the major portion of isotopes such as ^{10}B and ^{26}Al is accumulated in the ocean sediments whereas ^{3}H, and ^{7}Be and many other isotopes are absent. The greatest portions of ^{7}Be, ^{32}P, ^{33}P, ^{35}S, ^{37}Ar and ^{39}Ar are concentrated in the stratosphere and troposphere. The surface ocean layer and inland waters contain the majority of cosmogenic isotopes in significant amounts. Their concentration in groundwaters depends on conditions of interrelation between surface waters and groundwaters. Only those isotopes whose lifetimes are longer than that of infiltrated surface water recharge groundwaters. The varying proportions of concentrations of a given cosmogenic isotope in the water-bearing layer and its steady-state amount in precipitation, surface waters, or in the overlying water-bearing layer, provide a basis for studying processes of water circulation and hydrochronology.

An additional source of isotopes in the atmosphere is cosmic dust, the terrestrial accretion rate of which is about 10^{8}–10^{9} kg/year. The use of some cosmogenic isotopes, being components of cosmic dust, provides information on the accretion rate of the Earth in the past. Such isotopes are ^{53}Mn and ^{59}Ni, which are not produced in the Earth's atmosphere and ^{26}Al, the production rate of which in the atmosphere is less than the contribution due to cosmic dust.

Changes in the isotopic composition of cosmic dust and in the outer shells of meteorites result mainly from bombardment by low-energy cosmic particles of solar origin. The outer shell of a meteorite is usually melted and ablated during movement through the atmosphere. Therefore, while studying the total flux of solar cosmic rays and particularly low-energy protons, the most convenient object is cosmic dust accumulated in the ocean floor sediments and polar pack ices.

It should be pointed out that during the last two decades the concentration of the steady-state amounts of cosmogenic radioisotopes in nature has been broken due to the additional production of these isotopes during the course of nuclear and thermonuclear tests in the atmosphere. An intense flux of neutrons is produced at the moment of explosion, which interacts with the atmospheric constituents and results in the production of identical radioisotopes to those produced by the interaction between the atmosphere and cosmic rays.

The International Atomic Energy Agency (IAEA 1973) reported that from 1945 to 1973 936 nuclear tests were carried out, of which 422 took place in the atmosphere. The majority of those tests were before 1963. During the last decade 43 tests have taken place in the atmosphere. The most powerful output of bomb radioisotopes in the atmosphere took place during 1958–1959, i.e., related to the most frequent and most powerful thermonuclear tests. The concentrations of some radioisotopes have increased compared with the pre-thermonuclear steady-state values by one or two orders of magnitude. Thus, the major portion of ^{3}H, ^{14}C and ^{22}Na present in the atmosphere at present is of bomb origin. A steady-state level of concentration of a number of short-lived isotopes, such as ^{35}S and to a lesser extent ^{7}Be and ^{32}P has been distributed but at present their concentration has returned to normal. The distribution of ^{14}C and to a great extent of also ^{36}Cl and ^{81}Kr, has also been distributed.

The effect of these bombs will be manifested as a distinctive ‘mark’ for a long time in those reservoirs where the processes of water mixing and dilution are slow, such as in groundwater reservoirs. These marks may serve as a good indicator of groundwater motion and also of the individual water-bearing layers between each other and with surface waters.

10.2 Sources of Tritium Discharge into Natural Waters

Among the environmental radioisotopes tritium is the most attractive to those researchers who are studying the principles of water circulation in nature. It is a constituent of water molecules and, therefore, is a perfect water tracer. Interest in the application of tritium for hydrological and meteorological purposes increased greatly during the period of thermonuclear tests during 1953–1962 and also subsequently when a large amount of this artificially produced isotope had been injected into the atmosphere. The bomb-tritium, injected into the atmosphere by instalments after each nuclear test, is a kind of fixed time mark of water involved in water cycling.

Tritium is produced in the atmosphere by the interaction between secondary nuclear particles of cosmogenic origin, mainly neutrons and protons and nitrogen and oxygen nuclei. Neutrons produced by cosmic radiation originally have energies of about several dozens of MeV. Then, due to inelastic scattering on nitrogen and oxygen nuclei, they slow down. At energies greater than 1 MeV the prevailing nuclear reaction is $^{14}N(n, {}^{3}H)\ ^{12}C$.

Table 10.5 Main reactions with neutrons in the atmosphere

Reaction	Absolute rate, (neutron/cm^2 · sec)	Relative rate
Radiocarbon production	4.0	0.56
Tritium production	0.13	0.02
Other reactions	2.2	0.31
Loss	0.8	0.11
Total	7.13	1.0

Table 10.6 Reactions of cosmic-ray production of tritium in the atmosphere

Reaction	Energy of particles (MeV)	Cross-section of reaction (mbarn)	Production rate atom/cm^2 · sec
$^{14}N(n, ^3H)\ ^{12}C$		11 ± 2	0.1–0.2
$^{16}O(p, ^3H)\ ^{14}O$	>100	25	0.08
$^{14}N(p, ^3H)\ ^{12}N$			
$^{16}O(p, ^3H)\ ^{14}O$	10–100	–	0.01
$^{14}N(p, ^3H)\ ^{12}N$			
$^{14}N(p, ^3H)\ ^{12}N$	<10	–	0.05
$N, O(\gamma, ^3H)$	–	–	10^{-5}

The cross-section of this reaction is about 0.01 barn. Only 3–5 % of all the neutrons generated by cosmic rays in the Earth's atmosphere take part in the production of tritium (Table 10.5).

Beside the above reaction, tritium may be produced by other reactions, the main ones of which are presented in Table 10.6.

It follows from Table 10.6 that the first two reactions of interactions of ^{14}N with medium energy neutrons, fission of ^{14}N and ^{16}O nuclei by protons at energy higher than 100 MeV have the highest cross-section. The production rate of tritium by protons with energies ranging 10–100 MeV has been estimated to be 0.01 atom/cm^2 · sec because of an absence of reliable experimental data. The contribution of tritium production by the other components of cosmic radiation is 0.1–0.2 atom/cm^2 · s. This value is less than that actually observed, which is 0.3 atom/cm^2 · s. An additional tritium input to the atmosphere may take place during intense solar flares. It is most probably formed in the course of the reaction ^4He (p, 2p)^3H in the chromosphere of the Sun.

The steady-state amount of tritium on the Earth, formed by cosmic radiation, varies from 3 to 10 kg. The major part of tritium (~93 %) stays in the hydrosphere and only about 7 % is in the atmosphere (see Table 10.4). Due to insignificant amounts in natural objects, tritium is commonly expressed in Tritium Units (TU). A tritium unit corresponds to one atom of tritium per 10^{18} atoms of protium, which is equivalent to 7.2 disintegrations per minute per litre of water, or 0.119 Bq/kg. Tritium is a soft β-emitter, characterised by maximum particle energy equal to

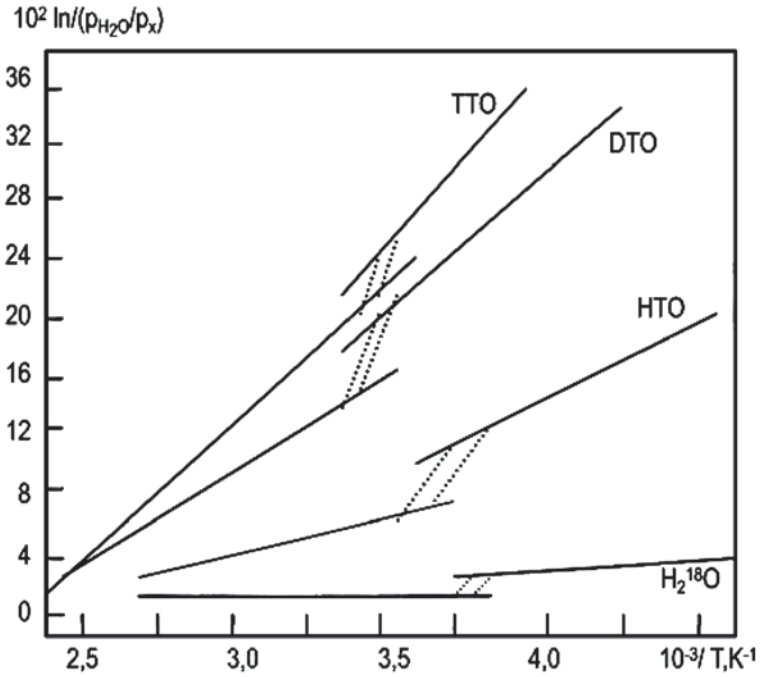

Fig. 10.6 Experimental relationship from vapour pressure of heavy and light water molecules and temperature. (Van Hook 1968; Ferronsky and Polyakov 2012)

18 keV and a half-life of 12.43 year. The final product of tritium decay is the stable isotope of ^{3}He.

Shortly after production, tritium is oxidised and forms molecules of water HTO. Since the masses of tritium and protium differ, fractionation occurs during phase transitions of water from gases to solid states and vice versa (Fig. 10.6).

It is for this reason that inhomogeneity is observed in tritium distribution between hydrogen-bearing systems in tritium-protium exchange reactions. Experiments involving different types of clays (kaolinite, montmorillonite and silty clays) have shown that in the course of their interaction with water labelled by tritium a marked exchange reaction between tritium and protium is observed. Protium constitutes the clay minerals and hydroxides (Stewart 1965). This effect may be considered as significant in groundwater dating and the large time-scale involved in the investigation of water motion in rocks based on tritium labelling

Before the first thermonuclear tests in the atmosphere (1952), the majority of tritium in nature resulted from cosmic-ray production. At that time only a few measurements of natural tritium on the Earth had been carried out. According to the data of Libby (Kaufmann and Libby 1954), who was the first to study its applicability in hydrology and carried out measurements in Chicago, the average content of environmental tritium in precipitation was about 8 TU. Brown (1961) measured tritium concentrations in the Ottawa Valley (Canada) and found that the mean level

Table 10.7 Distribution of tritium in the geospheres. (Burger 1979)

Geosphere	HTO		HT		CH^3T	
	Ci	TE	Ci	TE	Ci	TE
Ocean, top 100 m	$9 \cdot 10^8$	10–20	$(1–10) \cdot 10^3$	?	–	–
Troposphere, ($3.8 \cdot 10^{18}$ kg air)	$(2–8) \cdot 10^6$	–	$(8–18) \cdot 10^6$	$(3–7) \cdot 10^6$	$(6–20) \cdot 10^6$	$\sim 5 \cdot 104$
Stratosphere, ($1.3 \cdot 10^{18}$ kg air)	$(0.6–5) \cdot 10^8$	(2–8)	$(1–4) \cdot 10^4$	–	< 105	$\sim 5 \cdot 104$

of tritium was 15 TU. According to the calculations of Lal and Peters (1962), this value corresponds to 6 TU. Later on, when some principles of distribution and fall-out of corresponding amounts of tritium on the Earth were established, it became clear that tritium content varies within a large range both in space and time. This range may be estimated as being equal to 0.1–10 TU for both hemispheres at a constant rate of tritium production of about 30 atoms/cm^2 min relative to the terrestrial surface (Suess 1969).

Using data obtained by different authors, Burger (1979) reported the data of tritium distribution in individual geospheres given in Table 10.7. Estimations were made of tritium fallout on the Earth with cosmic dust and micrometeorites (Fireman 1967). It was shown that in stone meteorites, the tritium activity equals 200–400 disintegrn/kg min. For iron meteorites this value was 40–90 disintegrn/kg min. Thus, the tritium component contained in meteorites falling down on the terrestrial surface is insignificant and is less than 10^{-5} atoms/cm^2 s.

The results of measurements of tritium concentrations in lunar rocks, carried by the space crafts Apollo-11 and Apollo-12, gave 270–300 disintegrn/kg min (Bochaler et al. 1971), which appeared to be similar values to those in meteorites. The production of tritium in lunar rocks and meteorites occurs due to spallation reactions between cosmic high-energy protons and nuclei or rock-forming elements, such as Fe, Si, Al, etc.

Thermonuclear tests in the atmosphere, carried out since 1952, represent another source of atmospheric tritium. The output of tritium released during a thermonuclear explosion averaged from 0.7 to 5 kg per megaton of thermonuclear fusion and 0.07 kg per megaton of nuclear fission (Miskel 1973). A diagram of tritium injection to the atmosphere from thermonuclear explosions since their beginning is shown in Fig. 10.7 plotted on the basis of data obtained by Eriksson (Schell and Sauzay 1970). Curve 1 accounts for the residence time of tritium in the stratosphere, the main reservoir of accumulation. According to data obtained for precipitation, this residence time is about one year. The residence time in the reservoir is the time required for one half of the tritium present at the beginning to remain in the reservoir. Curve 2 shows the annual variations of the total amount of tritium in the stratosphere.

Energy tests of thermonuclear explosions of megaton energy were carried out by the USA in August 1958 at an altitude of 4–7.5 km. In 1957–1958, at a lower altitude, there were eight megaton tests carried out by the UK. Some portion of tritium produced during these explosions has moved into the stratosphere. The most powerful megaton explosions were made in 1961–1962 by the USA and the former USSR in various places of the globe and at high altitudes. As a result, a large amount of tritium (up to 400 kg) has been stored in the stratosphere (Ostlund and Fine 1979) and its concentration in individual places on the Earth (e.g., White Horse, Canada) in the spring-summer months reached 10,000 TE (Thatcher and Payne1965). It was found later on, after the interdiction of nuclear tests in the three spheres, that the estimation of the residence time of tritium in the stratosphere, which was accepted to be about one year, appeared to be imprecise. Its concentration in precipitation has decreased up to the present time but far more slowly than was assumed theoretically. Thus, the tritium concentrations in precipitation should have reached a natural level by 1970. However, in Western Europe, in the summer months of 1968–1970, the levels were still fixed as they had been at the end of 1960, amounting to about 30 TU.

During the last few years, up to 1970, some increases in tritium content of the atmosphere were observed due to thermonuclear explosions carried out by France and China. But the values of these tritium injections are insignificant compared with the previous ones (see in Fig. 10.7 the maxima corresponding to 1967–1970).

Atomic industries (power and research reactors, plants of nuclear fuel reprocessing, etc.) are also sources of environmental tritium. The output of tritium during uranium fission in different types of reactors depends on the choice of fuel, the energy spectrum of neutron flux and a number of technological factors. Depending on the type of reactor, tritium is produced in the course of the activation of boron, lithium and deuterium atoms by neutrons. In a controlled thermonuclear reactor, which is now under construction, tritium will be the main radionuclide. In this case the major portion of tritium will be ejected from nuclear plants into the environment in a gaseous state (HT, DT, T_2) and partly in liquid phase in the form of HTO.

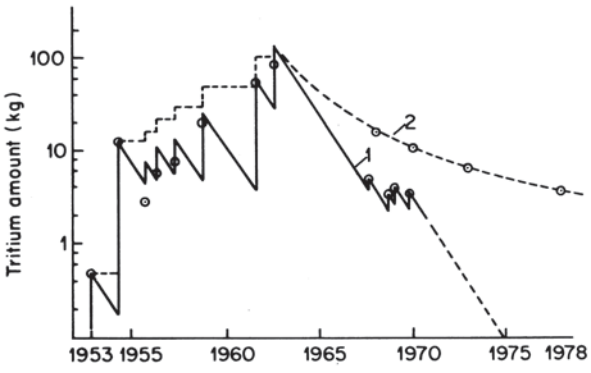

Fig. 10.7 Growth of thermonuclear amounts in the atmosphere taking into account its fallout (*1*), and the stratosphere taking into account its natural decay (*2*). (Ferronsky et al. 1975; Ferronsky and Polyakov 2012)

The gaseous tritium ejected into the atmosphere oxidises quickly and forms water molecules.

According to data obtained by Sehgal and Remport (1971), in the course of uranium and plutonium fission 0.8 atom of tritium is formed per 10^4 acts of ^{235}U fission, 0.9 atom of tritium for that of ^{238}U and 1.8 atoms of tritium for that of ^{239}Pu. Fluss and Dudey (1971) studied the dependency of tritium production on energy of neutrons for ^{235}U. According to them, when the energy of neutrons changes from 175 to 630 keV the yield of tritium increases from 2 to 3.4 atoms per 10^4 acts of uranium nuclei fission.

In the slow-neutron reactors, during ^{235}U fission, the yield of tritium amounts to $8.7 \cdot 10^{-3}$% (Taylor and Peters (1972) and in the fast-neutron reactors it corresponds to $2.2 \cdot 10^{-2}$% (Dudey et al. 1972). This efficiency of yield corresponds to the VVER and RBMK reactor that provides $1.1 \cdot 10^{-2}$ Ci/day · Mw (t) and for the fast neutron reactors—$2.8 \cdot 10^{-2}$ Ci/day · Mw (t).

During reactions proceeding in the control rods of the reactors, tritium is ejected in accordance with the reactions $^{10}B(\alpha, 2\alpha)^3H$; $^{11}B(n, {}^3H)^9B$; $^{10}B(n, \alpha)^7Li$; $^7Li(n, n\alpha)^3H$. The cross-section of these reactions increases with the energy of neutrons. Therefore, the yield of tritium in fast-neutron reactors is considerably higher than in reactors of the other type. Lokante (1971) reported that the tritium yield corresponding to fission reactions amounts to 11,000 Ci and for boron reactions is about 1380 Ci in the 3500 Mw boiling water reactor. In the 300 Mw breeder reactor the tritium yield is 1670 Ci for the fission reaction and 3980 Ci for the boron reaction. The tritium output from the heat-generating elements to the heat carrier depends on the material of the shell. Stainless steel passes up to 60–80% of the produced tritium and zirconium only 0.1% (Lokante 1971).

According to Broder et al. (1979), the tritium exhausts from typical VVER-440, VVER-1000 and RBKM-1000 reactors are equal to 0.6, 1.6 and 2.28 Ci/day, respectively. At the Novovoronezhskaya nuclear power station, for example, about 55% of the total amount of tritium is ejected into the atmosphere, 27% into surface waters and 13% into groundwaters. According to data for yearly observations, the tritium concentrations at 1 km downstream of the river are higher by one order of magnitude than in water upstream of the river.

As pointed out above, tritium is produced at nuclear power stations (reactors) both due to the process of uranium fission and due to interactions of neutrons of various energies with constructional materials and coolants. The following substances are some of those used as coolants: light and heavy water, noble gases, melted metallic sodium. The main nuclear reactions, in the course of which tritium is formed, are the reaction of fission of enriched uranium (X) leading to the formation of the fission products $X(n, f)^3H$; $X(n, f)^6He \rightarrow {}^6Li(n, \alpha)\ ^3H$; $^{10}B(n, 2\alpha)\ ^3H$; $^2H(n, \gamma)\ ^3H$; $^9Be(n, 2\alpha)\ ^3H$ and so on.

In Table 10.8 data on the tritium yield in different types of reactors due to the above-mentioned reactions are given. In Table 10.9, data on tritium input into the atmosphere and surface waters for various nuclear reactors and nuclear fuel processing plants are presented.

Table 10.8 Tritium production in various types of reactors. (Bonka 1979)

Nuclear reaction	Tritium production in Ci/Mw(e) per year					
	BWR[a]	PWR[a]	HWR[a]	AGR[a]	HTR[a]	FBR[a]
Efficiency	0.33	0.33	0.32	0.41	0.41	0.41
Fuel element						
Fission	18	18	20	15	12	30
^{6}Li in fuel, 0.05 ppm	0.3	0.3	0.8	1	0.2	0.1
^{10}B in fuel, 0,05 ppm	$4 \cdot 10^{-5}$	$4 \cdot 10^{-5}$	$3 \cdot 10^{-5}$	$5 \cdot 10^{-5}$	$1 \cdot 10^{-5}$	$2 \cdot 10^{-5}$
^{6}Li in graphite	–	–	–	–	0.5	–
^{9}Be in graphite	–	–	–	–	$1 \cdot 10^{-4}$	–
^{10}B in graphite	–	–	–	–	$3.5 \cdot 10^{-3}$	–
Coolant						
^{1}H in water	$8 \cdot 10^{-3}$	$8 \cdot 10^{-3}$	–	–	–	–
^{2}H in water	$4 \cdot 10^{-3}$	$4 \cdot 10^{-3}$	150	–	–	–
^{10}B in water	–	0.8	–	–	–	–
^{3}He in helium	–	–	–	–	1	–
^{6} Li in sodium	–	–	–	–	–	2
^{9}Be in sodium	–	–	–	–	–	0,01
^{10}B in sodium	–	–	–	–	–	0,01

[a] BWR is boiling-water reactor; PWR is pressurised water reactor; HWR is heavy-water reactor; AGR is advanced gas-cooled reactor; HTR is high-temperature reactor; FBR is sodium-cooled fast breeder reactor

Table 10.9 Tritium emission rates from nuclear power reactors under normal operation and reprocessing plants without tritium retention. (Bonka 1979)

Nuclear facility		Emission rate (Ci/year)	
		Atmosphere	Surface water
Reactor (1000 Mw(e))	BWR	30	150
	PWR	20	900
	HTR	10	900
	FBR	100	200
Reprocessing plant (40,000 Mw(e) full load)	BWR and PWR	$7 \cdot 10^{-5}$	1000
	PWR	$7 \cdot 10^{-5}$	1000
	HTR	$6 \cdot 10^{-5}$	1000
	FBR	$6 \cdot 10^{-5}$	1000

In the report made by the National Council on Radiation Protection and Measurements of the USA (Eisenbund et al. 1979) the following data on tritium yield due to diverse sources are given. The global amount of tritium produced by cosmic radiation equals 70 MCi (1 kg of tritium is equivalent to about 10 MCi), i.e., its production rate is about 4 MCi per year. In 1963 an amount of tritium, estimated at 3100 MCi, was injected into the atmosphere and hydrosphere as a direct result of nuclear and thermonuclear tests. Thus, the natural level of tritium (70 MCi) may be attained as a result of a decay process up to 2030. The production of tritium in nuclear reactors of the PWR type due to fission reactions ranges from 12 to 20 Ci/day per Mw of the thermal power. The activation of light elements gives an additional yield of tritium that averages from 600 to 800 Ci/year per Mw of electrical power. These values are equal to 63 Ci/year for the reactors of the BWR and PWR types with light-water cooling. The average residence time of tritiated water vapour in the troposphere ranges from 21 to 40 days.

The main residence time of HTO molecules in the mixing ocean layer (50–100 m thickness and equal to 75 m on average) is approximately 22 year. The average time of half-removal of tritium from the human body depends upon individual biological features and is equal to hundreds of days. For two arbitrarily chosen and absolutely healthy men of middle age, the time of half-removal was found to be 340 and 630 days.

Some portion of tritium is injected into the environment from research centres, medical institutions and industrial plants dealing with works involving the application of artificial tritium. According to data reported by König (1979), tritium activities of $(1.2–2.1) \cdot 10^3$ Ci/year have been released into the atmosphere from the Nuclear Research Centre in Karlsruhe (Germany) since 1969. Krejči and Zeller (1979) reported that a large amount of tritium is ejected into the atmosphere from the luminous compound industry, producing tritium, gas-filled light sources and tritium luminous compounds. The urine of the operators working on one of the plants producing luminophor contains about 25 Ci/l of tritium (1TU = 3.2 pCi/l). In the waste water within the plant area the concentration of tritium is about 0.3 Ci/l and in water at the exit from the cleaning installations the concentration is 0.004 Ci/l. In precipitation at a distance of 50 m from the ventilation system of the tritium department the concentration of tritium is 0.1 Ci/l, at a distance of 200 m it amounts to 0.02 Ci/l and at 2000 m it is equal to 0.001 Ci/l. A large amount of tritium is now used for the production of liquid crystal displays for digital electronic readouts. The annual production of tritium by different industries in the USA is shown in Fig. 10.8 reported by Combs and Doda (1979). According to their estimations the amount of tritium used for the production of backlighted digital watches would reach (and it did reach) 4 MCi in 1979.

A considerable amount of tritium in the environment originates from the nuclear fuel reprocessing industry. Daly et al. (1968) showed that the nuclear fuel reprocessing plant situated in New York State ejects about 200 Ci of tritium per day, 25 % of which is released into the atmosphere, 65 % is contributed in liquid form to the river and 10 % goes into the soil.

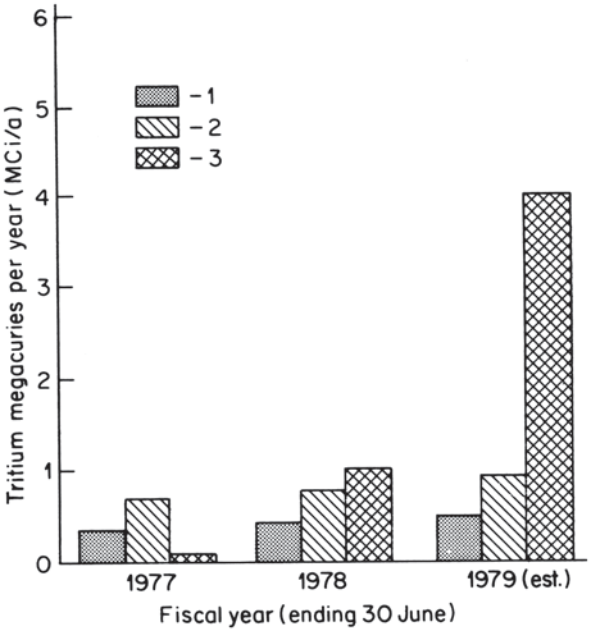

Fig. 10.8 Quantities of tritium produced annually in the United States of America for digital watch lighting (*1*), by power reactors (*2*) and for other commercial products (*3*). (Combs and Doda 1979; Ferronsky and Polyakov 2012)

Taking into account the modern trend of development of nuclear power stations in most countries of the world, it is easy to estimate that by the beginning of the twenty-first century the production of technogenic tritium, which will be continuously ejected into the environment, will overcome the amount of cosmogenic tritium produced in the atmosphere.

In fact, the tritium production rate from all the nuclear plants (power reactors and nuclear fuel reprocessing plants) of the world by 2000 was four times the rate of its natural production by cosmic radiation. But the release of tritium into the environment is negligible since its major portion is collected and buried as radioactive waste. Besides, the tritium produced by nuclear plants cannot reach the stratosphere, where it would be subjected to global redistribution. Therefore, its ejection into the precipitation, surface and groundwaters is of a local character, related to the neighbourhood of the organisation that is studying surface and groundwaters involving tritium measurements.

According to Katrich (1990), some amount of tritium was injected into the environment as the result of the Chernobyl accident. Concentration of tritium over the European part of Russia in May 1986 increased by 2–5 times compared with May 1985. But in June–July the level of contamination dropped to a normal level because the tritium only reached the troposphere.

At least some portion of tritium will be released into the atmosphere due to nuclear explosions used for peaceful purposes (such as the performance of underground oil, gas and water capacities, excavation of rocks in the course of construction works

etc.). But the major portion of tritium precipitating in the hydrological cycle in the near future will be, as previously, the bomb-tritium released in the period from 1952 to 1962.

10.3 Global Circulation of Tritium Water

At present the total amount of tritium on the Earth exceeds its pre-bomb level only by 1.5–2 times. This situation is explained by the continuous decay of tritium and isotopic exchange with the ocean's waters.

From the atmosphere, which is the only source of natural and thermonuclear tritium, the tritium water molecules together with air flows enter the troposphere where they form tropospheric moisture. The other effects that determine incoming of tritium into the tropospheric moisture is evaporation from the ocean surface and the molecular exchange between the surface ocean layer and atmospheric moisture. The continental atmospheric precipitation of high tritium content forms river runoff, lake and groundwaters and glaciers. Some part of precipitation evaporates. Concentration of tritium in river water is close to that in precipitation and in lakes it depends on the residence time of water: the longer residence time, then the less content of tritium because of its decay. The same relates to groundwater basins. In glaciers, especially in polar latitudes (Greenland, Antarctic), water looks like it is conserved and in the deep layers tritium is completely decayed. The non-decayed part of the molecules HTO from the rivers, lakes and groundwater arrives to the oceans together with surface and underground runoff.

The oceans' waters are divided into two layers: the upper well mixed layer with a depth of several hundred metres and the lower layer, divided from the upper by the thermocline, with a water exchange time of several hundreds and even thousands of years. The thermocline may be absent in Polar regions and in this case the most favourable conditions for vertical water mixing appear. In the upper layer are observed maximum concentrations of tritium, which lower to the deep and mixed long time and lose tritium at its decay.

Thus, the stratosphere is the source of tritium in the hydrologic cycle and the reservoir for tritium runoff is deep ocean waters and glaciers where it decays. It follows that definite regularities should be expected in distribution of tritium in all chains of the hydrosphere.

10.3.1 Tritium in Atmospheric Hydrogen and Methane

Except water, which is the main object for study of tritium distribution on the Earth, there are two other hydrogen-bearing compounds. They are the molecular hydrogen H_2 and methane CH_4. The study of their behaviour is important for understanding of the geophysical and physical-chemical processes in the atmosphere. Of a

special interest are H_2O, H_2 and CH_4 cycles, which have a close relationship in the atmosphere. Their passage from one form to another may be used as a tracer for determining the residence time of hydrogen in its compounds, for estimation of the exchange rate between the hemispheres, for study of the air exchange between the troposphere and stratosphere and for understanding the nature of the compounds origin.

At present the concentration of molecular hydrogen in non-industrial regions amounts to 0.575 ppmv in the northern hemisphere and 0.550 ppmv in the southern hemisphere (Schmidt 1974). On a global scale, 50% of molecular hydrogen is of anthropogenic origin. The most significant natural source of H_2 in the biochemical process occurring in the ocean is molecule dissociation with hydrogen photosynthesis occurring in the atmosphere (Romanov and Kikichev 1979) also contributing significantly to H_2 concentration.

The majority of tritium in atmospheric hydrogen is of cosmogenic origin. The principal reaction leading to the production of HT molecules, according to estimations made by Harteck (1954) for tritium generated by cosmic rays, is the recurrent photodissociation of TO_2 and the subsequent exchange reaction of the form:

$$T + H_2 \rightarrow HT + H.$$

Only 0.1% of the tritium produced by cosmic rays exists in the form of HT molecules and 99.9% is in the form of HTO molecules. The bulk of the HT molecules are formed at altitudes ranging from 10 to 40 km. The total mass of the HT molecules of cosmogenic origin in the atmosphere is about 5 g (Rowland 1959).

Besides the release of tritium from the device itself during thermonuclear explosions, tritium is produced according to the following main reaction:

$$D + D \rightarrow T + H + 4\text{MeV}.$$

It is considered that approximately the same relative content of bomb-tritium is contained both in the molecules of H_2O and H_2, which is the result of isotopic exchange between H_2O and H_2 in the expanding and cooling thermonuclear sphere. In this case, the main reactions are:

$$T + O_2 \rightarrow TO_2,$$

$$TO_2 + O \rightarrow TO + O_2 + 61\,\text{kcal},$$

$$TO + H_2 \rightarrow HTO + H + 17\,\text{kcal},$$

$$HTO + H_2 \leftrightarrow H_2O + HT.$$

In the course of underground thermonuclear tests the increase of tritium content in atmospheric hydrogen was not accompanied by an increase of tritium content in

the atmospheric moisture. This is likely due to the lack of conditions necessary for oxidising reactions in the medium where the explosion took place.

The main sources of technogenic tritium, as pointed out earlier, are nuclear power plants, which release a considerable amount of tritium in the form of HT molecules.

Tritium was first measured in atmospheric hydrogen in 1948 near Hamburg, where its concentration was found to be equal to $4 \cdot 10^3$ TU (Faltings and Harteck 1950). Later on, due to thermonuclear tests, the concentration of tritium in atmospheric hydrogen sharply increased. It can be seen from figure that the concentration of tritium increased from $4 \cdot 10^3$ to $4 \cdot 10^6$ TU from 1948 to 1973 (Ehhalt 1966; Östlund and Mason 1974). In tropospheric HT its concentration reached maximum values with a delay of about 2–2.5 year. Ehhalt (1966) assumed this to be the effect of removal of HT molecules from the stratosphere, which is the main reservoir of tritium accumulation during thermonuclear explosions, into the troposphere after a certain long time, corresponding to what was observed.

After thermonuclear tests were stopped in the three media, the tritium content in molecular hydrogen remained approximately unchanged from 1963 to 1973 at a level of $(2–4) \cdot 10^6$ TU. The constancy of the HT concentration in the atmosphere can only be explained by ejection of tritium into the atmosphere from some sources in order to maintain the corresponding partial pressures of the HT molecules and compensate the natural losses caused by radioactive decay and other processes of removal.

According to existing estimations (Martin and Hackett 1974) the total anthropogenic release of tritium into the atmosphere should amount to $1.2 \cdot 10^6$ Ci/year in order to maintain the average concentrations of tritium in atmospheric hydrogen at the level of about 80 atoms per mg of air. These sources of anthropogenic tritium release are likely to be atomic industry plants and underground tests.

In contrast to the distribution of HTO, the spatial distribution of tritium in atmospheric molecular hydrogen is characterised by a high homogeneity in the whole atmosphere. According to data of Östlund and Mason (1974), the concentration of tritium was about 50 atom/mg of air in 1971–1972. Only at high latitudes (60° N and higher) does the concentration of tritium increase up to 80 atom per mg of air. According to limited data, the tritium concentration in the stratosphere decreases with altitude following barometric law. Thus, in North Alaska at 70–75 °N the tritium content in the lower stratosphere varies with altitude from 80 to 30 atom/mg of air (Östlund and Mason 1974). The exceptions to these principles are the regions of anomalous release of molecular hydrogen of industrial origin with zero concentration of tritium and also the regions where nuclear industries are located, characterised by raised tritium content. The global content of HT molecules in the atmosphere during the period 1968 to 1978 is shown in Fig. 10.9 (Mason and Östlund 1979).

According to data of Ehhalt (1974), the methane early production is $(5.4–10.6) \cdot 10^{14}$ g, from which 80% have biogenic origin and the tritium concentration is more than 10^4 TU (Ehhalt 1974). Creation of CH_3T molecules in the atmosphere occurs as a result of nuclear and exchange reactions between HT and CH_4. But as investigations show, these reactions have small efficiency (Begemann and Friedman 1968). It is assumed that the main sources of tritium in methane are

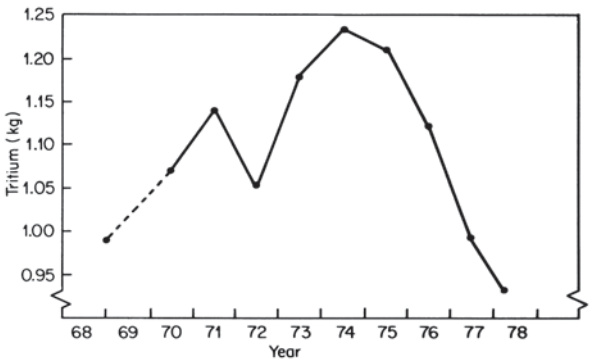

Fig. 10.9 Inventory of global atmospheric HT for 1968–1978. (Mason and Östlund 1979; Ferronsky and Polyakov 2012)

research laboratories and institutions of atomic industry, the technology of which relates to tritium (Burger 1979).

Molecules CH_3T of biochemical reactions have the same T/H ratio as environmental water. It is obvious that atmospheric HT takes part in biogenic methane. As a result of this process, the tritium content in methane correspondingly increases. The exchange time of methane in the atmosphere is about 4–7 year.

10.3.2 Tritium in Atmospheric Water Vapour

As pointed out above, the upper layer of the atmosphere, its stratosphere (15–17 km), is the reservoir where the bulk of natural tritium is accumulated. Despite the small amount of stratospheric moisture it is the main source of tropospheric tritiated water falling to the Earth's surface as precipitation. It will be shown that the stratosphere is also a reservoir accumulating thermonuclear tritium.

Martell (1963), using a supposed production rate of natural tritium of 0.3 atom/$cm^2 \cdot s$, obtained a value of tritium concentration of about 10^6 TU. The first measurements of stratospheric tritium in the air above Minneapolis in 1955–1958, at an altitude of 14–28 km carried out by Hagemann et al. (1959), showed that the tritium content was equal to $1.1 \cdot 10^6$–$1.52 \cdot 10^7$ atom per gram of air. On the basis of these measurements and with the ratio of T/C^{14} it was found that the amount of tritium in the stratosphere is equal to $6 \cdot 10^{23}$ atoms (6 kg). Later, Scholz et al. (1970) obtained a tritium concentration of $2.2 \cdot 10^6$–$8 \cdot 10^7$ T.U. using their own experimental data.

The most complete studies of tritium distribution in the troposphere were carried out by Ehhalt (1971). Measurements were conducted from November 1965 to January 1967 at continental (Scottsbluff, Nebraska) and oceanic (near California) stations up to an altitude of 9.2 km. The results of Ehhalt's measurements showed that concentrations in water vapour increase with altitude. The lowest concentrations were found at an altitude of 2300 m above sea level in the spring-summer seasons

(1200 TU) and maximum values at an altitude of 9 km (26 000 TU). It was found that the altitude of the seasonal variations at amplitude of 7.5–9 km is greater by a factor of 10 than the variation of tritium concentrations at the Earth's surface.

Detailed data concerning the distribution of HTO molecules with height were reported by Mason and Östlund (1979). Water and hydrogen samples were taken with the help of a molecular trap, placed on a special aircraft, up to a height of 13 km. Differences in the HTO distribution both with altitude and latitude were observed between 1976 and 1977, caused by an atmospheric thermonuclear test conducted by the People's Republic of China on 17 November 1976, which resulted in the release of a large amount of tritium into the stratosphere. According to the estimations of Mason and Östlund, the inventories of atmospheric tritium were about 1 kg of HT molecules and 5.3 kg of HTO at the end of 1977. A major portion of HTO (about 5.1 kg) has been stored in the stratosphere and 0.2 kg has been in transit to the ocean surface through the troposphere.

Bradley and Stout (1970) carried out individual measurements in order to obtain tritium distribution profiles in atmospheric moisture in Illinois State (USA) up to amplitude of 5 km. They obtained three different types of distribution of tritium with altitude. The first type is characterised by an increase of tritium concentration with altitude, the second type by a constancy of tritium concentration and the third type by a decrease of tritium concentration with altitude up to 2.5 km and then by a subsequent increase in concentration. These tritium distributions were explained by Bradley and Stout as the result of different conditions of formation and mixing of atmospheric moisture in the lower troposphere and also in terms of different sources of tritium.

In mountainous regions the vertical distribution of tritium in the atmosphere can be estimated using data of precipitation measurements at different altitudes. These studies were carried out by Romanov (1978) in Caucasus near the Aragats Mountain (Table 10.10). It was found that the average annual concentrations of tritium in precipitation sampled at an altitude of 850–3500 m in 1971 and 1972 increased by factor of three. Assuming the equilibrium conditions of condensation of atmospheric precipitation, it may be assumed that such relationships reflect the actual vertical distribution of tritium in water vapour.

The data obtained by the same author on tritium concentration in the annual layers of the Pamir glacier at an altitude of 4500 m (Table 10.10) were found to be lower. This was explained by a difference in the origin of the atmospheric moisture (Indian Ocean), which forms the sampled precipitation.

Table 10.10 Relationship of tritium concentrations with altitude in Aragats Mountain (Caucasus)

Sampling place	Altitude (m)	Mean annual concentration in precipitation (TE)	
		1971	1972
Oktemberian	850	37	82
Garnovit	1100	114	162
Aragatz	3238	143	201
Pamir (Abramov glacier)	4500	65	72

10.3.3 Tritium in Precipitation

The applicability of environmental tritium as a tracer of air mass circulation in the atmosphere and the formation of precipitation and discharge on the continental surface and in groundwaters is based upon experimental data of tritium content in precipitation on a global scale. This work was initiated in 1961 by the IAEA and the WMO jointly. In order to detect the tritium, deuterium and oxygen-18 content in precipitation, more than 100 meteorological stations linked to the WMO, located in different countries, were involved (see Fig. 9.7). The ocean samples were collected on islands and weather ships. Thus, the network of stations included the most characteristic points of the globe both on continents and oceans in both the northern and southern hemisphere.

In 1965, in connection with the International Hydrological Decade program (1965–1974), the network of stations included additional stations for water sampling from rivers. But the majority of rivers fell out of this network of stations and therefore a representative river network was not established. Up to present, the network includes more than 100 stations plus many national points of observation at which the tritium content is measured. Measurements of tritium content in precipitation continue.

Sampling and analysis were performed according to techniques developed by the IAEA. Samples of atmospheric waters, taken every month, correspond to the monthly average tritium content in precipitation. Tritium content in water samples was measured in low-level counting laboratories in the IAEA and in Canada, Denmark, India, Israel, New Zealand, Germany, Sweden, USA, USSR and other countries.

All these data are being collected by the IAEA and after processing together with the results of analysis of stable isotopes (deuterium and oxygen-18) content, measured in the same samples and also together with meteorological data, are published in special issues of Environmental Isotope Data (IAEA 1969).

The tritium concentrations in precipitation may have a substantial difference in individual fallouts, depending on their origin and trajectory of motion. But in principle, distribution of the fallouts depends on the mechanism of circulation of the atmosphere. Seasonal and annual variations are observed. Seasonal variations are related to the strengthening of the air masses exchange between the spring-summer stratosphere and the troposphere. The effect leads to occurrence of the so-called spring-summer maximum in the annual tritium distribution. Weakening of this process in the winter and autumn leads to occurrence of the autumn-winter minimum.

The long-term variation of tritium concentration of natural origin can be related to phases of solar activity. This is because it occurs at an anti-phase with the intensity of galactic cosmic rays, which are accepted as a source of tritium.

Some researchers have tried to study the correlation between long-term tritium variations, which were observed in Greenland glaciers formed before 1952, with solar activity. But a single-valued result was not found. For example, Begemann (1959) with the Greenland glaciers discovered a negative correlation between

tritium concentration and solar maximum activity. Ravoire et al. (1970) with Antarctic snow (1950–1957) found this correlation to be positive. And Aegerter et al. (1967) discovered both types of correlation.

During atmospheric thermonuclear tests, tritium in the form of HTO occurs both in the stratosphere and in the troposphere. A proportion of its amount depends on the height and power of the explosion. The tropospheric component of HTO must have a residence time compared with that of the tropospheric moisture, i.e., equal to several weeks. Experimental data prove this conclusion (Buttlar and Libby 1955). The period of removal of half of the tritium from the troposphere is 45 days. A figure close to this was obtained by Buttlar and Libby by measurements of tritium in precipitation in Chicago.

The stratospheric tritium part is removed substantially lower. The velocity of this process corresponds with the velocity of exchange between the tropospheric and stratospheric air and has seasonal cyclic character. The annual tritium concentration changes in the Ottawa River water are shown in Fig. 10.10 (Brown 1970). Figure 10.11 demonstrates the annual means of tritium concentration changes over Moscow and in the Moscow River (Russia) during the period of 1953–1969, obtained by the authors.

It follows from Figs. 10.10 and 10.11 that the entering of tritium into the atmosphere occurred during the 1954, 1956, 1958 tests. In the period of moratorium from 1959 up to its interruption in September 1961 the tritium concentration within the Moscow region dropped from 760 to 200 TU. The period of removal of the half tritium value for this time interval was equal to about 1 year. In September 1961, the thermonuclear tests were renewed and continued up to December 1962. In that period the main part of bomb-tritium accumulated in the stratosphere, which is observed up to now.

The maximum yearly means of tritium concentrations over the Moscow region reached 3900 TU (Fig. 10.11). After the thermonuclear test ban treaty in the three spheres had come into force the stratospheric tritium reserve started to decrease with a period of 1.2 year up to 1967–1968. After that the decrease slowed down. During 1969–1974, the period became equal to about 3 years. This value was obtained by the authors on the basis of data over vast territories and, therefore, may be considered adequately authentic. One more explanation of the above phenomenon can be redistribution of tritium in the stratosphere between the northern and southern hemispheres. During recent years, this transfer has decreased due to approaching a quasi-equilibrium state.

It was shown in the work of Weiss et al. (1979) that, starting from 1970 over Central and Western Europe, technogenic tritium plays a notable role in formation of its occurrence in precipitation. From here it follows that sampling stations should be placed at an appropriate distance from industrial plants and institutions.

Variations of tritium concentrations in precipitation during spring and summer are determined by specific conditions of the mass air exchange between the stratosphere and the troposphere, resulting from easier connection.

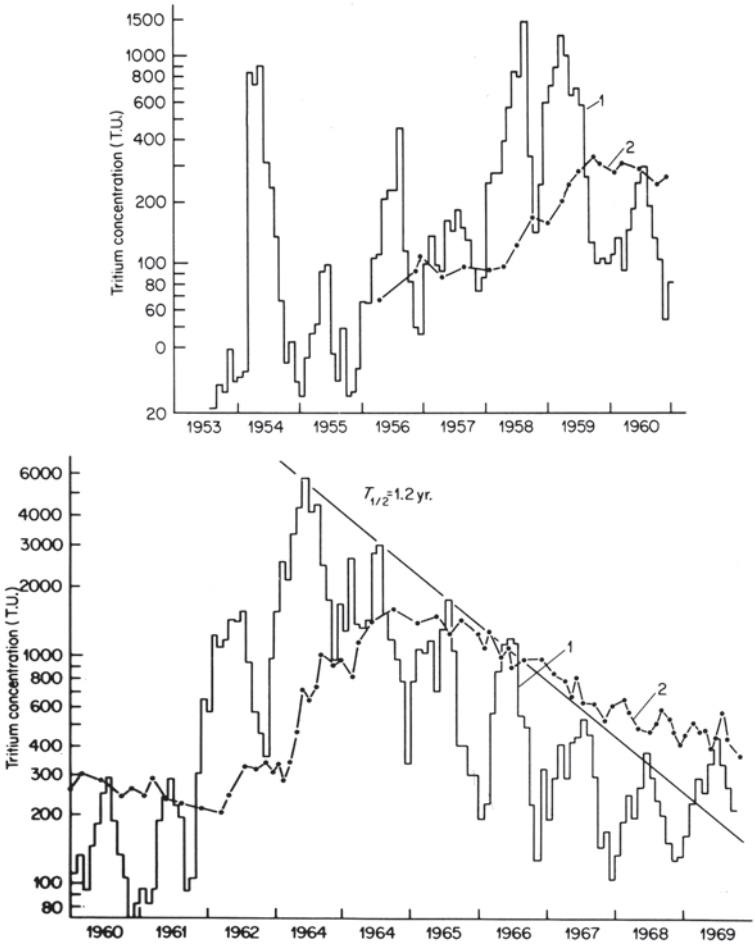

Fig. 10.10 Tritium concentration change during 1953–1969 in precipitation (*1*) and in Ottawa River water (*2*). (Brown 1970; Ferronsky and Polyakov 2012)

The peak of the tritium concentrations in precipitation for the northern hemisphere is observed, as a rule, in June and in the southern hemisphere in September. But very often deviations from this rule occur due to meteorological peculiarities of differed years. These peaks occur very seldom. In this connection, it is better to average data for a number of regions with more or less identical physical-geographical characteristics at the same time interval. Tables 10.11 and 10.12 are an example of such an average. The tables were prepared on the basis of data published by the IAEA (1969) using more than 250 stations of the Earth's globe. For the former USSR area the author's own data were used. Sometimes a substantial deviation in mean monthly tritium values from these seasonal variations is observed.

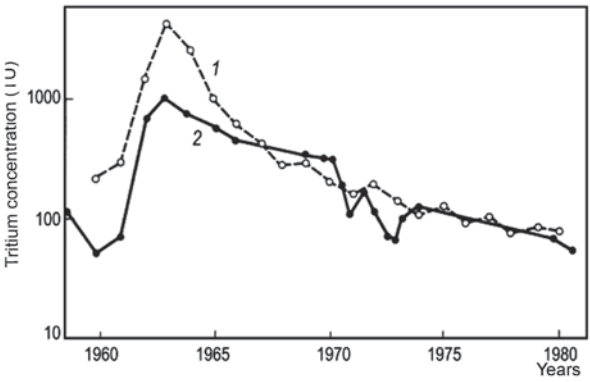

Fig. 10.11 Mean annual distribution of tritium concentration in atmospheric precipitation over the Moscow region (*1*) and in Moscow River water (*2*) 1958–1981. (Ferronsky and Polyakov 2012)

10.3.4 Formation of Tritium Concentrations in the Atmosphere

General principles observed from the picture of tritium concentration, related to latitudinal distribution and seasonal cycles, indicate the existence of a strict mechanism that governs the process of tritium distribution and concentration to precipitation.

In the period of intensive thermonuclear tests, the release of tritium into the stratosphere occurred periodically from individual points where the explosions took place. At the same time the average concentration of tritium fallout does not depend upon the place of injection but is related to latitude and time of the year. This fact resulted in the conclusion that the upper layer of the atmosphere (its stratosphere) is the reservoir where the accumulation and latitudinal redistribution of tritium occurs on a global scale and from which seasonal tritium releases to the lower atmospheric layer (troposphere) take place. Precipitation is formed in the troposphere. Such a reservoir exists for each hemisphere independently and the relationship between them is rather restricted. The mechanism of formation of tritium concentrations is presented as follows. The oceanic water, evaporated from its surface and having low tritium concentration, moves by the rising up air flows with a velocity of about 3–5 м/sec. In the case of unstable thermal atmospheric stratification, the velocity may overreach 10 m/sec. The created water vapour during the day and night is moved several kilometres high. From the other side, the process of mixing of the stratosphere and troposphere leads to interference to the last of enriched tritium water vapour.

The vertical distribution of tritium shows that its interference into the upper layers of the troposphere begins in December and continues up to June-July. In winter time the tritium transfer is made by eddy flows and in spring and summer by high tropic cyclones. In the Antarctic, in winter time, a direct condensation of vapour from the overcooled lower stratosphere is possible (Jouzel et al. 1979). The process of tritium moisture enrichment in clouds is continued due to molecular exchange.

Table 10.11 Seasonal distribution of tritium concentrations in precipitation for stations of the northern hemisphere

Month	Yearly means of concentration in precipitation (TU)					
	1964	1965	1967	1968	1969	mean value
0–20 °N						
January	1.09	1.13	1.26	0.94	0.99	1.07
February	1.17	1.29	1.18	1.06	1.04	1.12
March	1.17	1.28	1.20	1.24	1.23	1.19
April	1.30	1.07	1.27	1.09	1.03	1.13
May	1.31	1.23	1.07	1.16	1.04	1.13
June	1.34	1.40	1.30	1.10	1.09	1.22
July	1.44	1.24	1.13	1.27	1.34	1.35
August	0.96	0.84	0.92	1.09	1.24	0.99
September	0.71	0.66	0.83	0.88	0.92	0.78
October	0.51	0.62	0.66	0.72	0.77	0.64
November	0.51	0.62	0.68	0.75	0.66	0.63
December	0.49	0.62	0.51	0.70	0.64	0.58
20–90 °N						
January	0.89	0.63	0.73	0.46	0.63	0.70
February	1.09	0.98	0.90	0.80	0.76	0.89
March	1.18	1.20	1.09	1.04	1.04	1.08
April	1.46	1.46	1.22	1.19	1.11	1.29
May	1.67	1.54	1.60	1.42	1.49	1.57
June	1.70	1.73	1.58	1.59	1.62	1.64
July	1.41	1.51	1.36	1.44	1.47	1.45
August	0.99	1.10	1.17	1.28	1.29	1.18
September	0.56	0.60	0.88	0.86	0.80	0.74
October	0.43	0.43	0.54	0.60	0.63	0.53
November	0.31	0.35	0.48	0.54	0.50	0.44
December	0.32	0.36	0.46	0.77	0.64	0.50

The idea of the accumulation of radioactive products of thermonuclear tests in the stratosphere, with their subsequent redistribution and injection into the troposphere where precipitation is formed, was first suggested by Libby in 1956 (Libby 1963). Later on, attempts were made to develop this idea and to construct a box model of interacting exchangeable reservoirs: the stratosphere, the troposphere and the ocean. Investigations were mainly aimed at determining the residence time of a radioactive tracer in each of the exchangeable reservoirs. The final goal of these studies was to fix a relationship between the residence time of a tracer in the stratosphere and the motion of air masses in the stratosphere and troposphere.

In estimating the residence time of tritium in the stratosphere, it was assumed that the release of tritium into the troposphere is exponential. Thus, the residence

Table 10.12 Seasonal distribution of tritium concentration in precipitation for stations of the southern hemisphere

	Yearly means of concentration in precipitation (TU)					
Month	1965	1966	1967	1968	1969	Mean value
0–20 °S						
January	1.26	1.01	0.94	1.22	1.15	1.15
March	0.96	1.10	0.89	0.88	0.91	0.95
April	0.70	1.20	0.86	0.82	0.86	0.93
May	0.75	0.89	0.71	0.74	0.76	0.77
June	0.94	0.76	0.73	0.88	0.93	0.85
July	0.93	0.98	1.22	1.04	0.93	1.02
August	1.03	1.06	1.03	0.98	1.11	1.04
September	1.16	0.69	0.94	1.21	1.12	1.02
October	1.03	0.71	1.30	0.99	0.99	1.02
November	0.94	1.28	1.06	0.91	0.87	1.01
December	1.00	1.14	1.17	0.98	1.10	1.08
0–20 °N						
January	1.06	0.94	1.02	1.00	1.05	1.01
February	1.01	0.87	0.79	1.29	0.89	0.97
March	0.67	0.90	0.78	0.67	0.67	0.74
April	0.77	0.64	0.86	0.70	0.70	0.73
May	0.63	0.73	0.79	0.71	0.73	0.86
June	0.72	0.59	0.70	0.71	0.75	0.69
July	0.82	0.88	0.98	0.86	0.84	0.88
August	1.43	1.18	1.27	1.38	1.43	1.34
September	1.56	1.66	1.35	1.54	1.60	1.54
October	1.29	1.43	1.16	1.22	1.27	1.27
November	0.97	1.06	1,02	1.00	1.,06	1.02
December	1.06	1.10	1.28	0.93	0.90	1.06

time of tritium in the reservoir was taken, by analogy with its half-life, to be the time required for one half of the amount to be discharged from the stratosphere.

On the basis of experimental data concerning tritium concentrations in precipitation measured after 1953 at the two stations of Vienna and Valentia, which represent typical continental and coastal regions in terms of fallout, it was found that the residence time of tritium in the stratosphere is equal to one year (Schell and Sauzay 1970). According to data of Brown (1970) for the Ottawa River Valley it is equal to 1.2 year. As a result of the observed residence time of tritium in the stratosphere, its total storage (Fig. 10.2) and half-life removal, it can be estimated that by 1970 the tritium concentration in precipitation should already have been close to natural concentration. At the same time, according to experimental data obtained for Western and North America (see Fig. 10.10) from the beginning of 1967, the tritium content

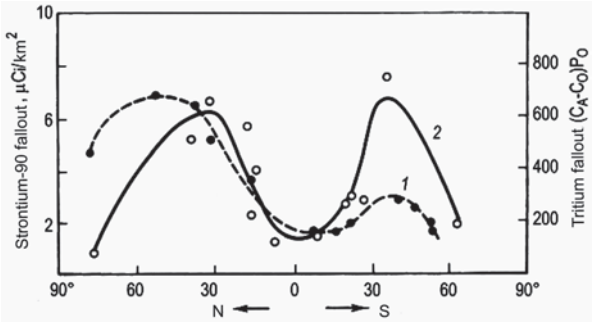

Fig. 10.12 Latitudinal fallout of tritium (*1*) and srtontium-90 (*2*) from the stratosphere over the Atlantic Ocean in 1969. (Ferronsky and Polyakov 2012)

in precipitation in the northern hemisphere remains constant at a level of 150–200 TU and by Romanov's estimations (Romanov 1978), decreases with a half-life removal time of about 3 year. This tritium content is an order of magnitude greater than natural tritium concentrations in precipitation. Different causes of this phenomenon were considered, particularly those related to the injection of tritium from thermonuclear tests conducted in the atmosphere during the preceding years. But in accordance with the measures carried out at a number of stations (e.g., in Tokyo), the increase in tritium concentration in fallout is insignificant because these explosions were not very powerful and provided only small concentrations of tritium to the stratosphere (see Fig. 10.2), where the maximum concentration occurred between 1967 and 1970. Another source of tritium contribution to the atmosphere may be the various installations of the atomic industry. This idea has been well demonstrated by Weiss et al. (1979). But as pointed out earlier, the possible input of tritium into the stratosphere from this source should be negligible and this tritium should have only a local effect upon sampling stations located near to nuclear plants.

Therefore, the residence time of tritium in the stratosphere (1–3 years) does not remain constant and the distribution and mixing of tritium in the atmosphere is a more complicated process than that described by the model of exchangeable reservoirs.

The questions of interpretation of global tritium distribution in precipitation have been studied by a number of researchers (Eriksson 1965a; Libby 1963; Taylor 1968). In one of the works an attempt was made to develop a general model of tracer release from the stratosphere into precipitation in which the injection, exchange, evaporation and condensation of the water vapour would be related to the meteorological parameters of the troposphere.

The model is based on the following physical reasoning. The exchange of air masses between the stratosphere and troposphere occurs mainly due to powerful air streams being thrown down periodically into the troposphere as a kind of trough or trench. This process coincides with the observed spring maximum of radioactive falls in precipitation at mid-latitudes of the northern hemisphere. Therefore, in the general mechanism of air masses exchange between the two reservoirs, the process

of stratospheric air transfer to the troposphere due to diffusion is a secondary factor. The periodic rushes of dry stratospheric air into the troposphere, which contain excessive concentrations of radioactive substances and have large potential velocities, determine the mechanism of stratospheric-tropospheric exchange of air masses.

Another process responsible for the ejection of highly radioactive stratospheric air concerns powerful convective storm fluxes rushing into the stratosphere. These air fluxes, containing a large amount of water vapour, are mixing with radioactive substances and return with a high radioactive content as subsequent precipitation.

It has been found that the greatest concentrations of various radioactive nuclei, e.g., ^{90}Sr, ^{14}C and T, in precipitation always occur in the spring-summer period. But the maximum T-values appear with a delay of one month compared with that of ^{90}Sr and one–two months earlier than the maximum ^{14}C-values at the same latitude. The reason for this lies in the differences in their masses and physiochemical properties relative to those of the other atmospheric constituents. In the stratosphere, the behaviour of tritium, a constituent of HTO water molecules, is the same as that of ^{90}Sr and ^{14}C since gaseous T is usually transferred through the air by eddy diffusion.

It has been found that the T/^{14}C ratio in the lower stratosphere exceeds that in humid air layers and is equal to 0.4. While approaching the humid layers of the troposphere, stratospheric HTO molecules may exchange with water at the ocean surface, re-evaporate and transfer into groundwater by infiltration,

The water circulation process in nature is as follows. Water with some tritium evaporates from the ocean surface. The water vapour rises and reaches the temperature of condensation by cooling. Dry air from the low stratospheric layers with a high tritium content exchanges tritium with the rising ocean water vapour, which contains low concentrations of tritium. The time of exchange appears to be an important factor; the longer the vapour stays in the atmosphere, the greater is the probability that it will become enriched in tritium. At some thermodynamic and meteorologic conditions precipitation is formed, which is a mixture of ocean and stratospheric water vapour.

The water balance equation is based on the relationship between radioactive fallout and meteorological parameters for a given atmospheric volume. Near the Earth this equation is:

$$\mathrm{E}-\mathrm{P}-\triangle\mathrm{F}=0, \tag{10.1}$$

where P is precipitation; E is evaporation–transpiration; ΔF is the derivation of the water flux in the considered air volume.

In order to establish the relationship between the equation and real conditions, it was assumed that water transfer is caused by winds characterised by velocities that vary in space. The balance equation at a concentration of the indicator C and for a vertical column of air relative to the Earth's surface, is as follows (Schell et al. 1970):

$$\iint(\mathrm{EC_E}-\mathrm{PC_P}-\mathrm{Q_tC_t})\,\mathrm{dxdy}=\iiint\left[\frac{\partial(\mathrm{QC_v}\cos\theta)}{\partial\mathrm{x}}+\frac{\partial(\mathrm{QC_v}\sin\theta)}{\partial\mathrm{y}}\right]\mathrm{dxdydz}, \tag{10.2}$$

where Q_t is an upward loss of moisture; C_E, C_P, C_t and C_v are the tritium concentration in evaporation, precipitation and atmospheric moisture at the border of air volume accordingly; Q is the flux of moisture; θ is the angle of wind direction. The equation may be simplified for computation:

$$<\overline{E}\overline{C}_E> - <\overline{P}C_P> - <\overline{Q}_t\overline{C}_t> = \frac{1}{L}\int_z \left(Q_2 v_2 C_2 \cos Q_2 - Q_1 v_1 C_1 \cos Q_1\right) dz,$$

where L is the distance between the observation stations and indexes 1 and 2 for the parameters Q, v and C relate to those stations.

The above model was applied for estimation of the relationship between the content of T, ^{90}Sr and ^{14}C in precipitation and meteorological parameters characteristic for a number of sites in Western Europe. Those calculations produced reasonable results.

In order to demonstrate the effects of the global distribution of tritium, Romanov (1978) made a number of assumptions in order to obtain a simpler expression describing the transfer of the atmospheric moisture. The balance equation then becomes:

$$\frac{dW}{dt} = E - P, \tag{10.3}$$

where W is the moisture content in the atmosphere; E and P are the amounts of moisture in evaporation and precipitation per unit of time.

The balance equation of HTO in the atmospheric moisture above the ocean is:

$$d(WC_A) = qdt - C_A Pdt + C_0 Edt - M(C_A - C_0)dt, \tag{10.4}$$

where C_A is the concentration of tritium in the atmospheric moisture; q is the rate of tritium release from the stratosphere; t is the residence time of an air mass over the ocean; C_0 is the tritium concentration in the surface oceanic layer; M is the rate of the eddy transfer of the atmospheric moisture to the surface oceanic layer. The fractionation of tritium during the phase transition is not accounted for.

The left-hand side of the equation expresses the change in the tritium content of atmospheric moisture over the time period dt. In the right-hand side the first term defines the discharge of tritium from the stratosphere, the second term corresponds to the removal of tritium in precipitation, the third term to the release of tritium from the ocean surface layer by evaporation and the fourth term to the injection of tritium into the ocean due to molecular exchange. The last term in Eq. (10.4), according to experimental data obtained by Romanov, is proportional to the gradient of the tritium concentration in the system: atmospheric moisture–ocean surface layer together with the water vapour.

In writing Eq. (10.4) it was assumed that the tritium content in precipitation is equal to its concentration in the whole of the upper atmospheric moisture layer and that the tritium concentrations in the ocean surface layer are little affected compared

with concentrations in the atmospheric moisture and the rate of tritium injection from the stratosphere is constant during the whole time of air mass transfer.

Using (10.3), Eq. (10.4) can be rewritten in the form:

$$\frac{dC_A}{dt} + C_A \frac{E+M}{W} = q + C_0 \frac{E+M}{W}. \tag{10.5}$$

The solution of Eq. (10.5) is:

$$C_A = C_0 + \frac{q}{E+M}\left\{1 - \exp\left[-\frac{E+M}{W}t\right]\right\}. \tag{10.6}$$

The integration constant can be defined from the initial conditions: $C_A = C_0$ at $t = 0$.

It follows from Eq. (10.6) that the tritium concentration in the atmospheric moisture is greater when the moisture content W is lower and when the interrelationship between the ocean and the atmosphere, expressed by parameters E and M, is weaker. This principle can be observed in nature by analysing experimental data on global tritium distribution in precipitation. The lower values of moisture content, evaporation and molecular exchange in high latitudes result in the observed latitudinal effect of tritium concentration exchange in precipitation.

Taking into account that the rate of water evaporation is proportional to the humidity gradient (p_o–p), the rate of molecular exchange is proportional to atmospheric humidity p and that both processes are identically related to wind velocity, Eq. (10.6) may be rewritten in the form:

$$C_A = C_0 + \frac{q}{kp_0}\left[1 - \exp\left(-\frac{tkp_0}{W}\right)\right], \tag{10.7}$$

where p_0 is the pressure of the saturated vapour at the ocean surface temperature t; k is the parameter determined from the relationship $M = kp$.

If value t is large enough, then:

$$C_A = C_0 + \frac{q}{kp_0}. \tag{10.8}$$

From Eq. (10.8) the velocity q of injection of tritium from the stratosphere can be obtained. The plot of dependence of the velocity from the latitude in Fig. 10.12 is presented. The values of T and ^{90}Sr content in the atmosphere are placed on the plot. It is seen that in both cases the maximum is located in the belt of 40–50 °N, which evidences the common nature of injection to the troposphere of bomb-tritium and strontium-90.

Let us determine the relationship between tritium concentration and the residence time of the air mass above the continent. The balance equation in this case is:

$$d(WC_A) + qdt - C_A Pdt + C_E Edt, \tag{10.9}$$

where C_E is the tritium concentration in the evaporating continental water.

Taking into account the insignificant difference between tritium concentrations in the surface continental water and in precipitation one can assume that $C_E \approx C_A$. In this case, using the balance equation for atmospheric moisture (10.3), a solution of (10.9) is obtained in the form:

$$C_A = \frac{q}{W} t + \text{const.} \tag{10.10}$$

The integration constant can be determined by the initial conditions $t = 0$ *at* which the tritium content in the atmospheric moisture is equal to its content in moisture transported from the ocean. Then:

$$C_A = C_0 + \frac{q}{W} t. \tag{10.11}$$

The last equation accounts for the observed continental effect. In fact the longer the air mass moves above the continent, the greater the concentration C_A becomes and the better the function $C_A(t)$ may be approximated by a linear dependence, which is confirmed by experimental data obtained in many regions of the world.

Further development of the models establishing the relationship between tritium concentrations in precipitation and meteorological parameters requires a deeper understanding of the natural principles governing air mass circulation in the atmosphere.

10.4 Tritium in Ocean Waters

Oceans are the main reservoir of the hydrosphere and the main source of atmospheric moisture on the Earth. From continental runoff, direct falls of precipitation and exchange with the atmosphere, the oceans receive the majority (about 90 %) of natural and bomb-tritium. Therefore, the oceans are the main reservoir of tritium accumulation on the Earth. The distribution of tritium in the surface and deep ocean layers is of interest while studying the principles of water circulation of the oceans together with atmospheric moisture and, in particular, of the ocean itself.

Before the thermonuclear tests the tritium concentrations in the ocean water, measured at different sites, had characteristic values from ~0.5 TU (Kaufmann and Libby 1954). to 1 TU (Begemann and Libby 1957). After the thermonuclear tests in March 1954 tritium concentrations increased at an average to 1.9 TU. It was difficult to measure such a concentration by the time techniques that existed then with appropriate accuracy.

After 1980, systematic measurements of tritium concentrations in the oceans started. The obtained results allowed Östlund and Fine (1979) to calculate the approximate amounts of tritium in different ocean regions (Table 10.13).

Table 10.13 Tritium inventory in the oceans. (Östlund and Fine 1979)

Ocean	Tritium (kg)
North Atlantic	66
South Atlantic	7
Arctic Basin	6
North Pacific	59
South Pacific	14
Antarctic	6
Indian Ocean	6
Total	164

Tritium content in the ocean waters is defined by effect of interaction between the ocean surface and atmospheric moisture, which is developed in precipitation, by evaporation and molecular exchange, by the life time of the surface layer existence, depending mean time on the vertical mixing of water and by interaction of water masses having different origins and tritium concentrations.

The general character of tritium content variations in the surface waters of the ocean reflect the picture of tritium input into precipitation including the rise of tritium content during the period of thermonuclear tests and seasonal cycles in each year. At the same time, it follows from the data that the input to the surface layer is delayed and the amplitude of tritium concentration is decreased because of dilution in a larger water volume. Figure 10.13 shows variation of tritium concentration in a surface water layer along 30 °N in the Atlantic Ocean plotted by the data of a number of researchers (Östlund and Fine 1979; Münnich and Roether 1967).

The corresponding changes in tritium content, because of a series of thermonuclear tests in 1958 and 1961–1962, are obvious. But the peaks are shifted to 2–3 years compared with concentrations in precipitation. The maximum of the amplitudes with higher tritium concentrations is observed in the middle and high

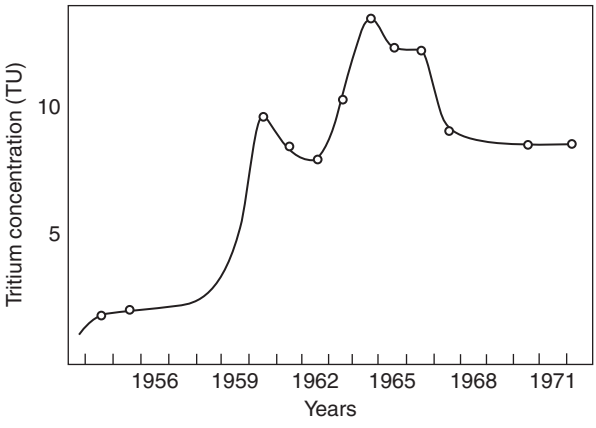

Fig. 10.13 Latitudinal variation of tritium concentration along 30 °N in the Atlantic Ocean during 1954–1972. (Ferronsky and Polyakov 2012)

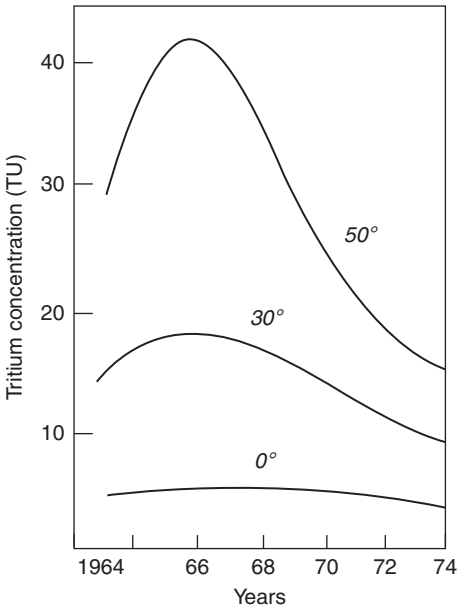

Fig. 10.14 Maximum changes in tritium concentrations in a surface layer of the Pacific Ocean. (Östlund and Fine 1979; Ferronsky and Polyakov 2012)

latitudes (Östlund and Fine 1979) (Fig. 10.14). The effect is strongly smoothed in the equatorial latitudes.

Tritium content variations in the surface layer differ seasonally. In the summer time, surface concentrations are higher because of its high content of atmospheric moisture, higher velocity of molecular exchange and lower dilution of surface layer by deep low-active oceanic water due to the thermocline effect. Dockins et al. (1967) studied tritium concentrations in the Pacific Ocean between 14 °S and 52 °N during 1959–1966. The highest concentrations correspond to the summer maximum in the northern part of the ocean, which are smoothed in the low latitudes. In the southern hemisphere the tritium concentrations in the surface layer decline quickly, which is in agreement with tritium the general picture of tritium falls in precipitation.

Münnich and Roether (1967) studied tritium variations in the surface and depth profiles of the Atlantic Ocean. As for the Pacific Ocean, the latitudinal distribution of tritium in the surface water has maximum concentration in the mid-latitudes of the northern hemisphere. The minimum concentrations of tritium were observed in the equatorial region (not more than 1–3 TU), being obviously close to the natural level observed before the bomb tests. The depth of the tritium mixing layer also increases with latitude from 100 m near the equator to several hundreds of metres in high latitudes. The absolute values of tritium concentrations in the Pacific Ocean are higher than those in the Atlantic Ocean due to more intensive vertical mixing.

Rooth and Östlund (1972) studied the distribution of tritium in the North Atlantic surface waters during 1963–1968. They confirmed the latitudinal increase of tritium content there. Longitudinal variations in concentration are small. They proposed a model applicable for calculation of the vertical turbulent transfer through the ocean thermocline, including advection.

Bainbridge (1963), Michel and Suess (1975) and other researchers, using the ratio between tritium content in the surface ocean layer and in atmospheric moisture, carried out an assessment of residence time in that layer. For this purpose they applied a box model where the ocean was divided into two reservoirs: the first was the surface well mixed layer and the second was the deep layer with lower tritium concentration compared with the surface one. Thus, it was assumed that tritium input is provided only through the dividing border between the atmosphere and the ocean and the tritium loss is a result of the radioactive decay in the well mixing layer. Horizontal advection is refused here because the horizontal tritium gradient in the open ocean is, as a rule, very small.

Applying the box model, Michel and Suess (1975) found that the water exchange time for 12 stations in the Pacific Ocean for the period of 1967–1973 is equal from 7.5 to 26 year. At the same time, they found that the maximum velocities are in the subtropical latitudes and the minimum in the equatorial zone. Values close to the above but calculated by a modified methodology, were obtained by Romanov (1982) for the Black and Caspian Seas (10–15 year) and for the margin seas of the Arctic Ocean.

Vertical tritium distribution in ocean water has its specific features related to its circulation on the globe. A typical picture of vertical tritium distribution is shown in Fig. 10.15. It is specified by the presence of a density jump at the thermocline, which is confined to the surface layer with a relatively high level of tritium content and the deep layer with almost zero tritium content. The two layers are divided by

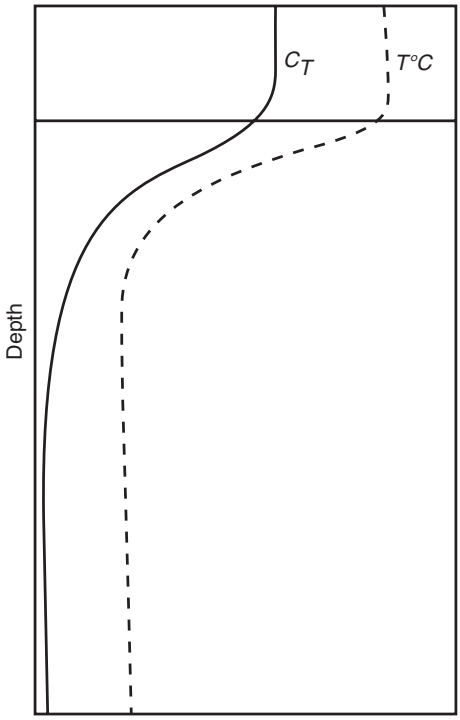

Fig. 10.15 Typical vertical tritium distribution in oceanic waters. (Ferronsky and Polyakov 2012)

an intermediate thin layer where the vertical turbulent mixing of tritium takes place. Such conditions are characteristic for the equatorial and low latitudes.

Applying the tritium gradient of concentration, it is possible to calculate the coefficient of vertical turbulent diffusion K_z. Roether et al. (1970) used this method and for the northern part of the Pacific Ocean obtained $K_z = 0.15$ cm^2/sec. Rooth and Östlund (1972) for the Sargasso Sea obtained a value of K_z close to the calculated one. In order to obtain this parameter the authors compiled an equation that takes into account the processes of turbulent diffusion and vertical advection. In this case the change of tritium concentration $C(x, y, z, t)$, as a conservative radioactive inform:

$$\frac{dC}{dt} = \frac{K_z \partial^2 C}{\partial z^2} + K_H \left(\frac{\partial^2 C}{\partial x^2} + \frac{\partial^2 C}{\partial y^2} \right) - \bar{V} \nabla C - \lambda C.$$

The coefficient of turbulent diffusion K_H in the horizon plane (at x and y) is taken as the same. The vector of velocity of advective transfer $\bar{V}$ appears to be the vectors sum on all the three space coordinates.

Romanov (1982), in order to determine the coefficient of vertical diffusion for the Black Sea, applied a simplified equation in the form:

$$\frac{dC}{dt} = \frac{K_z \partial^2 C}{\partial z^2} - \lambda C.$$

Its solution for non-stationary conditions is:

$$C = \frac{1}{2} C_n \left[\begin{array}{l} \exp\left(-\sqrt{\frac{\lambda}{K_z}} z \right) \left(1 - \operatorname{erf} \frac{z - 2\sqrt{K_z \lambda} t}{2\sqrt{K_z t}} \right) \\ + \exp\left(\sqrt{\frac{\lambda}{K_z}} z \right) \left(1 - \operatorname{erf} \frac{z - 2\sqrt{K_z \lambda} t}{2\sqrt{K_z t}} \right) \end{array} \right],$$

where $C_п$ is the tritium concentration in the surface layer of marine water.

Because the tritium concentration $C_п$ in the surface layer is not expressed in analytical form due to occasional character of thermonuclear tests, then a numerical solution with presentation of $C_п$ in a histogram form is used. After that the value of C for each step is found. This was the method used for interpretation of the Black Sea data, where the value of $K_z = 0.1$ cm^2/sec was obtained.

In high latitudes, where the process of air masses vertical mixing is more powerful, vertical tritium distribution appears to be more complicated. The same picture of tritium distribution for regional concentrations and divergence of ocean water is observed.

In 1972 tritium content studies at the deep water stations in the western Atlantic Ocean from 3 °N to 74 °N were carried out as part of the GEOSECS program. The results obtained were mainly in agreement with those obtained by Münnich and Roether (1967) and supplemented their profiles to the north and south. Penetration of bomb-tritium, with a concentration more than 0.2 TU, in the north latitudes, was observed up to the depth of 3500 m, whereas in the equatorial region a sharp decrease in content was observed at a depth of only 200 m.

Analogous profiles, obtained by the same authors for the Pacific ocean, show that bomb-tritium here has not fallen so deep as in the Atlantics at the north and most was in the upper layers that circulate in the reverse side in both hemispheres.

The northern and southern currents divide these systems. The deepest tritium penetration (up to 1000 m) is in the northern part of the Pacific Ocean. The most complete mixing, especially up to 500 m, is in the region of 20–40 °N. The maximum tritium concentrations in the near-equatorial current (8–20 °N) are at a depth of 200 m and at the surface. This is because the formed at higher latitudes and moving along constant density oceanic water are dropped. Analogous results and conclusions were obtained in earlier works by Michel and Suess (1975).

Asymmetric distribution of tritium concentrations in both oceans relative to the equator is explained by prevailing fallout in the northern hemisphere.

Note that the marked influence on the distribution of tritium in the surface oceanic layer in near-shore and continental regions effects the river runoff. There is also a good correlation between tritium concentrations and salinity and temperature of sea water.

10.5 Tritium in Continental Surface Waters

The continental surface waters, together with precipitation, are an important transport chain of global water circulation on the Earth. At evaporation they markedly affect the isotopic composition of atmospheric moisture. The surface continental waters are the main source for the groundwaters recharge and to a significant degree determine conditions of formation of isotopic composition and salinity of the marginal seas. A study of isotopic composition of the surface waters helps in obtaining valuable information about the parameters of water dynamics of river and lakes basins. Thus, the study of regularities in tritium distribution of surface waters is an important scientific problem.

10.5.1 Tritium Content in River Water

The factors that determine tritium content in river waters are tritium concentrations in precipitation over an area of the river catchment basin and the residence time of the infiltrating precipitation water in the soil through which it discharged into the groundwater and the river.

Let us express an analytical relationship between the tritium concentration in river water and the water exchange velocity in a river basin. Assume that river water in a basin represents the surface runoff and groundwaters that are well mixed. The age spectral function of river water can be written as $a(t)=\varepsilon \exp(-\varepsilon t)$, where $a(t)$ is the relative portion of precipitation in river water with age t and ε is the exchange velocity (the ratio of total annual recharge to the water volume of the catchment basin). Here value $1/\varepsilon$ has dimension of time (in years). Therefore,

$$\int_0^\infty a(t)\,dt = 1.$$

The tritium concentration in the river water C_r can be expressed by the equation:

$$C_r = \int_0^\infty C_p(t)\varepsilon e^{-\varepsilon t} e^{-\lambda t} dt,$$

or

$$C_r = \varepsilon \int_0^\infty C_p(t) e^{-(\varepsilon+\lambda)t} dt, \tag{10.12}$$

where λ is the tritium decay constant; $C_p(t)$ is the tritium concentration in precipitation at the time moment t.

At $C_p(t)=\text{const}=C_p$ (e.g., during the pre-thermonuclear period) one obtains:

$$C_r = \frac{\varepsilon C_p}{\varepsilon+\lambda}. \tag{10.13}$$

In order to obtain the solution of Eq. (10.12) when $C_p(t)\neq\text{const}$. (after the beginning of the tests) the function $C_p(t)$ should be rewritten in the form of a histogram. Then:

$$C_r = \frac{\varepsilon}{\varepsilon+\lambda}\left\{\sum_{i=1}^{n}\left[C_{p_{i=1}} - C_{p_i}\right]\exp\left[(\varepsilon+\lambda)(t_i - t_{i-1})\right]\right\} + \frac{\varepsilon}{\varepsilon+\lambda} C_{p_n}, \tag{10.14}$$

where C_{p_n} is the concentration of tritium in precipitation for the time interval $(t_i - t_{i-1})$; n is number of the time intervals in a period t.

Eriksson (1963) proposed another model for the interpretation of tritium data. It is based on the assumption that groundwaters, which are recharged by precipitation, move in parallel to the watershed. Then the precipitation waters, which fall at different distances from the watershed, do not become mixed. According to this model $a(t)=\varepsilon$ for t ranging from 0 to $1/\varepsilon$, equal to the residence time of infiltration water during its course from the watershed to the bed of the river. Then, the concentration of tritium in the river is as follows:

$$C_r = \varepsilon \int_0^{1/\varepsilon} C_p(t)\, e^{-\lambda t} dt. \tag{10.15}$$

At $C_p(t) = \text{const} = C_p$ one has:

$$C_r = \frac{C_p \varepsilon}{\lambda}(1 - e^{-\lambda/\varepsilon}). \tag{10.16}$$

Note that the ratio of the C_p-values, obtained from expressions (10.13) and (10.16), is equal to 1.3. Putting the expression for $C_p(t)$ written in the form of the histogram into (10.16), one obtains:

$$C_r = \frac{\varepsilon}{\lambda}\left\{C_{p_0}\left(e^{-\lambda t} - e^{-\lambda/\varepsilon}\right) + \sum_{i=1}^{n} C_{p_i} e^{-\lambda(t-t_i)}\left(1 - \exp\left[-\lambda\left(t_i - t_{i-1}\right)\right]\right) + C_{p_n}\left(1 - e^{-\lambda t}\right)\right\}. \tag{10.17}$$

Here the value of t should be less than that of the maximum residence time $1/\varepsilon$.

But a more reliable method for the estimation of water exchange rates in river basins is a balance method, proposed by Eriksson (1965b). In a somewhat simplified form it is as follows (Romanov 1978).

The spectral function of water's age can be represented by a number of fixed values a_0, a_1,…, a_i, where index i corresponds to the portion of infiltration water characterised by the age t_i. Thus the portion of precipitation falling in the year of observation is denoted by a_0, which in the previous year was a_1 and so on.

The balance equation of water is:

$$\sum_{i=0}^{\infty} a_i = 1. \tag{10.18}$$

An expression for tritium concentration in river runoff can be written as:

$$C_r = \sum_{i=0}^{\infty} a_i C_{a_i} e^{-\lambda t}. \tag{10.19}$$

Before the thermonuclear tests, n years ago, $C_a = \text{const} = C$, then:

$$C_r = \sum_{i=0}^{\infty} a_i C_{a_i} e^{-\lambda t} + C \sum_{i=0}^{\infty} a_i e^{-\lambda t}. \tag{10.20}$$

While studying river basins, the second term on the right-hand side of Eq. (10.20) can be neglected, so that:

$$C_r = \sum_{i=0}^{\infty} a_i C_{a_i} e^{-\lambda t}. \tag{10.21}$$

One should write n equations, such as (10.21), for the solution of the problem. In practice, the upper limit of summation can be bounded. For example, the value of $n = 1/\varepsilon$ has been determined beforehand from the conditions $i = 3$, i.e., for the coefficients a_0, a_1, a_2. The other coefficients were made equal to each other. Then:

$$C_{r_0} = a_0 C_{a_0} + a_1 C_{a_1} e^{-\lambda} + a_2 C_{a_2} e^{-2\lambda} + \left[1 - (a_1 + a_2 + a_3)\right] \exp\left\{-\frac{1}{2\varepsilon} + 1{,}5\right\} \frac{1}{1/\varepsilon - 2} \sum_{3}^{1/\varepsilon} C_{a_i} e^{-i\lambda},$$

$$C_{r_2} = a_0 C_{a_2} + a_1 C_{a_3} e^{-\lambda} + a_2 C_{a_4} e^{-2\lambda} + \left[1 - (a_1 + a_2 + a_3)\right] \exp\left\{-\frac{1}{2\varepsilon} + 1{,}5\right\} \frac{1}{1/\varepsilon - 2} \sum_{3}^{1/\varepsilon} C_{a_{ii+2}} e^{-i\lambda},$$

$$C_{r_i} = a_0 C_{a_i} + a_1 C_{a_2} e^{-\lambda} + a_2 C_{a_3} e^{-2\lambda} + \left[1 - (a_1 + a_2 + a_3)\right] \exp\left\{-\frac{1}{2\varepsilon} + 1{,}5\right\} \frac{1}{1/\varepsilon - 2} \sum_{3}^{1/\varepsilon} C_{a_{ii+1}} e^{-i\lambda}. \quad (10.22)$$

Treating the system of Eq. (10.22), one can obtain the values of a_0, a_1, a_2. In a similar way any number of equations can be written and solved.

Applying the balance method, Eriksson (1965b) re-estimated the partition function of the age of runoff in the Ottawa River. Using his solution and the box model, Romanov (1978) reported that the value of ε for the Moscow River in 1964–1965 was 0.195. This value coincides with results obtained on the basis of the laminar flow model, following from Eq. (10.17). In this case the values of the coefficients are $a_0 = 0.25$; $a_1 = 0.18$; $a_2 = 0.14$; $a_i = 0.07$ at $i = 3$–8.

The tritium content in river water, as well as in the atmosphere, is varied in time and space. Long-term distribution of tritium concentrations is governed mainly by that of tritium content in precipitation. Figure 10.11 shows annual means of tritium content in precipitation over the central part of the former USSR territory and in the Moscow River water from 1958 to 1981 (Romanov 1982). The maximum tritium values in river water were observed in 1963 and are accounted by 0.25 part compared with precipitation. The decrease of HTO values in the river water was smoother than in precipitation. After 1971 the tritium level in the river and precipitation were equalising.

Weiss and Roether (1975) carried out analogous observations, starting in 1957, for Rheins River. A study in the Ottawa River, as well as in precipitation, started in 1953. Pre-thermonuclear concentrations were measured only in two tributaries of the Mississippi River near St Louis (Illinois, USA): in January 1952 it was 5.6 ± 0.6 T.U. and in August 1952 it was 1.15 ± 0.08 TU (Stewart 1965).

Figure 10.16 shows variations of tritium content in the Colorado, News, Arkansas, and Potomac rivers during 1963–1964 according to USGS data (Stewart 1965). One can see in the figure that the tritium peak of 1963 is presented in precipitation (1) and in waters of all the rivers (2). The tritium peak in rivers appears with an average delay ranging from several days or even hours for the mountain regions (Fig. 10.16a) to a year or even more for the plain regions (Fig. 10.16b), depending on the geological and geographical conditions of their recharge. The traveltime taken by a tracer to move from the catchment area to the river bed is an important parameter, characterising drainage properties and the capacity of a basin. This parameter and also the general character of tritium variations in the river water

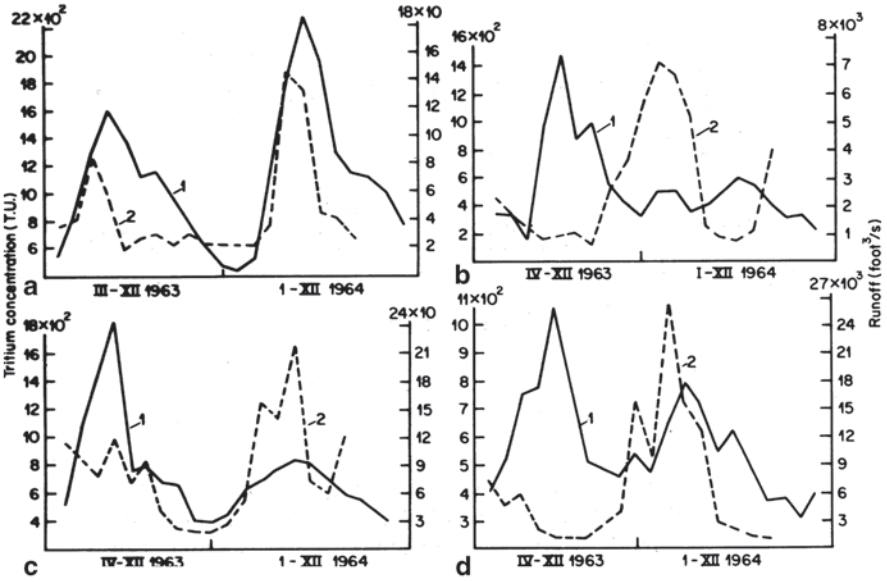

Fig. 10.16 Variation of tritium concentrations in precipitation (*1*) and in river water (*2*) of Colorado (**a**), News (**b**), Arkansas (**c**), and Potomac (**d**). (Stewart 1965; Ferronsky and Polyakov 2012)

and precipitation over time, permits estimations of the residence time of tritium in the drainage to be gained.

The seasonal variations in tritium concentration are markedly lower than in precipitation. The minimum tritium values are observed in the flood period, when the river recharge is mainly provided by melted winter snow, where tritium concentrations are 1.5–2 times lower than the mean annual (Romanov 1982].

After the flood passes, the rivers are recharged by the groundwaters of the catchment, where tritium accumulates by the previous fallouts in precipitation. Such a result was obtained in the Upper Angara River in autumn 1973, where after precipitation with about 250 TU of tritium content the river water activity contained about 350 TU (Romanov 1982].

The seasonal, annual and long-term variation of tritium concentration has been successfully used by many researchers for calculation of hydrographs in different river basins, for determination of residence time of water and water exchange time. For example, Brown (1970), using a box model, found for the Ottawa River that about 75% of the river volume of water represents the surface runoff with a mean residence time of about one year and the volume rest of about 25% is the underground runoff that has a residence time of about 6 years.

Weiss and Roether (1975), on the basis of tritium concentrations in the Rheins River water and precipitation during 1961–1973 and by appropriate modelling, discovered three components in the surface runoff separated. It was found that 25% of the runoff has a value of residence time less than one year, 35% has 5 years and 40% do not involve tritium at all. It seems that was old groundwater.

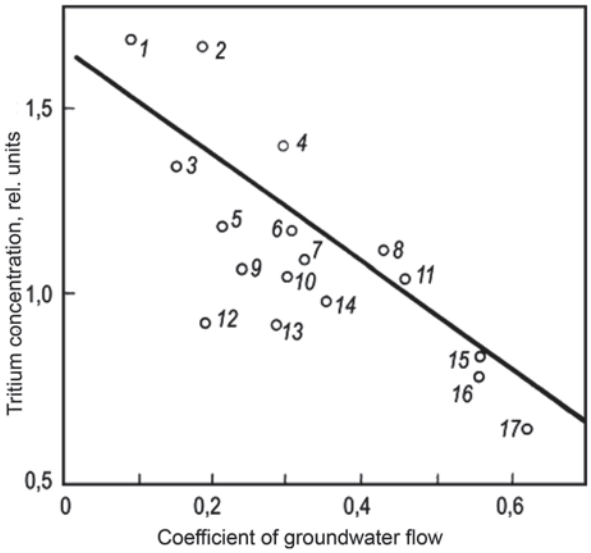

Fig. 10.17 Dependence on tritium concentration in river water from the coefficient of the underground water runoff for the rivers: Indigirka (*1*), Kolima (*2*), Amur (*3*), Lower Tunguzka(*4*), Lena (*5*), Enisey (*6*), Onega (*7*), Dnepr (*8*), Moscow (*9*) Kama (*10*), Upper Angara (*11*), Pechora (*12*), Southern Bug (*13*), Western Dvina (*14*), Ural (*15*), Don (*16*), Oka (*17*). (Ferronsky and Polyakov 2012)

The values of the runoff coefficients of tritiated water are equal to the ratio of the tritium value discharged by the river to the sea and the amount of isotope that fell out with precipitation over the catchment. The runoff coefficient is always equal to the runoff coefficient of the water but sometimes is rather different from it. An attempt was undertaken to compare the ratio of these values and also with the ratio of the annual mean value of tritium concentration and the coefficient of the underground runoff. Figure 10.17 shows the dependence of this value (relative to tritium concentration) on the underground runoff coefficient for the Russian rivers where the values were taken from the work of Domanitsky (1971)

The relationship between these values may be expressed by the regression equation in the form $C_r/C_p = 1.4K_n + 1.65$, where C_r and C_p are the tritium concentration in the river water and precipitation over the catchment area of a corresponding river; K_n is the coefficient of the underground water runoff of the river basin. The correlation coefficient of the regression equation is $r = -0.762$.

The geographical distribution of the relative tritium concentration in river water, for the European part of the former USSR territory, is characterised by a lower or close to unit value. At the same time, for the Siberian and Far East regions this value is within 1.05–1.69 and is increased towards the east. This tendency is well expressed for the northern rivers (Fig. 10.18). The relative tritium concentrations in waters of the north rivers located between Northern Dvina and Kolyma are

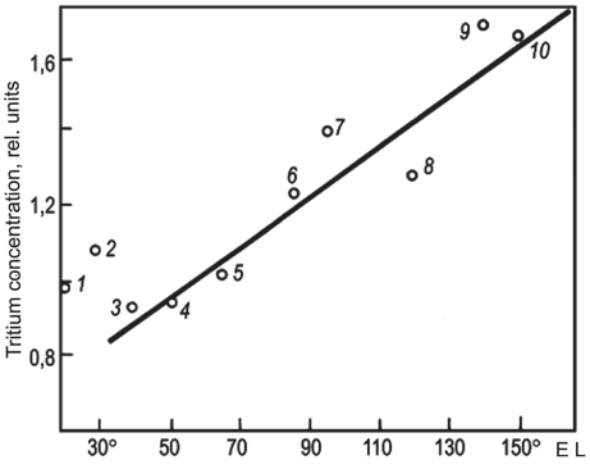

Fig. 10.18 Variation of relative tritium concentration in river waters depending on their longitude: Western Dvina (*1*), Onega (*2*), North Dvina (*3*), Pechora (*4*), Ob (*5*), Evisey (*6*), Lower Tunguzka (*7*), Lena (*8*), Indigirka (*9*), Kolima (*10*). (Ferronsky and Polyakov 2012)

described by the regression equation $C_r/C_p = 7.15 \cdot 10^{-3}\lambda + 0.56$ where the correlation coefficient $r = -0.95$ (λ is the degree of the eastern longitude)

The space distribution of the relative tritium concentration in river waters can be explained by the groundwater discharge where its value is lower. In the case when the relative concentration is higher than the modern precipitation water displaces the groundwater with lower tritium content.

There are experimental data that permit to assess tritium concentrations in groundwaters that take part in the river recharge by use of the equation of isotope balance, such as $C_r = C_p\,(1 - K_п) + C_п K_п$, where $C_п$ is the tritium concentration in groundwaters. Some results of the corresponding calculations are in Table 10.14.

The calculated tritium concentrations in groundwaters are very high and correspond to its content in precipitation fallout 10–15 years ago. In this regards, it is interesting to note that the appropriate groundwater tritium measurements in Yakutiya, carried out earlier, show similar high tritium concentrations (Afanasenko et al. 1973). At the same time, the tritium content in groundwaters of the European part of the former USSR, by multiple studies, very seldom overtopped its value in precipitation (Romanov 1982).

The attempts in finding a relationship between tritium content in river waters and some other hydrological parameters have failed.

From the general picture of space distribution in tritium concentration in river waters the data for Svir, Neva and Angara are of special interest. This is because water of the above rivers represents mainly runoff from large lakes like Onega, Ladoga, and Baykal where formation of isotopic composition is defined by some other conditions.

Table 10.14 Tritium concentrations in groundwaters taking part in river recharge)

River	Tritium concentration in groundwater (TE)	C_r/C_p
Pechora	68	0.65
Onega	101	1.28
Western Dvina	65	0.96
Dniester	93	1.29
Yuzhny Bug	55	0.75
Don	53	0.66
Oka	34	0.44
Moscow	83	1.26
Kama	117	1.17
Ural	78	0.71
Yenisey	193	1.61
Upper Angara	154	1.12
Lower Tunguska	309	2.,38
Lena	364	2.35
Kolyma	325	4.64
Amur	502	3.24

10.5.2 Tritium in Lakes and Reservoirs

While studying water exchange in lakes and water reservoirs with the help of a tritium tracer, a number of peculiarities should be taken into account that affect the tritium distribution patterns in them. Among them are the regime of the recharge, the ratio of the catchment area and that of the reservoir itself, the existence or absence of runoff, the temperature regime and many others. All these peculiarities determine whether a reservoir has a steady-state thermocline or a seasonal one, characterised by a complete mixing of water during cold times. Saline and some tropical reservoirs are of the first type. The majority of other lakes correspond to the second type. For the latter the balance equations of water and tritium under a study regime can be written in the form:

$$\frac{dV}{dt} = \sum_{i=1}^{n} R_i + P - E \pm U - A, \tag{10.23}$$

where dV is the lake volume change; R_i is the river runoff; P is the precipitation; E is the evaporation; U is the groundwater discharge; A is the surface runoff from the lake.

At a steady-state regime ($dV/dt = 0$), then the equation of tritium balance is written as:

$$\frac{d(CV)}{dt} = \sum_{i=1}^{n} C_i R_i + PC_p - EC_p - M(C - C) - \lambda CV - AC \pm UC_U. \tag{10.24}$$

Here C, $C_{i,}$ and C_p are the tritium concentrations in the lake water, river runoff and precipitation; M is the rate of the turbulent exchange between the atmospheric moisture and the surface water of the lake (Östlund and Berry 1970); C_U is tritium concentration in the groundwater discharge; λ is the tritium decay constant.

Omitting the value $\pm U = 0$ due to small groundwater tritium discharge in Eqs. (10.23) and (10.24), one obtains:

$$\frac{dC}{dt} = \bar{C}_i \bar{R}_i + PC_p - \bar{R}C + PC - M\left(C_p - C\right) - \lambda CV, \tag{10.25}$$

where

$$\bar{R} = \sum_{i=1}^{n} R_i; \quad \bar{C}_i = \sum_{i=1}^{n} C_i A_i.$$

Introducing the relative balance components $\bar{r} = \bar{R} / V$; $p = P/V$; $m = M/V$, we obtain the first-order differential equation:

$$\frac{dC}{dt} + C(\bar{r} - p - m - \lambda) = \bar{C}_i \bar{r} + C_p P. \tag{10.26}$$

In integral form, the last equation becomes:

$$C = \exp\left[-\left(\bar{r} - p - m - \lambda\right)t\right] \int_0^t \left(\bar{C}_i \bar{r} + C_p p\right) \exp\left[-\left(\bar{r} - p - m - \lambda\right)t\right] dt + \text{const}. \tag{10.27}$$

The solution of Eq. (10.27) can be obtained by the summation of the integrand if the variables $\bar{C}_i \bar{r}$ and $C_p p$ are written in the form of a histogram.

The estimation of the water cycle time in Baikal Lake, the largest in the world, carried out on the basis of the analysis of tritium patterns in the lake water, influents and precipitation, showed that this problem can be treated with the help of the box model. Using the balance method and corresponding experimental data on the tritium content in the water sources, it was shown that complete water exchange in this lake lasts 330 year, whereas that in the river basins is 2–3 year (Romanov et al. 1979). These results are in good agreement with hydrological estimations (Afanasyev 1960).

Table 10.15 demonstrates the main hydrological characteristics and the data on tritium concentrations in lake waters of the former USSR territory. In order to exclude the influence of geographic differences on tritium content in precipitation over the lake and river catchment areas, the value of relative tritium concentration is used. This value is equal to the ratio of tritium concentration in water and that over the catchment is of the lake or river. This value is used for comparison with the value of time exchange of the lake or river water (see Table 10.15).

Table10.15 Tritium concentrations and some hydrological characteristics for the lakes of the former USSR territory (1979–1980)

Lake, reservoir	Water volume (km^3)	Annual recharge (km^3/year)	Tritium concentration		Water exchange time (year)	C_i/C_p
			Lake C_i (TU)	Precipitation C_p (TU)		
Ladoga	908	79.8	122	66	11.4	1.85
Onega	295	13.6	138	67	21.6	2.06
Sevan	58.5	1.26	80	64	44	1.26
Issyk-Kul	1730	5.25	35.5	115	330	0.31
Baykal	23000	70.2	40	128	330	0.31
Valday	0.55	0.044	110	62	12.5	1.78
Aral	1023	60.3	217	100	17	2.17
Ribinsk reservoir	25.4	36	86	76	0.71	1.13

The results of a tritium study of lakes on the former USSR territory are shown in Fig. 10.19. Here the maximum relative tritium concentrations in reservoirs were found with the water exchange time of about 17 year (the Aral Sea and Onega Lake). It is interesting to note that 17 year before the lake water was sampled the maximum fallout took place.

The box model can be applied to treatment of experimental data for open water reservoirs. The conditions for such a treatment are as follows: first, equality of the mean value tritium concentration in the system itself and in the discharged water and second, constancy of the volume of the reservoir in time. In fact, the reservoirs with a constant water level and with well mixed water satisfy these conditions.

The box model has been used in calculation of water exchange time for river basins, lakes and reservoirs by many authors (Brown and Grummit 1956; Begemann and Libby 1957; Romanov 1978).

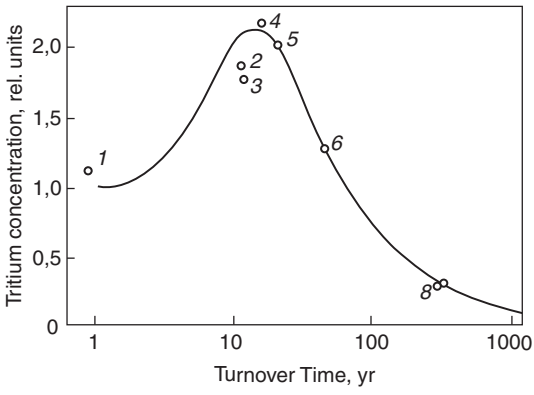

Fig. 10.19 Dependence of relative tritium concentration on the water exchange time for: Ribinsk Reservoir (*1*); lakes Ladoga (*2*); Valday (*3*); Aral (*4*); Onega (*5*); Sevan (*6*); Issyk-Kul (*7*); Baykal (*8*). (Ferronsky and Polyakov 2012)

10.6 Tritium in Groundwaters

The main source of tritium in groundwaters is precipitation water. But, as pointed out by Andrews and Kay (1982), some amount of tritium is created by the nuclear reaction (n, α) on nuclei of ^{6}Li in aquifers, especially those represented by acid rocks. The source of neutrons, in this case, is spontaneous natural uranium and thorium decay. By Andrews and Kay calculations, the above reactions in pore groundwater produce tritium concentrations up to 2.5 TU, which can be reached in a granite massif.

The shortest transition time of precipitation and surface water into groundwaters is observed in the case of a direct hydraulic connection between them, which occurs in the regions of tectonic fractures, fissures and karstic rocks and gravel-pebble sediments. The tritium half-life, equal to 12.43 year, is very often less than the groundwater exchange time. Therefore, the tritium radioactive decay is a significant factor decreasing its concentration. The intensive exploitation of groundwater for economic purposes is accompanied with development of depression funnels and washing of the rocks, intensifying the degree of relationship between the surface and groundwaters and affecting their tritium content.

In recent years, when the natural tritium content was disturbed by injection into the atmosphere of large amounts of bomb-tritium, the possibilities of the absolute dating of groundwater with the help of tritium were lost. At the same time the wide-scale investigations of tritium falls in precipitation on a global scale allow us to use the obtained data for studying the motion of groundwater from a somewhat different viewpoint.

Tritium was released into the atmosphere during the decade of nuclear weapon tests occurred in the form of individual pulses, which correspond to a single powerful or a series of moderate explosions. The tritium falls during the test period and during the subsequent period of time, mirrors its injection into the atmosphere in the form of individual pulses differing in magnitude over the yearly cycle. The knowledge of atmospheric water patterns in the underground part of the hydrosphere together with tritium dating information provides the basis for the solution of different time-dependent problems while studying groundwater dynamics

The study of problems dealing with the transition of tritium ‘marks’ in groundwater over time is based on systematic measurements of tritium concentrations in the precipitation of a studied region. The occurrence of tritium in groundwaters depends on their recharge conditions.

The most typical case of recharge of tritium from a surface aquifer is percolation of surface water through the unsaturated zone. Here, as a rule, the spring-summer component of the annual precipitation, containing the maximum tritium concentration, does not reach the aquifer. This portion of annual precipitation is lost mainly through evaporation-transpiration and partly by surface reservoir recharge. Some portion of the groundwater storage is similarly lost. During the autumn-winter period and in early spring, when tritium content in precipitation is minimal, the evaporation and transpiration of precipitation water is also reduced. During this period groundwaters are replenished. Thus, in this case tritium

concentrations in groundwaters are lower than the annual average concentration in precipitation.

Seasonal variations in tritium concentration have been observed (Andersen and Sevel 1974). The delay time of the peak annual concentrations ranges within about 1–3 months and the peak itself compared with the tritium peak in precipitation is considerably smoothed. The tritium concentrations in water of an unsaturated zone change in depth. Sometimes, the concentration maximum, which corresponds to the infiltrating precipitation of the peak fallout on a definite depth, was observed. This depth was dependent on the filtration properties of the soil of the unsaturated zone (Andersen and Sevel 1974; Atakan et al. 1974; Morkovkina 1978). Such a tritium distribution for determination of the infiltrated water velocity in the unsaturated zone was used.

According to experimental data of Münnich and Roether (1967) and Atakan et al. (1974), who carried out their studies on the alluvial plain of the Rhine River, bomb-tritium dating of shallow groundwaters can be used with a sufficient accuracy if the unsaturated soils and the aquifer itself are homogeneous in composition and properties. The tritium change in depth profiles over time, in an unsaturated zone composed of loess-loam soil and in an unconfined aquifer consisting of fine to medium-size and coarse sand, was studied by the authors. According to the tritium dating techniques, the average recharge rate of groundwaters in the fine to coarse sand material is 200 mm/year, which is in good agreement with that measured on the basis of routine hydrologic techniques.

By tritium distribution in time, the mean residence time of water is determined in the aquifer. Taking into account that aquifer water is drained by rivers then the portion of groundwater discharge to rivers can be calculated (Brown 1970). Or, if this value by some other method is obtained, then by balance relations the mean tritium concentrations discharged to the river are obtained. An attempt was undertaken to obtain these values for the large northern river basins of the former USSR (Romanov 1982). The results of these calculations, presented in the previous paragraph, show that tritium concentration in the groundwaters is increased from west to east of the basin location. And also, for rivers, located to the east behind Ural, their concentration is higher than in modern precipitation. This is because of the continental maximum over the catchment area and possibly due to the permafrost affect of the Siberian surface rocks, where safe tritium concentrations accumulated in the period of maximum fallout during 1962–1966. This idea is proved by the observational data of tritium in groundwater, rivers and precipitation obtained in Yakutia (Table 10.16).

The aquifers of fractured and karstic rocks have intensive recharge from precipitation. In this case there are good conditions for infiltration of water and restrictions for its evaporation. Here irregular distribution of tritium concentrations, due to the existence of a number of hydrologic subsystems or different ways of water transit, is observed.

Devis (1970) studied groundwaters in non-carbonate fractured rocks on the volcanic island CheYu in South Korea. Substantial variations in tritium content, discovered there, allow the mean residence time of the water in the range of 1–8 year

Table 10.16 Tritium content in natural waters of Yakutia. (Afanasenko et al. 1973)

Object	Tritium concentration (TU)
Water from a spring of Upper Nekharan	860
Water from a spring of Yust Nekharan	523
Water from the river mouth Nekharan	382
Snow	252
Precipitation	337

to be found. This is the normal 'age' for groundwaters. A similar study was done in Aragatz Mountain in Armenia by Vlasova and Brezgunov (1978). The transit time for precipitation between the points of recharge and discharge in the summer time was found to be 2–3 months and in the cold period is 7–8 months.

The tritium concentrations in such waters are, as a rule, high and close to precipitation. For example, high tritium concentrations in karstic waters with substantial seasonal variation were found in Southern Turkey (Dinçer and Payne 1971).

A number of researchers have found a good relationship between karstic and surface waters. The velocity of water movement in karstic rocks was found to be from several to hundreds of metres per hour (Fontes 1976).

The anthropogenic activity influence on the groundwater exchange rate is a problem of special interest. For example, concentration of tritium in water of the Middle Carboniferous rocks in the Moscow artesian basin, whose groundwaters have been intensively exploited, in 1978 was equal in average to about 50 TU. At the same time, in marginal parts of the basin, which are closer to the recharge area, the values very seldom exceed 10 TU (Zlobina et al. 1980). This shows that anthropogenic activity may lead to substantial disturbance of the natural circulation of groundwater.

Detailed studies of groundwater motion in saturated and unsaturated zones have been carried out by a number of researchers (Münnich et al. 1967; Andersen and Sevil 1974; Atakan et al. 1974; Allison and Hughes 1974; Verhagen et al. 1979; Morkovkina 1979).

10.7 Dating by Tritium

In view of the interpretation of isotope data and the solution of different problems elucidating groundwater dynamics, different models are widely used. The mathematical ground for the construction of these models is the balance equation of water masses and isotope tracers, together with the water dynamics in the system under investigation. Let us now consider some of the hydrological models.

One of the common problems in groundwater studies is the estimation of the residence (exchange) time of water in a hydrological system, or, as sometimes proposed, the age of the water. Several models applicable for the interpretation of experimental results have been suggested involving tritium tracers for determination of the age of groundwater (Nir 1964; Maloszewski and Zuber 1996).

10.7.1 Piston Flow Model

This model is based on the assumption that portions of water coming into the system follow each other along the flow and do not intermix. The model underestimates the residence time in hydrological systems since water mixing does occur in nature. But it is useful for estimations of the minimal residence time in a system.

According to this model the concentration of radioactive isotope C at a sampling point located a distance x_0 from the recharge zone is defined as:

$$C = C_0 \exp(-x_0/vT) = C_0 \exp(-t/T), \tag{10.28}$$

where C_0 is the concentration of radioactive isotope in recharge water; v is the rate of groundwater motion; T is the lifetime of an isotope ($T = T_{1/2}/\ln 2$).

Introducing a dimensionless parameter $k = t/T$, one obtains:

$$C/C_0 = \exp(-k). \tag{10.29}$$

Thus, the residence time of water from the recharge region of a basin to the sampling point is determined by the ratio C/C_0. Equation (10.28) can be readily transformed into one that corresponds to the common exponential law of radioactive decay:

$$C = C_0 \exp(-\lambda t), \tag{10.30}$$

where t is the age of the water, λ is the decay constant of an isotope $\lambda = 1/T = \ln 2/T_{1/2}$.

Therefore, the age of water at a sampling point for the piston flow model is:

$$t = \frac{T_{1/2}}{\ln 2} \ln \frac{C_0}{C_t} = \frac{1}{\lambda} \ln \frac{C_0}{C}. \tag{10.31}$$

In the framework of this model it has been admitted that C_0 is a constant and that intermixing of waters of different ages does not occur in the system.

10.7.2 Dispersive Model

According to this model the hydrodynamic dispersion and intermixing of waters, entering the system at different times, results in a Gauss' distribution of transition times along the flow. As in the previous case, assuming the spatial distribution of an isotope tracer being dependent on one coordinate x, one has:

$$C(x_0, t) = \frac{C_0}{(4\pi Dt)^{1/2}} \exp\left[-\frac{(x_0 - vt)^2}{4Dt}\right] dx, \tag{10.32}$$

or

$$C(x_0, x) = \frac{C_0}{(4\pi D_m x)^{1/2}} \exp\left[-\frac{(x_0 - x)^2}{4D_m x}\right] dx, \tag{10.33}$$

where $D_m = D/v$ is the coefficient of hydrodynamic dispersion being characteristic for a given hydrogeological system.

Expression (10.33) represents the concentration of tracer $C(x_0,t)$ at a distance x_0 from the source of recharge. When the tracer passes the average distance $x = vt$, the amount of tracer remains unchanged in time and is equal to $C_0 dx$. The average lifetime of the tracer is T and the concentration at a point x can be estimated from the equation:

$$C(x_0, x) = \frac{C_0}{(4\pi D_m x)^{1/2}} \exp\left[-\frac{(x_0 - x)^2}{4D_m x} - \frac{x}{vT}\right] dx. \tag{10.34}$$

If the concentration of the tracer at the input of the hydrogeological system varies within time, which it does for natural isotopes, the variation of the concentration at the output will depend mostly on the input parameters of the tracer.

Let us consider a hydrological system of volume $V(t)$, having an inflow of water $a(t)$ and an outflow $q(t)$. In this case the water age t is:

$$t = V(t)/q(t).$$

For the steady hydrodynamic state the input concentration of the tracer in discrete form can be given as follows (Martinec et al. 1974):

$$C(t) = \sum_{t=0}^{\infty} p(t) C_a(\theta - t) e^{-\lambda t}, \tag{10.35}$$

where θ is the year of sampling; t is the age of the water; λ is the constant of tritium (0.056 year^{-1}).

The distribution function of the water's age $p(t)$, in a hydrogeological system, is given in fractions of annual replenishment at the output of a system at the moment of sampling.

In the case of the dispersive model the distribution function of the water's age for a semi-infinite aquifer is as follows:

$$p(t) = \frac{2}{\sqrt{\pi D t}} \exp\left[-\frac{(t - t_0)^2}{Dt}\right] - \frac{2\exp(4\pi t_0/D)}{D} \operatorname{erfc}\left(\frac{t + t_0}{\sqrt{Dt}}\right). \tag{10.36}$$

The result of the above expression depends on two parameters, having dimensions of time: $t_0 = x_0/v$ (t_0 is not equal to the average residence time of water in the system) and $D = 4D_m/v^2$, (x_0 is the coordinate of a sampling point), where D_m is the hydrodynamical dispersion. Using a radioactive isotope tracer, one should introduce into Eq. (10.36) a term to account for its decay to the moment of sampling.

Dispersive models have been used by a number of researchers for estimating the residence time of water in hydrological systems (Martinec et al. 1974; Burkhardt and Fhöhlich 1970; Zuber 1994; Maloszewsky and Zuber 1996).

10.7.3 Complete Mixing Model

According to this model, water input at different times mixes quickly. It is not possible to account for water flow lines, as has been done in previous models, only to speak of water residence time in a system obeying exponential distribution. The model, as a rule, gives higher values of the residence time in a system if the distribution function of time is expressed by a continuous function.

In the interpretation of the observed results of tritium concentration changes in the Ottawa River basin, Brown (1961) used a box model that assumes complete mixing of the meteoric and groundwater in the bed flow. In this case, at the output of a hydrological system, the relative fraction of water of a certain age is expressed as an exponential dependency of the form:

$$p(t) = (1/\tau)\exp(-t/\tau), \tag{10.37}$$

where τ is the average value of residence time of water in a system; $1/\tau = \varepsilon$is the water exchange rate, i.e., the ratio of the total annual inflow of water to the volume of the basin.

Due to the function of water distribution (10.37), this model in literature is often called 'the exponential model'.

The distribution of tritium concentration in water at the output of the system, in discrete form and in accordance with Eq. (10.35), is:

$$C(t) = \sum_{1953}^{\theta} \alpha C_a(\theta - t)p(t)e^{-\lambda t}. \tag{10.38}$$

where α is the statistical distribution of the input function, determined as a function of the seasonal precipitation, participating in the recharge of a system compared with the annual amount of precipitation.

During the pre-thermonuclear era when $C_a = \text{const}$ we have expression (10.13) and when $C_a \neq \text{const}$ we have expression (10.17).

In practice it is not always convenient to estimate $C(t)$ by a method of successive approximations. Expression (10.38) can be simplified by letting $e^{-1/\tau} = \kappa$. In this instance, at $1/\tau << 1$, expanding the function $\kappa = e^{-1/\tau}$ in a power series of $1/\tau$, one obtains:

$$K = 1 - \frac{1}{\tau}, \tag{10.39}$$

or

$$\tau = 1 - \frac{1}{K} \tag{10.40}$$

Substituting the last expression into the age function $p(t)$, coming into Eq. (10.38), one obtains:

$$P(t) = (1 - K)\, K^t, \ (K < 1). \tag{10.41}$$

Then, taking $\alpha = 1$, Eq. (10.38) becomes (Dinçer and Payne 1971):

$$C(t) = \sum_{1953}^{t=n} C_t(\theta - t)(1 - K)K^t e^{-\lambda t}. \tag{10.42}$$

Here, as a rule, the summation is carried out over all the years since the beginning of thermonuclear tests, i.e., 1953 and $C_t(\theta - t)$ is accepted as an average tritium concentration in precipitation for a corresponding year. For practical purposes, the values C_t estimated at different values of κ (0.1, 0.2, 0.3, etc.), are indicated in the plot together with the experimentally measured values of tritium in the aquifer. Then, comparing the theoretical and experimental curves, the most probable value of the averaged residence time of water in a basin is determined.

The complete mixing model was used for estimating the residence time of groundwater in the karstic region of the Anatolian coast in Turkey (Dinçer and Payne 1971), for studying aquifers sited near Vladimir (Polyakov and Seletsky 1978), for studying the groundwater discharge characteristics of the Aragatz Mountain region (Vlasova et al. 1978) and for studying the water dynamics in the Moscow artesian basin (Zlobina et al. 1980).

It should also be pointed out that the age distribution of water, described by Eq. (10.37), does not always imply the existence of an underground or surface reservoir with good mixing. This model is also advantageous for studying aquifers drained by the aquifer thickness.

10.7.4 Symmetrical Binominal Age Distribution Model

According to this model the probability of the appearance of water characterised by an age t at the output of the hydrogeological system has the form (Martinec et al. 1974):

$$p(t) = \frac{1}{2N}\left(\frac{N}{t}\right), \quad t = 0, 1, 2, 3 \ldots \tag{10.43}$$

The parameter N in this case is dependent upon the mean residence time of water in the hydrogeological system and is given in the form: $N = 2\tau - 1$ or $\tau = (N + 1)/2$.

The numerical coefficient N/t represents the binominal coefficient defined by the binominal theorem:

$$(a+b)^N = \left(\frac{N}{O}\right)a^N + \left(\frac{N}{1}\right)a^{N-1}b + \left(\frac{N}{2}\right)a^{N-2}b^2 + \ldots + \left(\frac{N}{N-1}\right)ab^{N-1} + \left(\frac{N}{N}\right)b^N.$$

The following properties of this expansion are known: $N/0 = N/N = 1$ and the sum of all the binomial coefficients is equal to 2^N. Therefore, it is evident from the discrete binomial distribution that in the case of the continuous variation of the parameter t a normal distribution culminates with dispersion and average residence time depending upon the parameter N.

Figure 10.20 indicates some models of age distribution corresponding to the groundwater basin of the Dischma River (Switzerland).

10.7.5 Model of Mixing Waters of Different Ages

This model accounts for the case when discrete differences in the distribution of residence times are observed. For example, young waters in an aquifer may mix with very old waters. If the volume of the whole system is V and the volume of an individual constituent is V_i, then their relative contribution is:

$$p_i = \frac{V_i}{V}, \tag{10.44}$$

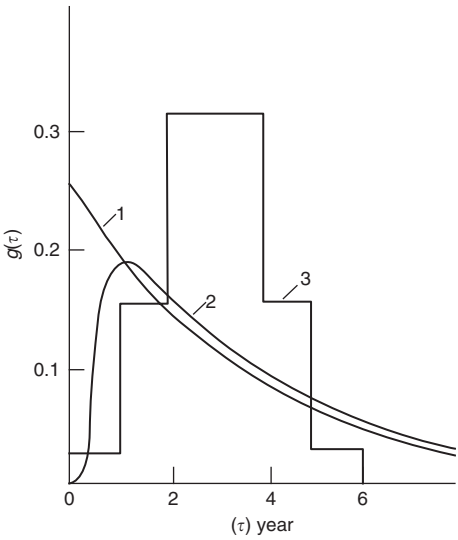

Fig. 10.20 Models of age distribution for the groundwater basin of the Dischma River: (*1*) experimental data, $\tau = 4$ year; (*2*) dispersive, $\tau = 4.8$ year; (*3*) binominal, $\tau = 3$ year. (After Martinec et al. 1974; Ferronsky and Polyakov 2012)

where $V = \sum V_i$ and $\sum p_i = 1$.

If the true age of an individual component is t_i, then the age of a mixture is:

$$t_\Sigma = \sum p_i t_i = \overline{t}, \tag{10.45}$$

where $\overline{t}$ is the mean weighted age.

If the initial concentration of each constituent is C_{0I}, then at the moment of mixing its concentration is:

$$C_i(t_i) = C_{0i} e^{-\lambda t}. \tag{10.46}$$

After mixing in a system its concentration becomes:

$$C = \sum p_i C_i = \tau = \sum p_i C_{0i} e^{-\lambda t}.$$

While estimating the age of a water mixture, e.g., using the piston flow model, the formal application of expression (10.28) gives the age:

$$t' = \frac{1}{\lambda} \ln \frac{C_0}{C} = \frac{1}{\lambda} \ln \left[\sum p_i \exp\left(-\lambda t_i\right) \right]^{-1}. \tag{10.47}$$

Comparing expressions (10.45) and (10.47) we find that actually $t' \neq \overline{t}$. Therefore, it follows that the true age of a mixture of waters of different ages is equal to the average age of its components. Further, the isotope age of the water mixture does not normally equal the true age and its theoretical value has nothing in common with that for a real system in the framework of the piston flow model. In principle, the problem of the mixing of waters of different ages can only be solved while taking into consideration the behaviour of several radioisotopes and counting out the time from the moment the waters become mixed. In this way the problem is reduced to the solution of the system of equations:

$$C_k = \sum^{m} p_i C_{0ik} \exp\left(-\lambda K t\right), \ \sum^{m} p_i = 1, \tag{10.48}$$

where C_{0ik} is the concentration of the κth isotope on the ith constituent of a mixture at $t = 0$; p_i is the contribution of the ith constituent; λ_k is the decay constant of the κth isotope; t is the time elapsed since the moment of mixing; m is the number of constituents in a water mixture.

Using the stable isotopes only, i.e., those for $\lambda_k = \infty$, system (10.48) is reduced to that describing simple mixing. For more details the reader is referred to Ferronsky et al. (1977); IAEA (1996).

10.7.6 Complicated Model

Such a model is indicative of most natural systems. In this model the output function of a system of one type becomes the input function of a system of another type. For example, the groundwater basin with a normal distribution of transition times is connected to a basin characterised by complete mixing and so on. Studies of the complicated systems, involving tritium and another tracer, require a detailed knowledge of the geology and hydrology of a basin.

Besides the above-mentioned models other combinations and varieties are used in hydrogeological studies.

A number of authors have carried out measurements of tritium concentrations in groundwater up to depths of several hundreds of metres. These studies were carried out in various hydrogeological conditions: in the Vienna basin situated near the Alps, in the hydrothermal regions of New Zealand and Iceland, in the limestone and dolomitic formations of Transvaal in South Africa and elsewhere. It was found that tritium concentrations decrease sharply with depth. Seasonal variations of tritium in the depth of an aquifer were not observed, indicating the continuous replenishment of the aquifer during the year with a constant rate of recharge. Considerable variations of tritium content exist for various boreholes located within a basin at short distances from each other, indicating the various conditions of recharge and rates of inflow. While studying geothermal regions the applicability of the techniques for the estimation of the inflow rate of surface waters to the zone of heating and their subsequent time of circulation, was demonstrated (Theodorsson 1967; Gonfiantini and Panichi 1982; Pinneker et al. 1978).

Tritium techniques are an effective instrument for the investigation of pollution problems, especially release of radio-nuclides into groundwater from nuclear power plants and atomic wastes. The last problem is relevant with active construction of nuclear power plants. In the last decade these studies have intensified (Sokolovsky et al. 2007; Polyakov and Golubkova 2007; Tokarev et al. 2005).

In 1969 Tolstikhin and Kamensky (1969) proposed the helium-tritium method of groundwater age determination. By this method water age is calculated as:

$$t = \frac{1}{\lambda} \ln\left(\frac{^3\mathrm{He}*}{^3\mathrm{H}} + 1 \right),$$

where ^{3}He* is the heliun-3 concentration in groundwater appearing after tritium decay.

It is not necessary in the determination of the input function $C_a(\theta - t)$ in Eq. (10.38). This method is used, first of all, for the study of ‘young’ groundwater (Schlosser et al. 1988, 2000; Plummer 2005).

10.8 Radiocarbon in Natural Waters

Carbon has always played an important role in geochemical processes that take place in the upper layers of the Earth and, in the first instance, in the formation of the sedimentary terrestrial layer and the evolution of the biosphere. Radioactive carbon ^{14}C is often used as a tracer of various natural processes such as the circulation of natural waters, their redistribution between natural reservoirs, water dynamics of the hydrosphere and its elements and is applicable for estimating the age of such waters. The age of geological formations and groundwater within the time scale up to 60,000 year is of a great interest for modern geology and hydrogeology. The data of radiocarbon distribution in different carbon-bearing natural objects are used for reconstruction of their paleoclimatic changes and for solving astrophysical problems related to variation in time of cosmic rays. In this chapter, the main focus is the distribution and application of radiocarbon in respect to the dynamics of natural waters.

10.8.1 Origin and Distribution of Radiocarbon in Nature

As was shown in Sect. 10.1, radiocarbon is formed in the atmosphere in the course of the interaction of secondary neutrons generated by cosmic rays, mainly with nitrogen-14, according to the reaction:

$$^{14}N + n = {}^{14}C + p + 0{,}626\ \text{МэВ}. \tag{10.49}$$

The cross-section of the reaction is 1.81 ± 0.5 barn. Table 10.17 shows the main reactions responsible for radiocarbon production in the atmosphere. But their contribution to the total ^{14}C balance comparing with the reaction (10.49) is insignificant.

The radiocarbon produced is usually oxidised to $^{14}CO_2$ after several hours in the atmosphere, which is characterised by approximately the same carbon isotopic composition and takes part in a general global circulation of carbon dioxide. The total equilibrium amount of radiocarbon on the Earth (in the atmosphere, hydrosphere and biosphere) can be theoretically estimated. According to Libby (1955) it is equal to 81 t and the estimations of Lal and other researchers gave 60–75 t, which is equivalent to an activity of about $3 \cdot 10^8$ Ci.

Despite considerable variations in the secondary neutron flux from the equator to the poles, which differs by a factor of 3.5, the ^{14}C isotope is sufficiently homogeneously distributed on the Earth. This effect was well studied by artificial bomb-radiocarbon that evidences the high rate of mixing of the atmosphere. Experimental data show that variations with latitude and altitude do not exceed 3–5 %.

Some amount of ^{14}C can be received on the Earth together with meteoritic matter, where it is produced by interaction with cosmic rays. Lunar soil and rock studies have shown that the carbon content in the sample No 14163 is 109 ± 12 g/t

Table 10.17 Reactions of radiocarbon production in the atmosphere by secondary neutrons action

Reaction	Reaction energy (MeV) +, exothermic; −, endothermic	Abundance relative ^{14}N	Relative rate production in the atmosphere
$^{13}C\ (n, \gamma)\ ^{14}C$	+8.17	$0.23 \cdot 10^{-5}$	$1.1 \cdot 10^{-9}$
$^{14}N\ (n, p)\ ^{14}C$	+0.626	1.0	1.0
$^{15}N\ (n, d)\ ^{14}C$	−7.98	$0.37 \cdot 10^{-2}$	$3.7 \cdot 10^{-5}$
$^{16}O\ (n, ^{3}He)\ ^{14}C$	−14.6	0.269	$2.7 \cdot 10^{-3}$
$^{17}O\ (n, \gamma)\ ^{14}C$	+1.02	$0.99 \cdot 10^{-4}$	$2.3 \cdot 10^{-5}$
$^{20}Ne, ^{21}Ne$ (split) ^{14}C	–	$0.12 \cdot 10^{-4}$	$1.2 \cdot 10^{-7}$

(109 ± 12 ppm together with a correction on the Earth's contamination (Fireman and Stoenner 1982)). The radiocarbon activity in two fractions, extracted by heating in oxygen at T = 1000 ºC, was 31.2 ± 2.0 disintegr min^{-1}/kg for the fraction of > 53 μ and 11.2 ± 2.0 disintegr min^{-1}/kg for the fraction of < 53 μ.

The above authors assumed that the values derived in this way for radiocarbon was produced by the action of solar wind. The carbon activity is approximately the same for both fractions (19.2 ± 2 and 21.0 ± 15 disintegr min^{-1}/kg). This is explained by interaction of cosmic rays with lunar rocks and direct partial production of the radiocarbon.

Studies of the dynamics of the carbon exchange between natural reservoirs, based on a ^{14}C tracer and theoretical investigations of radiocarbon redistribution between natural reservoirs (boxes) concluded their number is arbitrarily accepted from one (Gray and Damon 1970; Ralf 1972) to six (Craig 1957; Ekdahl and Keeling 1973). But the majority of works were performed using two or three box-models (Damon, 1970; Yang and Fairhall 1972; Keeling 1972).

Figure 10.21 shows the two-box model used by Sternberg and Damon (1979). In accordance with this model the radiocarbon, being produced in the upper parts of the atmosphere with the rate Q(t) atom. $cm^{-2} \cdot sec^{-1}$, is immediately moved into reservoir *A* composed of the atmosphere, biosphere and a mixing layer of the ocean. Between this reservoir and reservoir *B* of the deep ocean waters the radiocarbon exchange has rates of K_{as} and K_{sa}. Loss of radiocarbon from reservoirs A and B is due to the radioactive decay. The exchange rate K_{as}, as well as N_a and N_s, which are the total amount of carbon per 1 cm^2 of the Earth surface as well as in the reservoirs *A* and *B*, are accepted constant in time. The amount of ^{14}C atoms per 1 cm^2 in reservoirs *A* and *B* ($n_a(t)$ and $n_s(t)$ accordingly), is the function of $Q(t)$.

The two-box model can be described by two differential equations:

$$\frac{dn_a(t)}{dt} = Q(t) - K_{as} n_s(t) + K_{sa} n_s(t) - \lambda n_a(t), \tag{10.50}$$

$$\frac{dn_s(t)}{dt} = K_{as} n_a(t) - K_{sa} n_s(t) - K_{as} n_s(t) - \lambda n_s(t). \tag{10.51}$$

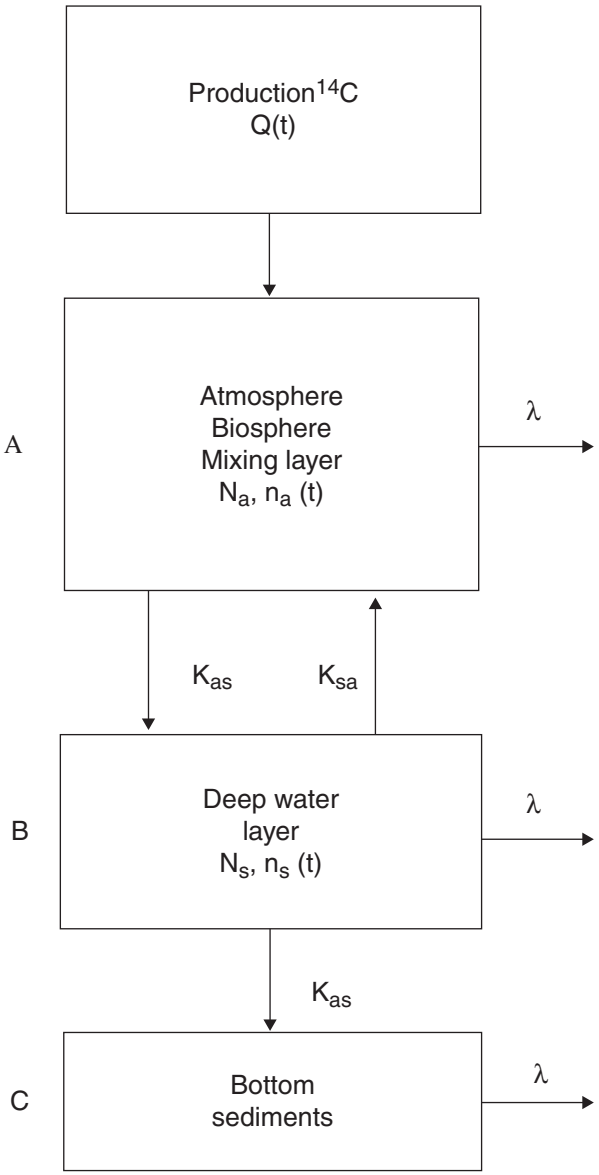

Fig. 10.21 Two-box radiocarbon exchange model. (Sternberg and Damon 1979; Ferronsky and Polyakov 2012)

Note that the reverse value of the exchange rate value is equal to the mean residence time t of radiocarbon in the reservoir. Taking into account that the specific activity of radiocarbon A_i in the ith reservoir is $\lambda n_i/N_i$, Eq. (10.50) can be written as:

$$\frac{d(\lambda n_a(t)/N_a)}{dt} = \frac{\lambda Q(t)}{N_a} - K_{as}\frac{\lambda n_a(t)}{N_a} + \frac{K_{sa}}{N_a}\lambda n_s(t) - \frac{\lambda^2 n_a(t)}{N_a}, \qquad (10.52)$$

$$\frac{dA_a(t)}{dt} = \frac{\lambda Q(t)}{N_a} - K_{as}A_a(t) + \frac{K_{sa}N_s}{N_a\left[\lambda n_s(t)/N_s\right]} - \lambda A_a(t) = \\ = \frac{\lambda Q(t)}{N_a} - K_{as}A_a(t) + \frac{K_{sa}A_s(t)N_s}{N_a} - \lambda A_s(t) \tag{10.53}$$

Analogously for the reservoir *B* one has:

$$\frac{dA_s(t)}{dt} = \frac{K_{as}A_a(t)N_a}{N_s} - K_{sa}A_s(t) - K_{as}A_s(t) - \lambda A_s(t). \tag{10.54}$$

In equilibrium conditions the process of carbon exchange between reservoirs *A* and *B* is satisfied to the equality:

$$K_{as}N_a = K_{sa}N_s \tag{10.55}$$

or

$$K_{as}/K_{sa} = N_s/N_a = \nu, \tag{10.56}$$

where *v* is the ratio of the carbon content in reservoirs *A* and *B*.

It follows from Eq. (10.56) that the carbon exchange rate is in reverse proportion to the total carbon reserve and vice versa, the residence time *t* is proportional to the carbon amount in the exchange reservoirs. The effect of carbon isotope fractionation at its redistribution between reservoirs should be taken into account while studying the parameters K_{as} and K_{sa}. As was shown by Craig (1957), the real value of the fractionation factor $\alpha_{s/a}$ is equal to about 1.012.

On the basis of experimental data, by Eqs. (10.53)–(10.56) one may calculate values of ^{14}C distribution and assess the effect of dynamics of carbon exchange between the reservoirs. For these calculations the values A_q, A_s, Q should be taken as the steady-state condition. The Q parameter, as a rule, is determined by means of the decay rate I of radiocarbon, which relates to 1 cm^2 of the Earth's surface. In the general case, I relates to $Q(t)$ by equation $I = -\lambda\int_0^\infty Q(t)e^{-\lambda t}dt$. It is obvious, if one considers that $Q(t)$ does not depend on time (which is not entirely correct), that $I=Q$. Equating the left-hand side of Eq. (10.53) to zero and replacing $K_{sa}N_s/N_a$ by K_{as}, for the stationary state condition one obtains:

$$K_{as} = \frac{\lambda(Q/N_a - A_a)}{(A_a - A_s)}, t_a = \frac{(A_a - A_s)}{\lambda(Q/N_a - A_a)}. \tag{10.57}$$

where t_a is the residence time of radiocarbon in reservoir *A*.

On the basis of experimental data Sternberg and Damon (1979) accepted the following mean values: $\overline{A}_a = 14.5$ ppm/g (C), $\overline{A}_s = 12.6$ ppm/g, $Q=I=108$ ppm/cm^{-2} and $N_a=0.361$ g (C)/cm^2. In this case the carbon residence time in reservoir

A is about 50 year. By the same theory, on the basis of more reservoir boxes, the residence time of carbon in the atmosphere exchanging with the fast mixing ocean layer can be estimated. For this case, Sternberg and Damon accepted the following parameters: $\overline{A}_a(1890) = 13.8$ ppm/g (C), $\overline{A}_{\text{П..с.}} = 0.965\overline{A}_s$ and $N_a = 0.125$ g(C)/cm^2. In this case $t \approx 5$ year. Similar estimates of the carbon residence time in the biosphere, in the fast mixing layer of the ocean and its deep layers, give mean values of 60, 10 and 1500 year correspondingly. These are the approximate results because of low accuracy in the parameters calculated. The values of carbon in a number of exchange reservoirs used for theoretical calculations are given in Table 10.18.

The possibility of ^{14}C production in nitrogen-bearing objects (in wood, for example) *in situ* by reaction with neutrons, generated by cosmic rays or occurring spontaneously in rocks at nuclear reactions, was considered.

Radnell et al. (1979) considered the possibility of radiocarbon accumulation in time in woods by thermal neutrons of cosmic origin irradiation. It was shown that in nuclear reaction with nitrogen-14 (fast neutrons) in bristlecone pine an activity of about $(1.7 \pm 0{,}6) \cdot 10^{-3}$ ppm/g (C) during 8000 year can be reached, i.e., this is only 0.03 % of natural ^{14}C radioactivity in wood of 8000 year age.

Zavelsky (1968) showed that the possibility of ^{14}C generation *in situ* is limiting the upper value of the measured radiocarbon age. According to his calculation, such a limit for a number of objects can be 80,000–100,000 year.

The theoretical specific activity of ^{14}C in modern carbon-bearing samples should be about 17 ppm/g (C) (Libby 1955). Numerous comparable studies in different regions have shown that the specific activity of ^{14}C in the biosphere varies from 14 to 16 ppm/g for inland specimens and from 13 to 17 ppm/g for ocean specimens. The average activity is 15.3 per gram of carbon. For the ocean carbonates this value averages around 16.0 ppm/g, i.e., approximately 5 % higher than for the biogenic ^{14}C. Later on these figures were refined

The major proportion of carbon, which participates in a cycle in the form of dissolved carbon dioxide, carbonates and bicarbonates (H_2CO_3–HCO_3– CO_3^{2-}), is in the oceans. If one accepts CO_2 contents in the atmosphere as $N_a = 0.62 \cdot 10^{12}$ t (C), then the ocean contains 65 N_a (C) and the biosphere 2.4 N_a (C), from which 90 %

Table 10.18 The amount of carbon in some exchange reservoirs

Reservoir	Carbon amount (g/cm^2)	
	Libby (1955)	Rubey (1964)
Ocean carbonates	7.25	6.95
Ocean dissolved organic substance	0.59	–
Biosphere	0.33	–
Living organisms and non-decomposed organic	–	0.775
substance		
Atmosphere	0.12	0.125
Total	8.29	7.85

is contained in oceanic plankton (Oeschger and Siegenthaler 1979). After death, organic substances are subjected to decomposition. Carbon is cycling through the biosphere about every 300 year. This process can be observed, for example, in biogenic ocean carbonates, the major portion of which is dissolved while precipitating on the ocean floor.

Besides that, the carbon present in the common exchangeable reservoir, which is contained in the sedimentary strata, representing its main terrestrial storage, takes part in the dissolution and admixing of cosmogenic radiocarbon. Sedimentary carbonaceous rocks are, on the one hand, being continuously formed and, on the other hand, are being constantly disintegrated. In this form of solutions and suspended particles the disintegrated rocks are carried out into the ocean. The amount of carbon contained in sedimentary rocks is estimated to be $2 \cdot 10^{22}$ g. If the process of the formation of sedimentary carbonaceous rocks has taken place over the last 3 billion year with a variable rate of formation in various epochs, then, according to different estimations, less than 3 % of the ^{14}C participates in this process at any one time.

An important question in radiocarbon dating concerns the efficiency of ^{14}C mixing in the main reservoirs over time. The homogeneity in ^{14}C distribution in a reservoir can only be attained if the mixing time is short compared with the lifetime of ^{14}C. The mixing time for the biosphere is not more than 300 year and in the atmosphere 10 year (Libby 1955). The mixing time of the Atlantic Ocean does not exceed 2000 year, that of the Mediterranean Sea is about 100 year and for the Black Sea it is about 2500 year. Another fact in agreement with the assumption of complete mixing of the ocean is the magnitude of the heat flux from the oceanic floor, which is equal to that of the terrestrial crust at 30 cal/cm^2 per year (Libby 1955). If this value is correct the absence of a heat inversion near the bottom suggests good mixing of the ocean in the framework of a radiocarbon scale of time.

The constant rate of radiocarbon production and the constancy of the amount of stable carbon in the exchangeable reservoir are of importance in the problem of radiocarbon dating. The constancy depends upon (Stuiver 1965): (a) the variation of intensity of cosmic radiation due to solar activity; (b) the variation of the magnetic dipole and field of the Earth; (c) the climate change of the Earth. Libby (1955, 1967) pointed out that considerable corrections in view of these factors should not be made since the ^{14}C lifetime is relatively small ($T_{1/2} = 5730$ year). However, in the cold periods of glacial times the stable carbon content in the ocean may drop and the specific activity of ^{14}C may increase by 5–10 %. The amount of living organic material has no effect on the specific activity of carbon (since its ratio in nature has always been small).

During the last 100 year the content of CO_2 has markedly increased in the Earth's atmosphere as a result of the industrial burning of fossil fuels (coal, oil and gas). This effect is known as 'the industrial effect' or 'Suess effect' consisting in a certain decrease (by about 3 % for the northern hemisphere) of ^{14}C (Houtermans et al. 1967; Oeschger and Siegenthaler 1979). But as a whole the natural equilibrium in ^{14}C content has settled during the last two decades due to thermonuclear explosions conducted in the atmosphere. Due to these, the ^{14}C content in the northern hemispheric atmosphere has more than doubled and become higher in the biosphere and

in the surface oceanic layer it has increased by about 20 % (Nydal et al. 1979). In wooden rings of 1963–1965 the ^{14}C increased up to 180–190 % compared with the pre-bomb level (Cain 1979).

10.8.2 Natural Variations of Radiocarbon in the Atmosphere and Biosphere

The specific activity of radiocarbon in the atmosphere and, as a consequence, in the biosphere is mainly governed by variation of the cosmic rays intensity at the Earth's surface. The natural ^{14}C variations can be divided into short-periodic ones, governed by the Sun modulation of galactic cosmic rays and long-periodic ones connected with the geomagnetic Earth's field and climate variation (Dergachev and Kocherov 1977; Sternberg and Damon 1979). Long-periodic variations of the ^{14}C level can also be effected by corpuscular radiation from super-nova flashes and possibly by occurrence of neutron flows during annihilation of meteoric matter. The last problem has a more exotic than practical meaning (Sternberg and Damon 1979). As Dergachev and Kocherov pointed out, the degree of correctness of solar activity (Wolf's numbers W) is high after 1749. Attempts were undertaken to extend the time scale up to 1610 and even to 648 BP (Dergachev and Kocherov 1977). But the correct measurements of the 11 year solar cycle by W numbers have been achieved only since 1749. Attempts have been made to check the last time of the 80 year (century) cycle but difficulty arose in connection with the short period of observations (230 year). In accordance with the calculations, the amplitude of specific ^{14}C activity for the 11 year cycle of solar activity is 5 % and for the century cycle about 1 %. Registration of the 11 year variation in the yearly wooden rings' radiocarbon content is a difficult instrumental task. Stenhouse and Baxter (1979) used two high-stability proportional counters of quartz and metallic for its solution. This allowed obtaining a relative error in the experiments equal to 6.4 ‰. In yearly oak rings over 1840–1890, he found ^{14}C peaks relating to 1851, 1869 and 1880 (at the level of about 1 %). ^{14}C fluctuations at a level of 0.3–0.4 % have not been reached and the 2–3 % variations have definitely not been found. The total ^{14}C activity from 1840 to 1890 decreased on average by 0.03 % per year. After 1890 an increase of ^{14}C concentration in the atmosphere fixing in the yearly wooden rings was observed. The radiocarbon variations in the past and changes in the solar activity during the last 300 year are considered in the work of Dergachev (1975). ^{14}C variation in atmospheric carbon dioxide during the last 1000 year is discussed by Stuiver and Quay (1981). Their results are presented in Fig. 10.22.

It follows from the experimental data that natural reservoirs of carbon do not stay in equilibrium relative to the atmospheric ^{14}C level. Before 1890, variation of the radiocarbon content resulted mainly due to solar activity changes. Since 1890, the ^{14}C activity decrease was connected mainly to dilution of the atmospheric carbon dioxide by the "dead" CO_2 coming from burning fossil fuel. But as was shown by Stuiver and Quay, ^{14}C content in atmospheric CO_2 during the 20th century is not

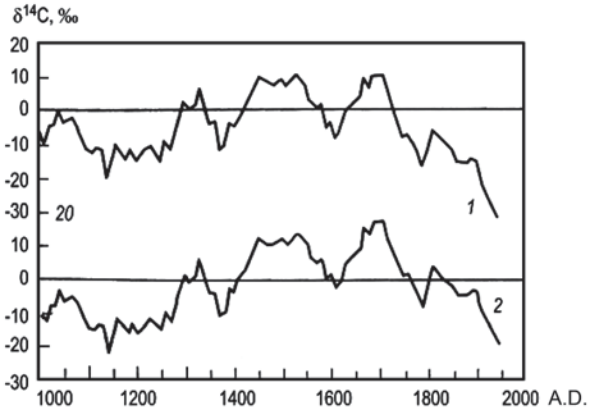

Fig. 10.22 14C variation in the atmosphere in the last 1000 year: non-corrected (*1*) and corrected on the basis of long-periodic geomagnetic field change (*2*). (Stuiver and Quay 1981; Ferronsky and Polyakov 2012)

distinguished by something specific (see Fig. 10.22, (1)). These changes are due to long-periodic variations of the geomagnetic field. If one makes a correction of ^{14}C long-periodic changes by means of a sinusoidal curve of a several thousand years period, then the ^{14}C level in atmospheric CO_2 (and biosphere) in the XX century, at least during the last thousand years, will be minimal (Fig. 10.22, (2)).

These data prove the anthropogenic influence on the increase of total carbon content in the atmospheric reservoir, which has led to a decrease in the specific activity of radiocarbon in the atmosphere, biosphere and a mixing ocean layer. By the data of Stuiver (1980), with reference to Douglas, the ^{14}C level in 1954 differed from the 'standard modern level" (0.95 activity of the NBS standard) by 24 ± 2 ‰.

The study of ^{14}C variation in time by the yearly rings of XVIII and XIX century woods is convenient because at that time the anthropogenic impact on the atmosphere was weaker, the level of solar activity (W-number) change is well known and the climate variations by the synoptic data can be restored. Currently there is a significant amount of data on ^{14}C concentration measurements in the yearly rings of woods from that time. By measurements of Stuiver (1965), over the time period from 1700 to 1870, a decrease in ^{14}C content by 2 % from 1700 to 1790 is noticed. The maximum difference in ^{14}C activity within the studied period reaches 2.8 %. It is worth noting that due to the small diameter of the rings, Stuiver measured ^{14}C activity in several rings simultaneously. In addition, the studies were performed on the ring slices of four trees from different locations of growth. This may lead to some errors depending on local conditions.

Analogous measurements on ^{14}C changes in yearly wooden rings of pines growing in Lithuania were performed by Dergachev and Kocherov (1977). Figure 10.23 shows their results of a series of measurements on 5 year rings during 1707–1859.

It is seen that the ^{14}C change curve has a sinusoidal form with amplitude of 1.5 %. The period of ^{14}C variations for the time interval from 1780 to 1840 is equal

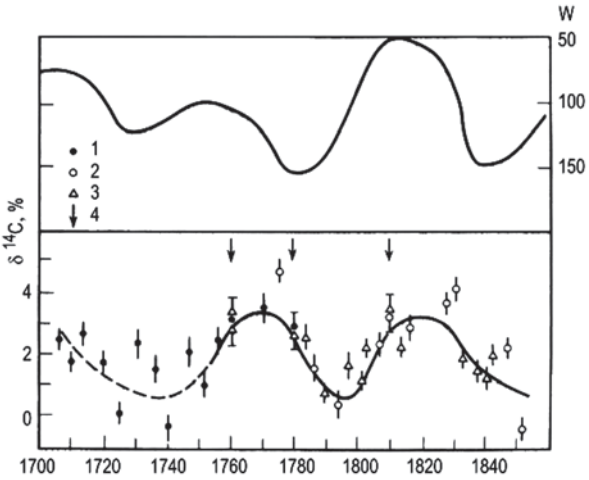

Fig. 10.23 Relationship between δ14C variations in pine rings and solar W-number during 1707–1850: (*1 and 2*) measured by proportional counter; (*3*) measured by scintillation counter; (*4*) calibration points. (Dergachev and Kocherov 1977; Ferronsky and Polyakov 2012)

to about 60 year. The curve itself shows an inverse proportionality in relationship to the solar W-numbers and radiocarbon content. The time shift, equal to about 10 year, is specified by the mean residence time of the carbon in the exchangeable reservoir (see Fig. 10.21, A) and depends on the period. The following expression of the changes rate of ^{14}C generation depending on the W-number for the considered solar activity cycle is proposed by Dergachev and Kocherov:

$$\Delta Q(W)/Q_0 = 0.4 - 0.01\ W,$$

where Q_0 is the equilibrium rate of ^{14}C generation.

Suess (1970) discovered in the yearly bristlecone pine rings a century ^{14}C variation with the period of 181 year within the time period of 7000 year (from the middle of the XX century up to 5000 year BP). The ^{14}C variation amplitude is about 2–3 % and the mean value of the ^{14}C activity is changed in time by sinusoidal law. In connection with solar activity changes and the corresponding climatic variation, it is worth noting that an ice core of 404 m length from the Greenland Camp Century Dansgaard covered the time interval from 1970 to 1200 year and by Fourier treatment $\delta^{18}O$ values equal to 78 and 181 year were derived (cited by Dergachev and Kocherov 1977). Obviously, the climatic changes result from solar activity and the 180 year period corresponds to the Suess data.

It seems the record in observation of the periodic climate changes based on solar activity and registered by isotope data belongs to Libby and Pandolfi (1979). They studied distribution of deuterium and oxygen-18 in the yearly rings of Japanese cedar (*Cryptomeria Japonica*) within the last about 1800 year and derived there eight cycles with periods of 58, 68, 90, 96, 154, 174, 204 and 272 year. The shorter cycles like 11 and 21 year were not discovered due to averaging of the measured

wooden rings within 5 years. And also the 174th cycle of the authors corresponds to the 183 year Suess period.

For the last relationship of δD and $\delta^{18}O$ in the Japanese cedar with radiocarbon in the bristlecone pine, measured by Suess for the same time intervals, Libby and Pandolfi discovered an inverse correlation. To the lower values of δD and $\delta^{18}O$ corresponds the higher ^{14}C values. These relations have the form:

$$\delta D = 0.677 \cdot {}^{14}C - 75.5(\text{SMOW}),\ r = 0 - 0.62,$$
$$\delta^{18}O = 0.0613\delta^{14}C - 22.5(\text{PDB}),\ r = 0 - 0.77.$$

The δD value was measured relative to the SMOW standard and $\delta^{18}O$ relative to the PDB standard. This relationship between stable hydrogen and oxygen-18 isotopes and the radiocarbon in wooden rings with ^{14}C amplitude of about 1% the above authors explain by climate change due to solar activity. The relationship between the rate of radiocarbon generation in the atmosphere and solar activity variation seems to have physical bases. But the problem of the influence of solar activity on galactic cosmic rays modulation and on the Earth's climate change has not been yet studied in detail. The search of cyclicity in the long and short-periodic processes has always attracted the attention of researchers. But as Gribbin and Lem (1980) pointed out, the cyclic attraction conceals in itself the risk to discover it, where there is a distribution of random values. To prove this, Gibbin demonstrated by a known graph, drawn by computer, generating random figures from 0 to 9, where deviation of the sliding average value from mathematical expectation appears to be equal to 4.5. On the graph of the random values distribution quasi-sinusoidal short-periodic fluctuations and a long-periodic 'temporal' trend are traced.

The long-periodic variation of ^{14}C content in the atmosphere and correspondingly in the biosphere was reliably fixed by the radiocarbon concentration measurement in the long-living woods. Figure 10.24, taken from work of Sternberg and Damon (1979) and drawn on the basis of results obtained by many laboratories in the world, traces sinusoidal changes in the wood ring's ^{14}C concentration during about 7500 year BP. The averaged data show that the minimal ^{14}C concentration (–5.5‰ from the level of 1890) comes approximately at 1400 year and the maximum (+85‰) at about 6500 BP.

Sternberg and Damon assumed that the observed ^{14}C variation is related to geomagnetic dipole moment changes. The relationship between the rate Q(t) of ^{14}C generation and the strength of the geomagnetic dipole moment has a reverse proportional dependence:

$$\frac{Q(t)}{Q_0} = \left(\frac{M(t)}{M_0}\right)^{-a}, \tag{10.58}$$

where Q_0 is the equilibrium rate of generation of the magnetic moment M_0; α is the coefficient changing within 0.4–0.6.

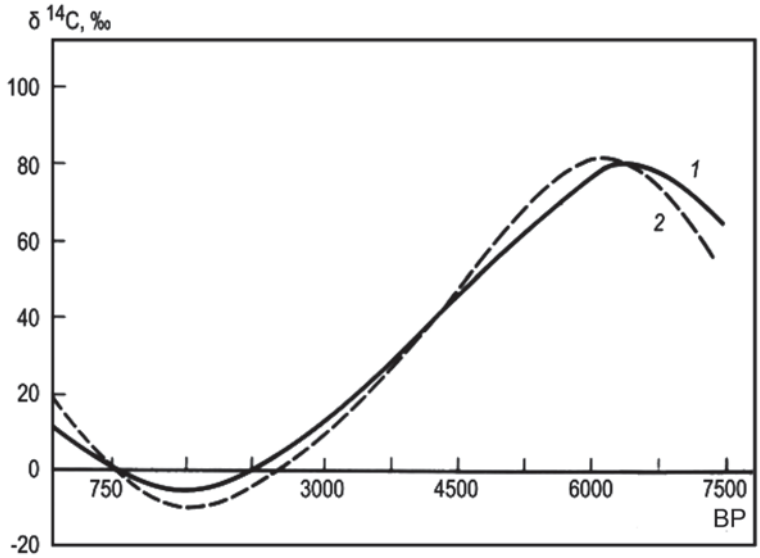

Fig. 10.24 Experimental and calculated data of 14C variation in yearly wooden rings: (*1*)experimental data approximated by a polynomial of the fourth degree; (*2*) the curve (*2*)obtained by calculation. (Sternberg and Damon 1979; Ferronsky and Polyakov 2012)

It was also found by the data of a paleomagnetic study that the magnetic dipole moment is varied in time within $(4–12) \cdot 10^{25}$ Gs · cm^3. It changes by quasi-sinusoidal law and during the last 10,000 years can be described by the equation:

$$M(t) = M_0 + M_1 \sin\omega(T - t + \theta),$$

where M_0 is the mean value of the dipole moment; M_1 is the amplitude variation; T is the period of oscillation; θ is the phase; $\omega = 2\pi/T$; t the time.

Denoting $T - t + \theta$ by t', Eq. (10.58) can be rewritten in the form:

$$Q(t) = Q_0 \left[1 + (M_1/M_0)\sin\omega t'\right]. \tag{10.59}$$

Applying the two-box model to the carbon exchanging reservoir (Fig. 10.21), Sternberg and Damon reached good accordance between the experimental and calculating data on the long-periodic variation of the radiocarbon change in the atmosphere at the following conditions: $T = 8500$ year; $M_{max} = 12.5 \cdot 10^{25}$ Gs · cm^3; $T_{Mmax} = 2500$ year; $\alpha = 0.45$; $\tau_a = 75$ year (see the residence time of carbon in a reservoir in Fig. 10.22); $K_{as} = 5 \cdot 10^{-4}$. The calculations were done by Eqs (10.53), (10.54) and (10.59). The value of ^{14}C (‰) was calculated by the equation $\delta A_a(t) = [(A_a(t) - A_0)/A_0] \cdot 1000$, where A_0 is the activity of the modern carbon standard

Figure 10.24 presents the compared experimental and calculated long-periodic changes of radiocarbon in the Earth's upper atmospheric layers. The authors note that a delay for several hundred years in the phase between the geomagnetic field

change and the radiocarbon variation in the exchange reservoirs is observed. This is due to the mean residence time of carbon in reservoir *A*, the ratio of exchanging carbon funds in *A* and *B* reservoirs and the period *T* of the geomagnetic field variation.

In addition to the astronomical and climatic factors effecting the distribution of the natural ^{14}C concentration in the atmosphere and biosphere, the dilution of atmospheric carbon dioxide by endogenic CO_2 may have an influence on local radiocarbon content changes, which is typical to the volcanic and breaking Earth's crust regions. It is suggested that in the modern volcanic regions, ^{14}C content in the biosphere is lower than the present day level. This is because of throwing out of endogenic carbon dioxide in the period of volcanic activity and CO_2 entering from the Earth's crust breaks (Sulerzhitsky and Frolov 1966; Karasev et al. 1981). On this basis Karasev et al. proposed a method of break discovery in active tectonic zones by radiocarbon measuring in plant samples. As was shown by the authors, in a break zone $\delta^{14}C = -50\,\%$ and at a distance of about 10 m $\delta^{14}C$ increases up to $+27\,\%$.

10.8.3 Natural Radiocarbon in Oceans

A number of works have been devoted to the analysis of radiocarbon in the oceanic water's carbonate system and water-bearing organic matter (Fonselius and Östlund 1959; Broecker et al. 1960; Broecker and Olson 1961; Bien et al. 1963; Fairhall and Young 1970; Fairhall 1971).

Starting in 1940–1950s, studies on ^{14}C distribution in the ocean water were difficult due to bomb-radiocarbon entering into the oceans. The artificial mark appearing in culminating tests in 1961–1962 allowed further detailed studying of the dynamics of CO_2 between the atmosphere and oceans exchange but became an obstacle for further study of ^{14}C space distribution in oceans and seas.

Radiocarbon enters into the oceans as a result of carbon exchange between dissolved marine carbonates and atmospheric CO_2. The radiocarbon entering into the surface ocean layer is rather quickly and uniformly distributed in an exchangeable layer ($h \approx 100$ m, $r \approx 10$–15 year). From there, by vortex diffusion and pelagic biogenic carbonate sedimentation, the radiocarbon enters the deep water layers, where its residence time (t), by different estimates, is equal to 1500–2000 year. As Craig (1957) noted, CO_2 exchange between the atmosphere and oceans is accompanied by isotopic effects. The mean isotopic content of stable carbon of the dissolver—hydrocarbonates of sea water—has a value of $\delta^{13}C = -7\,‰$ (here and further relative to the PDB standard). Thus, as a result of exchange processes the carbon of the hydrocarbonates becomes heavier by 7‰. Enrichment of oceanic ^{13}C can be described by means of the fractionation coefficients $\alpha_{13_C} = R_0/R_a$, where R_o and R_a are the ratio of $^{13}C/^{12}C$ in the ocean and atmosphere.

The value R can be presented as $(1 + \delta^{13}C/1000)$. Then the expression for α is rewritten as:

$$\alpha_{13_C} = \frac{1+\delta^{13}C_0/1000}{1+\delta^{13}C_a/1000}.$$

Analogously, for ^{14}C one has:

$$\alpha_{^{14}C} = \frac{1+\delta^{14}C_0/1000}{1+\delta^{14}C_a/1000} = \frac{\left(^{14}C/^{13}C\right)_0}{\left(^{14}C/^{13}C\right)_a}.$$

It is known (for example, Galimov 1968), that the fractionation constant increases by the square dependency on each additional neutron to the isotopic nucleus. Then, $\alpha_{14_c} = \alpha^2_{13_c}$. And applying the approximate equality $(1+x)^2 = 1+2x$ at $x << 1$, one obtains:

$$\alpha_{14_c} = \frac{1+\delta^{14}C_0/1000}{1+\delta^{14}C_a/1000} = \frac{1+2\delta^{13}C_0/1000}{1+2\delta^{13}C_a/1000}. \quad (10.60)$$

Using the last expression, it is possible to show that if ^{13}C of the ocean bicarbonate is enriched by 7‰, then at such enrichment ^{14}C should be equal to about 14‰. In the other words, $\varepsilon_{14_c} = 2\varepsilon_{13_c}$, where $\varepsilon_{13_c} = \delta^{13}C_0 - \delta^{13}C_a$. Later on this task is discussed in more detail.

Thus, theoretical consideration of the problem of CO_2 exchange between the atmosphere and the ocean shows that the surface oceanic water should be enriched in ^{14}C isotope by about 14‰ compared with atmospheric carbon. Analogously, it is possible to show that the biosphere should have ^{14}C in deficit by about 3% ($\delta^{13}C_a = -25$‰) compared with the atmosphere. As was shown earlier, the normalisation of ^{14}C content is provided for unification of the radiocarbon measurements (−25‰ is the normalising value for the studied samples). The formula for normalisation from Eq. (10.60) was obtained. It was pointed out by Libby (1955) that the oceanic carbonates have ^{14}C activity by 5% higher than biogenic carbon. His statement coincided with theoretical consideration of the natural exchange processes. But later studies have not proved this conclusion. In particular, it was shown that the hydrocarbons of the mixing layer in the Atlantic, Indian and Pacific oceans to the north from 40ºS have practically constant ^{14}C content close to that in the biosphere (without the isotope correction) (Fonselius and Östlund, 1959; Broecker et al. 1960; Broecker and Olson, 1961; Bien et al. 1963; Bien and Suess 1967). This fact is explained by an increase of ^{14}C content due to isotope fractionation in the exchanging processes eliminated at mixing with the deep layers.

Stuiver (1980) on the basis of works of Broecker, Östlund, Craig and other researchers, compiled a short report on ^{14}C distribution in ocean waters during the pre-bomb period. It follows from this summary that in nine surface water samples taken in the North Atlantic in 1955 $\Delta^{14}C = -49 \pm 2$‰. The data from 13 stations of the South Atlantic (to the north from 40 ºS.), sampled during 1956–1957, have slightly lower values, namely, $\Delta^{14}C = -57 \pm 2$‰. Up to that time of measurements, the decrease of the pre-industrial ^{14}C level in the surface oceanic waters was about 12‰. From this, we can accept that $\Delta^{14}C$ for the surface Atlantic waters before the intensive thermonuclear tests is equal to −40‰ from radiocarbon in the biosphere. It means that this value can be accepted as characteristic for the mixing layer over

the thermocline. In the depths from 100 to 600 m the content of radiocarbon decreases exponentially from −40 to −100 and deeper it remains constant. The value −110‰ was characteristic for the Atlantic deep layers in the pre-thermonuclear epoch. The studies of Stuiver (1980) showed that after thermonuclear tests the 'natural' distribution of radiocarbon in the Atlantic Ocean in 1970 was preserved only below 3500 m.

Significant amounts of experimental data were collected by dating of mollusk shells living in normal salinity marine water. Investigations of samples collected in the period between the middle XIX century to 1950 in near-shore areas of different oceans provide the basis for the conclusion that the radiocarbon content (without isotopic correction) in the mixing ocean layer during the pre-thermonuclear epoch was also lower than the biogenic level, determined as 0.95 activity of NBS oxalic acid. By the data of Gillespie and Polach (1979), who studied radiocarbon distribution in mollusk shells from the near-shore of oceans during 1840–1950, the conclusion follows that ^{14}C content in the mixing layer varies in natural conditions from +8 to −11% relative to the modern standard. And without taking into account the effects of fresh river water recharge and the Suess effect, the variation range is narrowing. In average, carbon is depleted by ^{14}C (without correction) by about 15‰. Correcting by 25‰ and by age, the value of $\overline{\nabla}^{14}C = -64.5$‰ (0.95 NBS). Then the "apparent age" of the shells related to the reservoir effect in the mixing layer appears to be 535 year. For the Australian shore area the mean value of $\overline{\nabla}^{14}C = -55 \pm 4$‰ (non-corrected value is ~5‰), which corresponds to the "apparent age" of 450 ± 35 year.

For the shells from the North and South American shore, taken in 1878–1940, the non-corrected value of $\delta^{14}C$ varies from +1 to −8% and the averaged value is about −3% (–30‰). The true ^{14}C value for the mixing layer in the pre-thermonuclear epoch is of great practical interest for radiocarbon dating using mollusk's shells. The ^{14}C differences in mollusk shells are hardly defined by the metabolic processes. They more likely reflect radiocarbon variations in offshore ocean layers, which affect the river runoff and discharge of the continental groundwaters. Sternberg and Damon (1979), after analyses of the great amount of collected experimental data, for theoretical calculation accepted that the mean radiocarbon activity in the mixing layer for the pre-thermonuclear epoch is equal to 0.965 with that in the biosphere in 1890 equal to 13.8 desintegrations/min · g (C).

The estimation of ^{14}C activity in different exchangeable reservoirs before 1950 can be done using the data from the work of Fairhall andYoung (1970) shown in Table 10.19.

On the basis of the above Fairhall and Young data it is possible to conclude that the ^{14}C activity of the mixing ocean layer in the pre-thermonuclear epoch should be 1% lower compared to the biosphere and about 3% than in the atmospheric CO_2. A number of researchers (for example, Oeschger and Siegenthaler 1979) in their theoretical calculations have accepted ^{14}C in the surface ocean layer before thermonuclear tests to be 95% from the atmospheric level in the middle XIX century. The carbon distribution in the deep layers, as the result of thermonuclear tests, inconsiderably changed due to the very long mean carbon residence time in this layer.

Table 10.19 Distribution of natural and thermonuclear ^{14}C at the end of 1962. (Fairhall and Young 1970)

Reservoir	Total amount of carbon (g)	^{14}C before 1950 (atom/g · 10^{10}C)	Natural ^{14}C, (atom · 10^{27})	Thermonuclear ^{14}C
Atmospheric CO_2	$6.8 \cdot 10^{17}$	6.07	41	54
Continental biosphere	$3.1 \cdot 10^{17}$	5.85	18	<1
Humus	$1.1 \cdot 10^{18}$	<5.8	<64	<1
Oceanic living biosphere	$3 \cdot 10^{15}$	6	0.2	<0.1
Oceanic non-decomposed rests	$2 \cdot 10^{16}$	6	1	<0.1
Dissolved organic matter in the oceans	$8 \cdot 10^{17}$	5.3	42	<1
Non-organic matter in the oceans				
upper 100 m	$1 \cdot 10^{18}$	5.8	58	~3
below 100 m	$3.8 \cdot 10^{18}$	5.1	1940	~1
Total	$42 \cdot 10^{18}$		2160	~60

By the data of Fairhall (1971), who summarised his own results and the results obtained during the 1958–1970 expeditions by Broecker, Bien, and Rafter before 1969 in the Atlantic, Indian and Pacific oceans, the non-disturbed picture in radiocarbon distribution below 500 m is observed and also its relative uniform distribution was fixed in the deep ocean layer. Radiocarbon comes to the deep layers from the mixing layer by vortex diffusion (Oeschger and Siegenthaler 1979) and partly due to sedimentation of mollusk shells, which dissolved in depth. By Fairhall's calculations the ^{14}C absolute concentration in ocean water before 1950 amounted to about $1.4 \cdot 10^9$ atoms per litre for the entire depth, for which the ^{14}C concentration depth gradient is equal to zero or correspondingly about 84 % of specific radiocarbon activity in the atmosphere (see Table 10.19). Using Fairfall's data, we may estimate the carbon mean residence time in the ocean deep layers. For this case, the following material balance can be used: $MdA_2/dt = q_1A_1 — q_2A_2 — MA_2\lambda$, where M is the carbon mass in the exchangeable layer; q_1 and q_2 are the carbon mass income; A_1 and A_2 are the specific carbon activities in the exchangeable and deep layers; λ the ^{14}C decay constant. In the stationary state, the left-hand side of the equation is equal to zero and $q_1 = q_2$. Taking into account that $M/q = \tau$, then one has $\tau = (A_1 - A_2)/A_2\lambda$.

Accepting that $A_1 = 0{,}965$, $A_2 = 0{,}835$ and $\lambda = 1.21 \cdot 10^{-4}$, then one obtains $\tau = 1300$ year. If $A_1 = 0.99$, which corresponds to many experimental data for the Atlantic ocean (Fairhall 1971), then $\tau \approx 1500$ year, which corresponds to Libby's (1955) estimation.

10.8.4 Technogenic Radiocarbon in the Atmosphere and Oceans

According to data obtained by different authors (Fairhall andYoung 1970), $6 \cdot 10^{28}$ atoms of ^{14}C have been released into the Earth's atmosphere during thermonuclear tests. Before the tests the ^{14}C content in the atmosphere was estimated to be $4.1 \cdot 10^{28}$ atoms and therefore the total amount of carbon atoms has increased by 2.5 times. Compared with the total equilibrium amount of the isotope on the Earth ($2.2 \cdot 10^{30}$ atoms) the bomb component amounts to 2.5 % (see Table 10.19).

On average, at a thermonuclear test $3 \cdot 10^{26}$ atoms of ^{14}C per 1 Mt are produced, which is equivalent to 7 kg of radiocarbon. By radiocarbon thrown into the atmosphere, over 200 Mt of total explosion power was performed up to 1962, which injected into the atmosphere about 1.4 t of artificial radiocarbon.

Numerous measurements (up to a thousand specimens) were carried out in order to determine ^{14}C content variations in the troposphere and stratosphere both with latitude and altitude (Fairhall andYoung 1970; Münnich and Vogel 1963; Fairhall et al. 1969; Hagemann et al. 1959). The most representative results of these studies according to the data of different authors for the troposphere CO_2 generalised from 1963 to 1966 are shown in Fig. 10.25.

There are distinct seasonal variations of ^{14}C concentrations in the northern hemisphere and a considerable latitudinal gradient of concentrations in 1963 indicated in Fig. 10.26 but the gradient quickly decreases to zero by 1967. Both of these effects are a consequence of seasonal variations in the release of bomb ^{14}C from the stratosphere into the troposphere and the longitudinal mixing that occurs in the troposphere. The most intensive release of ^{14}C into the troposphere, as in the case of tritium, is detected in spring and early summer. At the same time the most effective mixing of this isotope occurs in the longitudinal direction.

In contrast to the thermonuclear dust, which is removed as a rule quickly from the troposphere with precipitation, CO_2 has a rather long residence time in the troposphere. Therefore, the levels of bomb ^{14}C in the troposphere air were highest in the middle latitudes of the northern hemisphere and reached maximum concentrations late in the summer.

The longitudinal mixing of ^{14}C extends southwards. Annually, from September to February, the level of ^{14}C in the northern latitudes decreased and in the southern latitudes increased, up to the middle of 1966. Such a process took place until 1966 when the whole troposphere became homogeneous with respect to ^{14}C.

It has been pointed out (Fairhall and Young 1970) that the relative amounts of tropospheric air participating in the circulation at various latitudes should be taken into account when comparing the latitudinal variations of ^{14}C concentrations (Fig. 10.25). The convergence of the meridians and the decent of the tropopause at high latitudes result in a sharp decrease in the volume of tropospheric air with increasing latitudes, compared with the equatorial region. Thus, for the same ^{14}C ejection from the stratosphere its activity in high latitudes will be considerably higher than in the lower ones.

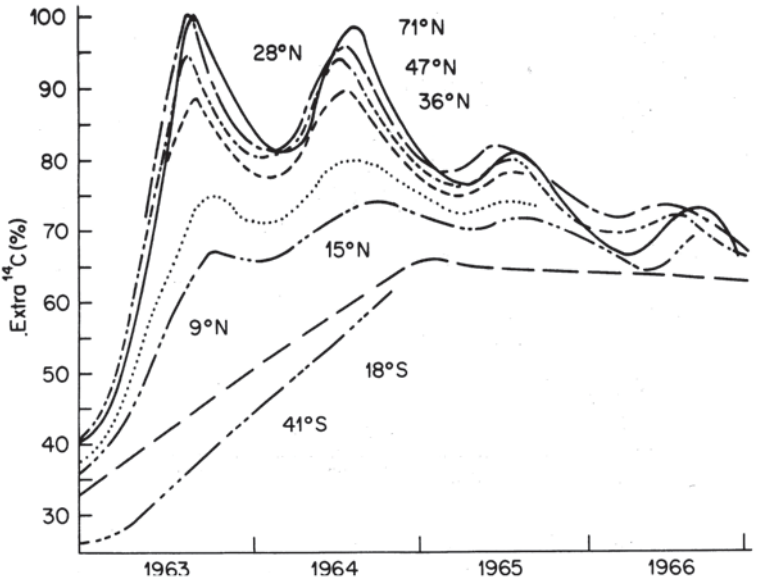

Fig. 10.25 Variation in time of ^{14}C concentrations in tropospheric CO_2. (Fairhall and Young 1970; Ferronsky and Polyakov 2012)

Figure 10.26 shows the variations with time of the absolute amounts of bomb-radiocarbon in the troposphere, stratosphere and atmosphere as a whole for the northern and southern hemispheres.

It follows from Fig. 10.26 that with the decrease in the ^{14}C concentrations in the northern hemisphere the opposite process took place in the southern hemisphere during 1963–1965. The theoretical estimation of the total amount of ^{14}C in the atmosphere based on experimental data shows that the time of half-removal of this isotope is equal to 3.3 year. In the next years the rate of ^{14}C removal from the atmosphere decreased. Its amount in the troposphere up to 1970 compared with 1963 decreased by two times and by 1977 only one third of it was left (Berger 1979). Before 1984 the ^{14}C amount in the troposphere was about 125 % with respect to the pre-thermonuclear level. The residence time of CO_2 in the troposphere calculated by decrease of ^{14}C activity during the period of 1963–1976 was about 10 year (7/0.693) and for 1970–1982 this time was about 15 year, which is close to the earlier estimates made by Arnold and Anderson (14–30 year) (Miyake 1969).

It is assumed that the rate of removal of bomb ^{14}C from the stratosphere is proportional to the difference (gradient) between its concentration in the stratosphere and the surface (mixing) ocean layer. While decreasing the gradient, the velocity of the radiocarbon removal from the troposphere is dropping. On this basis, the conclusion follows that during the 'peak' injections of radiocarbon (and tritium as well) into the atmosphere, the ^{14}C concentration changes, between the atmosphere and hydrosphere, take place in $^{14}CO_2$ but not in general CO_2. The sharp drop of ^{14}C

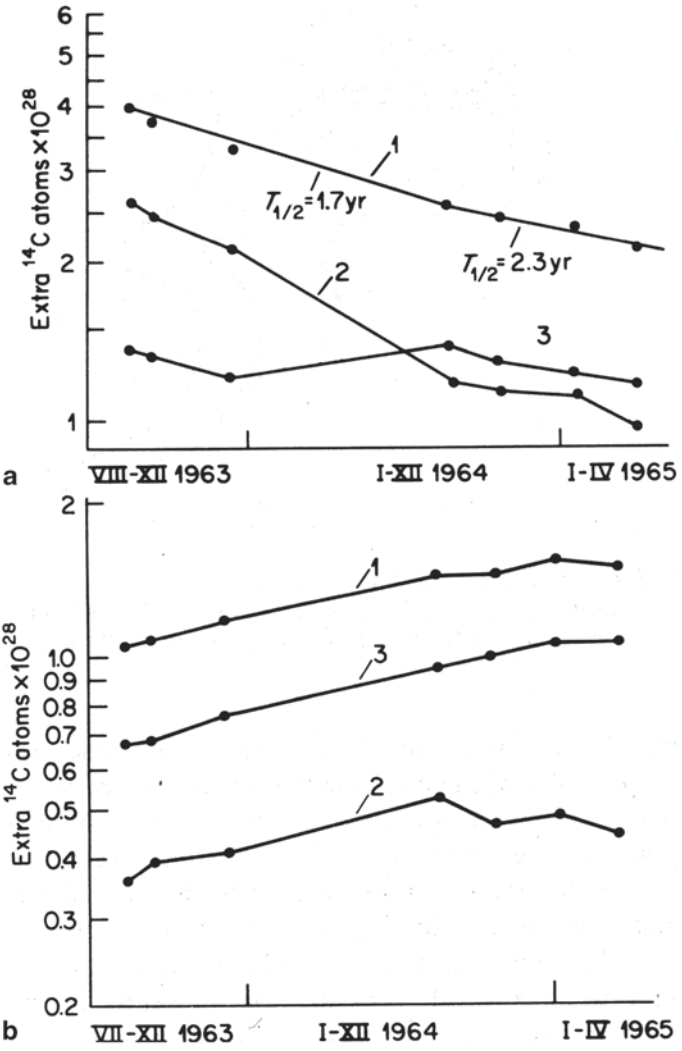

Fig. 10.26 Variation of total amount of bomb 14C in the northern (**a**), and southern (**b**) hemispheres for the atmosphere as a whole (*1*), the stratosphere (*2*) and the troposphere (*3*). (Fairhall and Young 1970; Ferronsky and Polyakov 2012)

half-removal from the atmosphere in the first years after the nuclear tests stopped in the atmosphere is shown in Fig. 10.26a. It is most probable that the ^{14}C half-removal, measured by its activity before 1966, characterised in reality not only the CO_2 exchange process between the atmosphere, ocean and biosphere but also ^{14}C activity decrease in the northern hemisphere as a result of its transfer with air masses into the southern hemisphere.

The altitudinal distribution of ^{14}C specific activity in the atmosphere is not uniform. In 1962, for example, ^{14}C activity in CO_2 of the lower troposphere was about

140% with respect to the natural level. In April 1962, before the USSR thermonuclear tests, at the height of 12.2 km at 36 °N, ^{14}C activity was measured to be three times higher than the natural one (Fergussen 1963). These measurements have shown that considerable amounts of ^{14}C were accumulated in the stratosphere as a result of the nuclear tests. This fact is proven by the summer maximum coming into the troposphere.

By the data of Fairhall and Young (1970) the radiocarbon concentrations in the troposphere and atmosphere are practically equalised. But the observed summer maximums during 1968–1974 evidence against this assumption (Berger 1979). In order to find the correct answer, CO_2 stratospheric sampling at 18 and 21 km heights was carried out during 1975–1977 in the framework of the NASA program. The results of this experiment are shown in Table 10.20.

As is shown in Table 10.20, the spring peak of ^{14}C concentration appears in the lower stratosphere, which looks like the summer maximum in the troposphere. In this regards, one may assume that the ^{14}C enriched air during the summer breaks the troposphere and arrives there from the lower stratosphere. By Berger's opinion, the mean residence time of CO_2 in the stratosphere is about 15–20 year.

In 1963, USSR, USA and the UK signed the treaty on cessation of nuclear weapon tests in the atmosphere, oceans and on the Earth's surface. Since that time, the exchange reservoirs have been insignificantly replenished by artificial ^{14}C during French and Chinese explosions. The peak ejections of radiocarbon into the atmosphere, which created in the atmosphere and stratosphere some kind of marks, allowed a more detailed study of the mass exchange between the atmosphere, oceans and the biosphere and also between different layers of the atmosphere and oceans. A wide program on the study of distribution of ^{14}C caused by the bomb-tests was carried out in the Trondheim Laboratory starting in 1962. In particular, the scientists who took part in the program since 1963 published their results on the study of CO_2 exchange between the atmosphere and oceans. A study on ^{14}C redistribution between the northern and southern hemispheres on a profile of Spitsbergen–Madagascar was also initiated. Before 1967, ^{14}C concentrations in the lower atmosphere of the Earth were practically equalised. This allowed the calculations of carbon exchange cycles to not take into account the time in different parts of the atmosphere.

Table 10.20 ^{14}C content in the stratosphere. (Berger 1979)

Sampling date	Samplingheight	Sampling place	$\delta\,^{14}C$ (‰)
13.06.75	19.8	Northern Sierra	+127.4
25.09.75	19.8	California	+90.7
03.12.75	18–21	San Francisco—Phoenix	+79.1
02.06.76	18–21	San Francisco—Salt Lake City	+85.6
30.03.76	19.8	San Francisco—Oregon	+107.0
23.09.76	19.8	San Francisco—Denver	+99.2
22.03.76	19.8	Pacific Ocean—Los Angeles	+199.6

The decrease of bomb ^{14}C in the atmosphere occurs due to its absorption by the terrestrial biosphere and CO_2 exchange between the atmosphere and the oceans. The latter reservoir is most important since more than 80% of atmospheric CO_2 is exchanged with the ocean and 20% is replaced through the inland biosphere. In view of the role of the oceans in the absorption of bomb-1^4C, considerable investigations have been carried out aimed at the measurement of its concentration in surface and deep oceanic waters (Bien and Suess 1967; Fairhall 1971; Fairhall et al. 1969). In contrast to the atmosphere, characterised by quick ^{14}C mixing (less than 10 year), the process of mixing in the ocean is more complicated and requires more time. The radiocarbon technique is advantageous in studying oceanographic processes such as mixing of the oceanic waters and their global circulation.

The spatial ^{14}C distribution in depths of the Atlantic Ocean was studied in the framework of the GEOSECS program (Stuiver 1980). Figure 10.27a shows the location of the stations and also the stations of the research ship 'Meteor' (Germany). The ship's route was adjusted for the GEOSECS program (Roether et al. 1980). The $\Delta^{14}C$ values distribution at the GEOSECS stations in 1972–1973 are presented in Fig. 10.27b, 10.27c. It is seen in Fig. 10.27c that the two main fields of the surface waters immersion into deep layers are observed. The first field is located between 36° and 40 °S and the second between 20° and 30 °S. The upward flow of the deep waters is traced around the equator. The two more localised upward flows are traced between 40–50 °S and 40–50 °N. It follows from Fig. 10.27b, 10.27c that significant amounts of bomb-radiocarbon entered into the surface ocean layer and reached the deep layers in 1972. An analogous picture on the longitudinal profile, obtained during the 23 rd route of the 'Meteor' in 1971, is observed (Fig. 10.28) (Roether et al. 1980).

As pointed out above, the ^{14}C mark that occurred in the atmosphere after the thermonuclear tests during a short period of time, is used to study the atmosphere and oceans dynamical characteristics. The carbon concentration increase in the Earth's atmosphere has a head form of δ-function at the well-known change of carbon concentration in the atmosphere and oceans. This gives the possibility for estimation of the exchange parameters of the reservoir, the main of which are the atmosphere, oceans and biosphere. Each reservoir can be presented by a number of 'boxes' (Dergachev 1977). For example, the oceans can be considered as a two boxes reservoir: the upper one over the thermocline (75 ± 25 m) in which intensive water mixing occurs and a lower, weakly mixing 'box' in which the carbon concentrates due to the diffusion process. The continuous carbon exchange between the deep ocean layer and ocean sediments takes place. The natural border in the atmosphere is the tropopause, which is at a height of 11–12 km. The tropopause divides the troposphere into a layer, well mixing in the vertical direction and a layer where the meso-longitudinal exchange is prevailing. The use of the box models, the possibilities of which were discussed earlier, on the basis of an experimental study of ^{14}C distribution in a reservoir in space and time, allows the rate of exchange processes and the carbon mean residence time in reservoirs to be estimated.

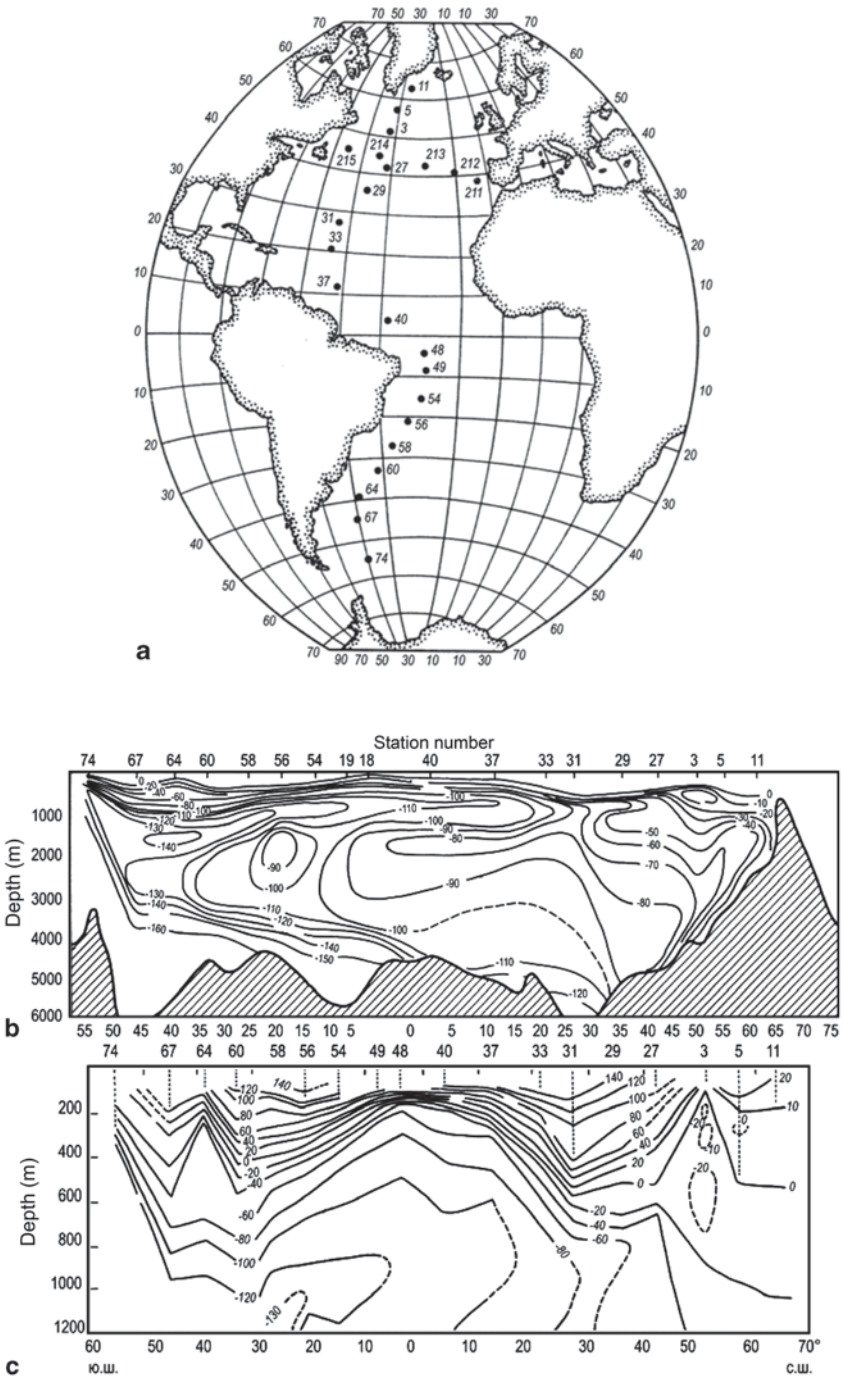

Fig. 10.27 Location of measurement and sampling stations for the GEOSECS program (1972–1973, № №5–74) and the 23rd 'Meteor' route (1971, №№ 211–215) (**a**) (Stuiver 1980; Roether et al. 1980); and $\Delta^{14}C$ vertical distribution in the western part of the Atlantic Ocean in 1972–1973 (**b**) (Stuiver 1980); the same for the depth up to то 1200 m (**c**) (Ferronsky and Polyakov 2012)

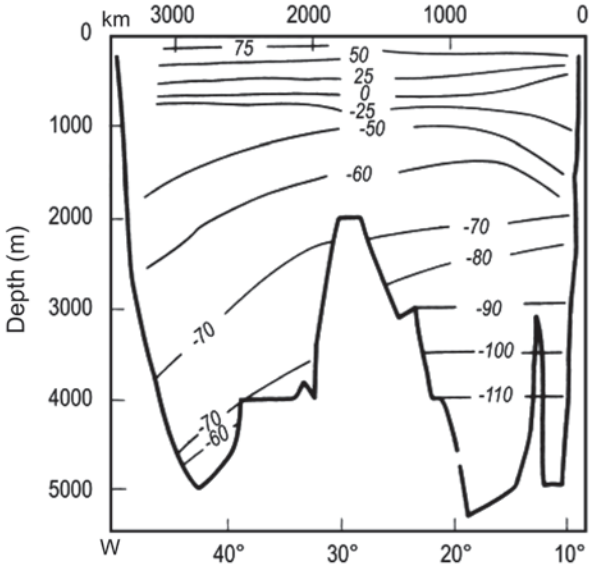

Fig. 10.28 $\Delta^{14}C$ vertical distribution obtained by ship 'Meteor' stations, 23rd route. (Roether et al. 1980); Ferronsky and Polyakov 2012

Dergachev (1977), after analysis of many works on the problem, came to the conclusion that the values of the exchange parameters, calculated on the basis of artificial ^{14}C distribution, are too scattered. This scattering is firstly due to incorrectness in determination of the reservoir borders of the exchange reservoir and secondly, because of confusion in the meaning of 'half-exchange time' and 'half-living time' of the ^{14}C in either part of the reservoir. The following values of the above parameters were obtained by Dergachev: the exchange time between the troposphere and stratosphere is equal to 1.5–2 year; the ^{14}C mean residence time in the stratosphere is 3.5–4 year and in the troposphere 1.5–2 year; the mixing time of the atmosphere between the hemispheres through the equator is about 1.5 year. The mean values for both hemispheres are:

$$\tau_{ma} = 9.1;\ \tau_{ma} = 7.1;\ \tau_{ma} = 8.7;\ \tau_{md} = 4.3;\ \tau_{md} = 2.8;\ \tau_{md} = 3.8\ \text{yr};$$

where m is the mixing layer; a is the atmosphere; d is the deep layer.

As Dergachev points out, the small values τ_{md} contradict the results of calculations by box models, by which $\tau_{md} \approx 10$ year. This is possible because of the dependence of the exchange rate between the atmosphere and different ocean layers on the ^{14}C concentration gradient in exchangeable reservoirs. In this case the decrease of the rate of the radiocarbon removal from the troposphere must lead to an increase in the mean residence time in the atmosphere and mixing ocean layer. The

Table 10.21 ^{14}C (%) content from the standard of modern carbon

Reser-Voir	Time (year)						
	1957	1958	1959	1960	1961	1962	1963
A	104	112	123	122	116	137	193
H_m	98	98	99	99	100	100	102
	1964	1965	1966	1967	1968	1969	
A	188	170	165	160	158	155	
H_m	105	108	110	112	114	118	
	1970	1971	1972	1973	1974	1975	
A	152	150	148	145	142	140	
H_m	116	116	115	115	114	113	

experimental data on ^{14}C distribution in the atmosphere and oceans, obtained in the last years, are evident of such as assumption. The author, applying the Trondheim Laboratory data, on the basis of the one-box model, estimated the residence time of radiocarbon in the mixing and deep ocean layers. Table 10.21 shows the function (A) of the radiocarbon change in the atmosphere and the ^{14}C concentration increase in the mixing ocean layer H_m used in the calculations.

The data for the atmosphere before 1963 were taken on the basis of ^{14}C measurements in alcohol of Georgian and Portuguese wines (Burchuladze et al. 1977; Lopes et al. 1977). For the mixing layer, ^{14}C concentration before 1963 was obtained by extrapolation of the data published in the works of Bien et al. (1963); Broecker et al. (1960). The calculations were carried out by the formula analogous to that used for tritium data interpretation:

$$A_t = \bar{A} + \sum_{1957}^{1975} \delta A_\theta \frac{1}{\tau} e^{-t/\tau -}$$

where A_t is the radiocarbon concentration in the mixing layer at t year after 1957; δA_Θ is the difference (%) between the biogenic radiocarbon level before 1950 (100%) in the calendar year Θ; $\bar{A}$ is the ^{14}C concentration in the mixing layer (98%).

The best coincidence of the calculated and experimental data is achieved at the value $\tau \approx 15$ year. The radiocarbon half-life has not been taken into account because of the short time interval compared with the ^{14}C half-life. Certainly, the one-box model used for estimation of the dynamical parameters in the system atmosphere-ocean (Gray and Damon 1970; Ralf 1972) gives an approximate result. But the carbon constant of the reaction transfer rate from the deep to mixing layer by substitution of the value $\bar{A}$ was taken into account. The carbon exchange time of the mixing layer by Eq. (10.55) can be estimated. Taking into account that $N_{п.с.} = 1.3N_a$, then one obtains $\tau = 13$ year, if τ for the atmosphere is equal to 10 year. As in this case the carbon exchange in the system mixing-deep layers was not taken into account, then the more realistic τ value for the mixing layer seems to be 10 year. This does not contradict the three-box model of Dergachev (1977). The ^{14}C distribution

in the surface layer of the central ocean parts is of interest. The observations of the Atlantic and Pacific Ocean stations show (Nydal et al. 1979) that ^{14}C concentrations in local areas do not stay constant in time but vary within 10‰ (and even up to 20‰). A positive correlation between radiocarbon content in the surface layer and the surface ocean temperature is observed.

In the study of Rafter and O'Brien (1972) the ^{14}C distribution in the Pacific surface waters after 1968 is discussed. They found that two belts of increased concentrations ($\delta^{14}C \approx 20\%$) near 27 ºN and 27 ºS and minimal values around the equator ($\delta^{14}C \approx +5\%$) are observed.

While considering the ^{14}C distribution in the surface Atlantic waters, Dergachev (1977) derived two maximum values: $\delta^{14}C \approx +7\%$ (70 ºN) and $\delta^{14}C \approx +19\%$ (27 ºN). It is interesting to note that the location of the above maximum values is unchanged up to the depth of 500 m. The nature of this phenomenon is not explained. The only thing clear is that the maximum salinity of the oceans coincides with those from Fig. 10.29. The water zones are characterised by higher evaporation of marine water and have a relationship with the global circulation of the air and water masses. It is obvious that before the thermonuclear tests, ^{14}C concentration in the surface ocean waters was not constant and changed under the same effects as after the tests.

The artificial radiocarbon from the mixing layer enters the deep ocean layers. According to Fairhall's (1971) calculations, the process of equilibrium state be-

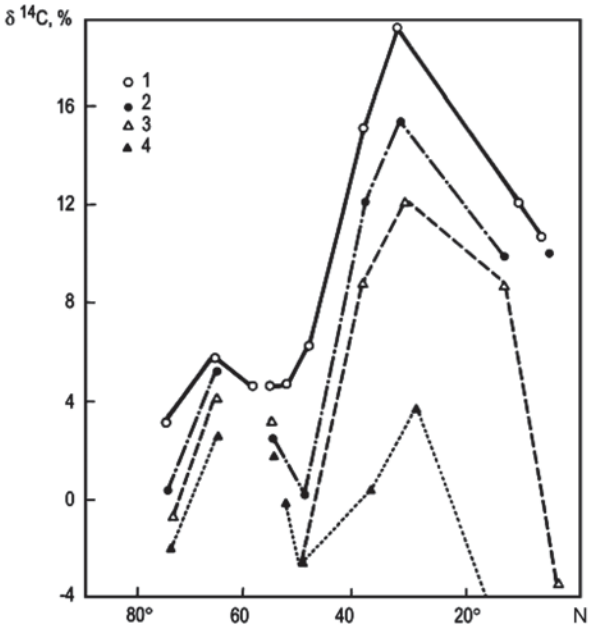

Fig. 10.29 Radiocarbon concentration change in the upper layers in the North Atlantic Ocean: (*1*) surface layer; (*2*) at depth 100 m; (*3*) at 200 m; (*4*) at 500 m (Ferronsky and Polyakov 2012)

tween the atmosphere and oceans will continue for 45 year (starting from 1970). An experimental study of this process will help in understanding the oceanic currents nature and the mixing time of ocean waters.

10.8.5 Forecast of Carbon Dioxide Increase in the Atmosphere

The carbon dioxide increase in the atmosphere, in addition to the ^{14}C specific activity dilution in the exchangeable reservoirs, play independent and important roles. Increase of the carbon dioxide content may lead to a considerable change in the mean yearly temperature on the Earth, which is a consequence of the 'greenhouse' effect. Carbon dioxide is practically transparent for solar radiation but it absorbs the thermal radiation of the Earth in a number of lines on the infra-red spectrum. If water and carbon dioxide are absent in our planet, then the infra-red radiation leaves it for space and the lower layers of the atmosphere to lose warmth. The carbon dioxide concentration growth leads to the stratosphere cooling and near-earth air growth (Table 10.22).

Oeschger and Siegenthaler (1979) used CO_2 to change in time the parameters for the main reservoirs, obtained on the basis of artificial radiocarbon distribution and to predict the possible increase of CO_2 content in the atmosphere. They proposed models that are based on the following assumptions.

1. The study of ^{14}C content in deep Pacific and Atlantic oceanic waters over 1957–1959 has shown that distribution of radiocarbon in the deep waters was not practically disturbed by the thermonuclear tests.
2. As a result of the thermonuclear tests, ^{14}C activity in surface oceans waters increased by 95 % with respect to the present carbon content (its 'pre-industrial' value for the atmosphere is equal to 100 %) in 1957 and by about 112 % in 1970.
3. About 19 %, with respect to the 'pre-industrial' amount of CO_2, has been injected into the atmosphere before 1970 but its concentration decreased only by 10 %.
4. Because of dilution of carbon dioxide due to combustion of fossil fuel, the ^{14}C specific activity in the atmosphere before 1950 decreased by about 2 %.

Oeschger and Siegenthaler (1979) assumed for their model that the carbon transfer from the mixing layer to the deep waters results from vortex (turbulent) diffusion (Fig. 10.30). Any increase of the partial pressure in CO_2 leads to its redistribution between the atmosphere and oceans. Such a redistribution can be described by a parameter called the 'buffer-factor'. For example, if the CO_2 partial pressure in the at-

Table 10.22 Assuming CO_2 growth in the atmosphere. (Kellog 1980)

CO_2 content change in atmosphere (%)	Assuming year of the change (year)	Growth of near-earth temperature (ºC)
+25	2000	0.5–1.0
+100	2050	1.5–3.0

mosphere increases by α %, then the total CO_2 concentration in the ocean waters, to be in equilibrium with the atmosphere, increases in waters only by α/ξ %. The biosphere in the model is represented by the well mixed reservoir, where the amount of carbon is 2.4 times more than in the atmosphere and its residence time is about 60 year. The partial pressure increase of CO_2 in the atmosphere leads to the photosynthetic activity of plants described by the 'growth-factor' ε. If CO_2 pressure in the atmosphere increases by α% then the carbon flow from the atmosphere to the biosphere increases by the value of $\varepsilon\alpha$%. According to Oeschger and Siegenthale (1979), the ε value varies for different conditions from 0 to 0.4. For prediction of the CO_2 increase in the atmosphere the following independent parameters were used (see Fig. 10.30):

N_a	CO_2 in atmosphere	Pre-industrial level	$0.62 \cdot 10^{18}$ g
N_b	CO_2 in biosphere		2.4 N_a
N_m	CO_2 in mixing layer		1.3 N_a
N_d	CO_2 in deep water layer		64.2 N_a
K_{am}	Exchange coefficient in the system atmosphere—mixing layer		1/7.7 year
K_{ab}	Exchange coefficient in the system atmosphere-biosphere		1/25 year
K	Coefficient of vortex diffusion		$3987\ m^2 \cdot sec^{-1}$
ξ	Buffer-factor of CO_2 absorption by the ocean		10
ε	Growth-factor connecting with CO_2 absorption by the biosphere		0.2

The authors give a prediction of the CO_2 content increase in the atmosphere at different input functions. For example, if single CO_2 concentration in the atmosphere increases by α%, then a new equilibrium is reached characterised by α_∞%. The ratio α_0/α_∞ can be obtained by the equation:

$$\alpha_0 N_a = \alpha_\infty N_a + (\alpha_\infty/\xi)(N_m + N_d) + \alpha_\infty \varepsilon N_b,$$

or

$$\alpha_\infty/\alpha_0 = N_a/[N_a + (N_m + N_d)]/\xi + \varepsilon N_b.$$

At ξ=10, ε=0.2 α_0/α_∞=0.125, i.e., one eighth of the total CO_2 input into the atmosphere. Here, a possible decrease of the α_∞ value as a result of oceanic carbonates dissolution and weathering of the rocks has not been considered. But because of too slow CO_2 transfer into deep ocean layers these processes will continue for a long time. If the CO_2 inflow into the atmosphere stopped in 1970, then $\alpha \approx 10$%, in 2000 the α value would be 7% and after several centuries it would reach an equilibrium value,

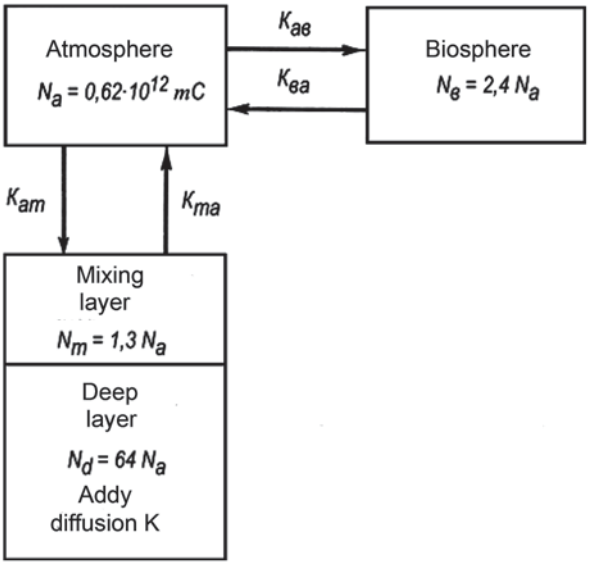

Fig. 10.30 Reservoirs of the carbon exchangeable system that take into account diffusion transfer to the deep ocean layers. (Oeschger and Siegenthaler 1979; Ferronsky and Polyakov 2012)

i.e., $\alpha_\infty \approx 2.3\%$. The carbon content in fossil fuel (oil, coal and gas) recalculated by CO_2 is 11.64 times more than CO_2 in the atmosphere during the pre-industrial epoch. According to present-day knowledge, the CO_2 production rate can be described by the equation:

$$P(t) = \frac{d}{dt}\left[\frac{11.65N_a}{1+61\exp(-t/22)}\right],$$

where t is the time in years (t = 0 in 1970).

The production rate P(t) after 1970 comprises 4.5 N_a per year (the mean velocity over 1960–1970 is about 5% per year). The calculations show that at this rate of fuel combustion more than 2000%, with respect to the pre-industrial level of CO_2, will be accumulated in the atmosphere up to 2050. This amount of carbon dioxide may lead to an increase of near-ground temperatures from 3º to 4ºC (Fig. 10.31). But it is unlikely. In the XXI century, fossil fuel use descended because other sources of energy are now available. In addition, according to recent scientific data on heat and mass exchange between the atmosphere and oceans, the greenhouse effect is by orders of 3–4 overestimated (Sorokhtin 2002).

By Kellogg's (1980) data, in this case the near-ground temperature will increase only by 1–1.5 ºC.

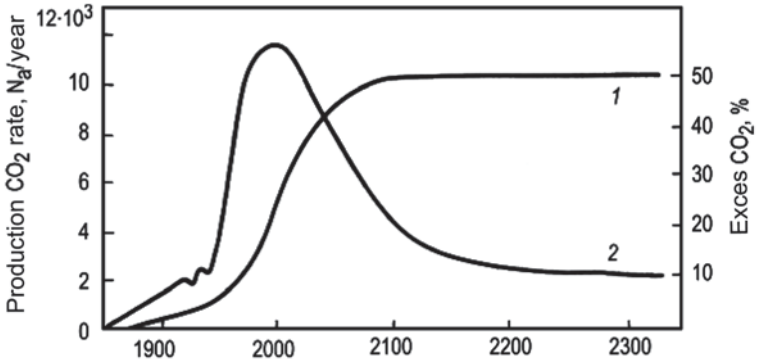

Fig. 10.31 Dependence of CO_2 variation in the atmosphere on present fossil fuel combustion (*1*) and on 30 % reduction of its present combustion (*2*). (Oeschger and Siegenthaler 1979; Ferronsky and Polyakov 2012)

10.8.6 Principles of Radiocarbon Dating

If any system exchange with atmospheric carbon dioxide is finished then the accumulated ^{14}C amount is decreased in time by the radioactive decay law:

$$A_t = A_0 e^{-\lambda t}, \tag{10.61}$$

where A_t and A_0 are the radiocarbon activity (or concentration) at time t and $t = 0$; λ is the radiocarbon decay constant; $\lambda = \ln 2/T_{1/2} = 0{,}693/T_{1/2}$; T is the period of the ^{14}C half-life.

If the exchange processes stop, for example due to death, then the formula (10.61) can be used for calculation of the time passed after the process has broken off (the object age):

$$t = (1/\lambda)\ln(A_0/A_t) = 8033\ln(A_0/A_t). \tag{10.62}$$

The half-life period equal to 5568 year was used in Eq. (10.62). In order to pass the 5730 year period, all the calculated age values by Eq. (10.62) should be multiplied by the coefficient 1.03. The method of obtaining radiocarbon dates on organic specimens was developed by Libby (1967).

Radiocarbon dating is based on a number of assumptions, the main of which are: (1) the intensity of cosmic radiation and, as a consequence, the ^{14}C concentration in the atmosphere, remained constant at least during the radiocarbon dating scale (0–80,000 year); (2) the time of exchange of atmospheric carbon with terrestrial carbon is considerably smaller than the half-life of carbon-14 and does not change with time; (3) secondary processes do not affect the isotopic composition of the studied specimens after sampling. This is equivalent to the assumption that the radiocarbon content in a specimen decreases only because of radiocarbon decay.

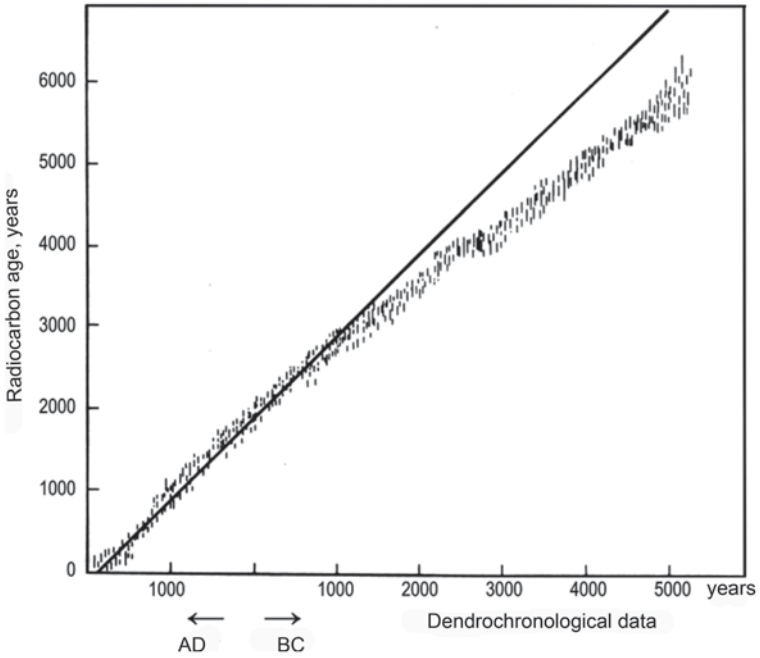

Fig. 10.32 Relationship between dendrochronological and radiocarbon ages of Sequola gigantea and Pinus aristata (Mook 1977; Ferronsky and Polyakov 2012)

In natural cases, the above-mentioned assumptions do not hold strictly, although in most cases the age determined on the basis of radioactive dating are in good agreement with those obtained using other techniques (Libby 1967).

In the case of ^{14}C variations in atmospheric CO_2 and in the biosphere (see Fig. 10.24) over long time periods starting from about 2500 year, the radiocarbon and dendrochronological time scales of the organic specimens differ (Fig. 10.32).

In order to reconcile the radiocarbon results with the dendrochronological ones within 0–8000 year, a number of correlation relations were proposed. According to Wendland and Donley (1971), the age correlation can be done by the third-degree polynomial:

$$T_{corr} = 112 + (0.710 T_{14_c}) + (1.610 \cdot 10^{-4} T_{14_c}^2) - (1.50 \cdot 10^{-8} T_{14_c}^3).$$

For this purpose there are also other correlation equations (Ralph and Klein 1979).

Radiocarbon dating on the basis of organic fragments has a wide application in archaeology, geology, geography, oceanography and other Earth sciences (Suess 1979).

Isotopic composition of the stable carbon in a carbonate system is used for correction of the radiocarbon age of groundwater. The processes of carbon isotope fractionation were considered above.

As follows from Eq. (10.62), the most carbon fractionation is between gaseous CO_2 and hydro-carbonate-ion (HCO_3^--ion is enriched in ^{13}C by about 10% at 0ºC compared with carbon dioxide). It is also obvious that the complete fractionation of carbon isotopes in the gas-solution and gas-solid phase system should depend on the medium pH.

Fractionation of the carbon isotopes in the thermodynamically equilibrium processes, stipulated by the kinetic factors (for example, in biochemical reactions), leads to the non-steady state in carbon isotopes of carbon-bearing matter of different natural objects.

Figure 10.33 indicates the isotope variation limits in carbon contained in various objects (Stiel et al. 1979). It is observed from the figure that the most ^{13}C-enriched

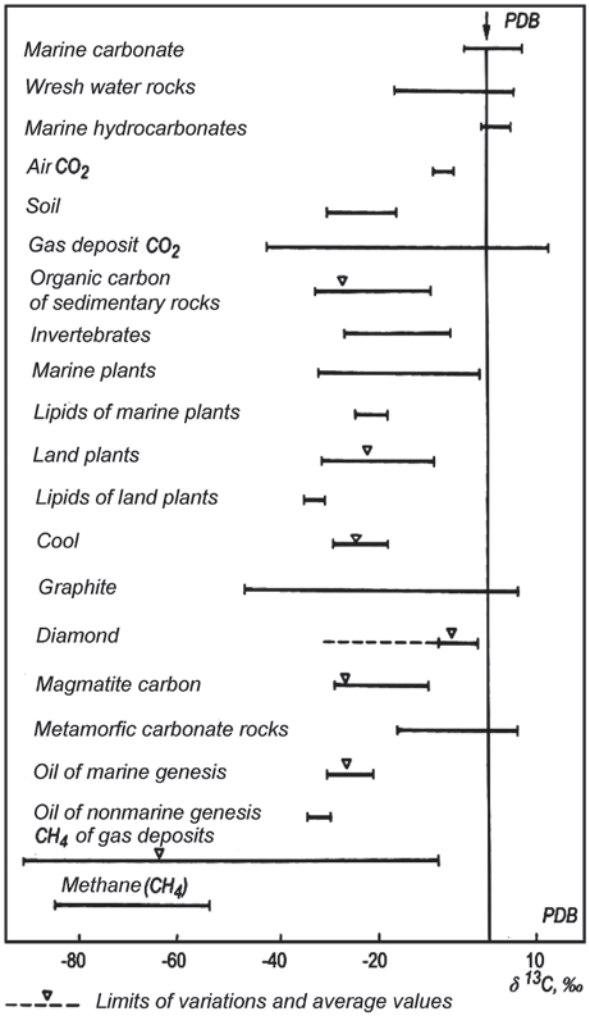

Fig. 10.33 Stable carbon isotope variations relative to the PDB-1 standard in various natural objects. (Stiel et al. 1979; Ferronsky and Polyakov 2012)

and relatively constant by isotopic composition are the carbonates precipitating from oceanic water (mean values of $\delta^{13}C = 0$). The PDB-1 isotope standard is composed of these carbonates. Compared with the standard, atmospheric CO_2 is enriched in the light isotope of carbon by −7‰. Plants are even more enriched in the light isotope. The average value for ground plants is $\delta^{13}C = -25$‰. Close to this value is the soil CO_2. A large value of shift ($\delta^{13}C = -30$‰) is detected in oil and maximum enrichment in ^{12}C is observed in natural methane formed in sedimentary rocks ($\delta^{13}C$ up to −90‰).

Since the isotope fractionation factor increases by its square with the addition of each neutron, the corresponding isotope shift in ^{12}C–^{14}C isotope fractionation will be twice as great. Therefore vegetation should be depleted in ^{14}C compared with the atmosphere and have $\delta^{14}C = -50$‰.

10.8.7 Radiocarbon Dating of Groundwater

At present, for groundwater age determination most researchers apply the piston model. It was earlier pointed out that the radioactive isotope concentration in a sampling point *A*, located at a distance x_0 from the recharge, is calculated by the expression:

$$A = A_0 \exp[-(x_0/v)\lambda] = A_0 \exp(-\lambda t), \tag{10.63}$$

where A_0 is the isotope concentration (activity) in the recharge area; *v* is the velocity of groundwater motion; λ is the ^{14}C decay constant; $\lambda = \ln 2/T_{1/2}$; *t* is the water age, determined as the transit time, during which the isotope reaches the distance from the recharge area to the sampling point.

The time *t*, from Eq. (10.63), can be obtained by the formula:

$$t = (T_{1/2}/\ln 2)\ln(A_0/A) = (1/\lambda)\ln(A_0/A). \tag{10.64}$$

As was noted earlier, the radiocarbon method of groundwater age determination was applied for the first time by Münnich (1968). The main assumptions of this method are as follows:

1. Radiocarbon concentration in the recharge zone is known and does not change at least over the range of the radiocarbon time-scale.
2. Radiocarbon does not enter the carbonate system of groundwater from outside the recharge zone.
3. If ^{14}C content in an aquifer decreases both due to radioactivity decay and other processes, then the effect of these processes can be taken into account.
4. The leakage of water from one aquifer into another (the mixing of water) is negligible.
5. The rate of movement of dissolved carbonates is equal to the rate of groundwater movement.

The reality of the above conditions is discussed later on.

It is worth mentioning that the term 'age' of groundwater has a great indefiniteness compared with, to-say, 'age' of a solid sample. In the general case, the age of groundwater can be defined by a certain period of time after some hydrogeological event has happened (Dubinchuk 1979). Such an event in radiocarbon dating is the discontinuation of the water exchange with the soil air or the atmosphere. In the framework of this definition, in the radiocarbon scale the natural waters appear to be modern if they are found in continuous exchange with the soil air or atmosphere, where radiocarbon concentration $A_0 = 100\,\%$.

In the general case, the water 'age' is more easily described in the form of the distribution function of residence time in the aquifer, applying corresponding models for a hydrogeological system, which satisfy its real structure (Ferronsky et al. 1977; Dubinchuk 1979). At the present time, for isotope data interpretation and for obtaining the groundwater's age characteristics, in addition to the piston model, there are the following models for mass transfer in hydrological systems: (1) model of complete mixing (exponential or box-model); (2) dispersion model; (3) mixing model of different age waters.

According to the complete mixing (exponential) model (Nir 1964), water input at different times mixes quickly. The relative portion of water of *t* age in the system is expressed as an exponential function in the form:

$$p(t) = (1/\tau)\exp(-t/\tau), \tag{10.65}$$

where τ is the average residence time of water in a system; $1/\tau = v/q$ is the water exchange rate, i.e., the ratio of the total annual inflow of water to the output of the system. Concentration of the isotope in the system ($A_{system} - A_{output}$) in the general case can be written as the following sum in discrete form:

$$A_{system} = \overline{A}/(1+\lambda\tau) + \sum_{\theta=1952}^{1952+t} \left[A(\Theta - t) - \overline{A}\right]/p(t)e^{-\lambda t}, \tag{10.66}$$

where Θ is the current year; $(\Theta - t)$ the time of input into the water system with a concentration of the isotope (^{14}C and others.) $A(\Theta - t)$, which happened by *t* year from the sampling moment; $\overline{A}$ is a steady-state concentration before the thermonuclear tests; other definitions are as previous. Applying the formula (10.66), by observed ^{14}C concentrations in the system (A_{system}), the mean residence time of water can be obtained if the function of the isotope distribution $A(\Theta - t)$ at the system entrance is known. The exponential model is used for interpretation of tritium data. But it can also be used for estimation of the dynamical characteristics of groundwater, applying the radiocarbon, because the function $A(\Theta - t)$ (radiocarbon input at the hydrogeological system entrance) is known.

Calculation shows that the effect of ^{14}C concentration change, induced in groundwater by the thermonuclear tests, in so much as the mean residence time in the system, is less. If the function $A(\Theta - t)$ is constant the ^{14}C radiocarbon residence time of water $\tau = v/q$ can be determined by the formula:

$$\tau = (A_{input} - A_{output})/A_{output}\lambda = 8033(A_{input}/A_{output} - 1), \quad (10.67)$$

where A_{input} and A_{output} are the radiocarbon concentrations (in % with reference to the standard of the modern carbon) at the entrance and outlet of the system.

It is not difficult to show that in the framework of the exponential model, if $A_{input}$is constant in time, then the water age t is related to the residence time τ by the expression $t=(1/\lambda)(1—\lambda\tau)$. Application of the integral or discrete expressions like (10.66) allow to estimate the residence time in the hydrological system at different forms of the distribution function $p(t)$. But, despite the wide application in tritium data treatment, interpretation of the radiocarbon data by such a way is not used.

As a special case, it is necessary to consider the model of different-age water (Evans et al. 1979). If the hydrogeological system consists of n components of water with the ages T_i, then its age can be determined as a mean-weighted value:

$$\overline{T}=\sum_{i=1}^{n} P_i T_i, \quad (10.68)$$

where P_i is the part of water of age T_i.

In such a system the mean-weighted isotope concentration (for example, ^{14}C) is established:

$$\overline{A}=\sum P_i T_i. \quad (10.69)$$

If the source of the radioactive isotope input is the same, then the values A_i will be differed due to partial radioactive isotope decay over the time T_i. Such a condition is satisfied for the radiocarbon concentration where in the recharge area it is constant and equal to A_0. Then the expression (10.69) can be rewritten as:

$$\overline{A} = A_0 \sum P_i \exp(-\lambda T_i). \quad (10.70)$$

Determining the mixing age by concentration $\overline{A}$ and using the exponential formulae, we may obtain the value:

$$T' = 8003 \ln(A_0/\overline{A}) \quad (10.71)$$

Comparing the expressions (10.71) and (10.68), we find that $T' \neq \overline{T}$. It follows from the above that: (1) the true age of mixture of different waters is equal to the mean-weighted age of the water components; (2) in the general case, the isotopic (radiocarbon) mixture of waters is not equal to the true age and its formal determination does not give unique time-information about a system. This problem can be solved correctly only in the case of independent measuring of the date and age for each component. For obtaining such information one may use, for example, the data

on distribution of other isotopes (D, ^{18}O, T and so on). Evans et al. (1979) calculated the possible change in radiocarbon age for a two-component mixture depending on a portion of the modern component ($A_0 = 100\,\%$). It follows from their calculations that the groundwater of radiocarbon age equal to 57,000 years may represent a mixture of 99.9 % of water with 100,000 years of age and 0.1 % of modern water. This result only slightly changes if the present-day component has 5,000 years of age. But despite the radiocarbon age of waters mixture not providing true information, it can be used to study a relationship between the aquifers, localisation of recharge areas and so on (Borevsky et al. 1981; Sobotovich et al. 1977; Seletsky et al. 1979; Fröhlich et al. 1977; Deak 1974).

Since under real conditions the initial radiocarbon concentration can always be estimated with some error, corresponding corrections should be done (see Ferronsky and Polyakov 2012).

10.9 The Other Cosmogenic Isotopes in Natural Waters

Besides tritium and radiocarbon, other cosmogenic isotopes are used in studying natural waters. While considering the amounts and production rates of primary cosmic rays and secondary nuclear particles with the three main constituents of the atmosphere, nitrogen, oxygen and argon were accounted for. But it has been pointed out that nuclei of neon, krypton and xenon and also those of volcanic and meteoric origin can make a certain contribution to the production of cosmogenic isotopes.

In the course of neon nuclei fission reactions, ^{7}Be, ^{10}Be, ^{3}H and other isotopes are produced. But the yield of isotopes occurring during these reactions is lower than for the argon fission reactions. Besides, in the atmosphere, the ratio of concentrations of Ne/Ar = 0.02. The content of krypton and xenon in the atmosphere is even lower and, respectively, the contribution of cosmogenic isotopes occurring from reactions involving these elements is also small. Moreover, only reactions of the (n, γ)–type on nuclei of ^{80}Kr, ^{84}Kr and ^{132}Xe can serve as a source of very small amounts of ^{81}Kr ($T_{1/2} = 2.1 \cdot 10^5$ year), ^{85}Kr ($T_{1/2} = 10.8$ year) and ^{133}Xe ($T_{1/2} = 5.3$ days). An approximate estimation of the cosmogenic ^{81}Kr yield by the (n, γ) reaction produces a value of $3 \cdot 10^{-7}$ atom/cm$^2 \cdot$ s.

Bartels (1972) suggested that the major portion of the cosmogenic isotopes of ^{22}Na, ^{32}Si, ^{32}P, ^{32}P, ^{35}S and ^{36}Cl may be produced by the reactions of cosmic rays on nuclei of the elements released into the atmosphere in the form of volcanic explosions. His suggestion is based on data on the rate of contribution of s number of elements, together with volcanic material, to the terrestrial atmosphere (Table 10.23).

The conditions in which the production of many cosmogenic isotopes takes place were considered by Lujanas (1975, 1979). He pointed out that the atmospheric concentrations of the elements, indicated in Table 10.23, are much less than those of

Table 10.23 Amounts of some elements released into the atmosphere from volcanic explosions

Elements	Released amounts (kg/year)
B	$7.3 \cdot 10^7$
F	$7.3 \cdot 10^9$
Na	$6 \cdot 10^9$
S	$1.7 \cdot 10^{10}$
Cl	$7.6 \cdot 10^9$
K	$2.3 \cdot 10^9$
Ca	$7.2 \cdot 10^9$

the main air constituents. Therefore, the effect of fission reactions on their nuclei will be negligible. But in a number of cases the cross-sections of reactions on slow neutrons are great. In order to estimate the yield of cosmogenic isotopes in these reactions let us write the expression for the production rate P_i of a given isotope relative to the production rate P_c of ^{14}C isotope in the reaction $^{14}N\,(n, p)\,^{14}C$ on slow neutrons:

$$P_i = \frac{P_c \sigma_i N}{\sigma_c N} P_i, \tag{10.72}$$

where σ_i and σ_c are the effective cross-sections of production of a given isotope and ^{14}C, respectively; N and N_c are numbers of atoms in a nuclei-target and in the atmosphere column with a unit section.

One can find, for example from expression (10.72), that in reaction $^{10}B\,(n, p)\,^{10}Be$, at $\sigma_i = 4010$ barn, $\sigma_i/\sigma_c \approx 2300$ and $N/N_c = 1.9 \cdot 10^{-11}$, the value of $P_i = 8.7 \cdot 10^{-7}$ atom/cm$^2 \cdot$ s is less than the rate of yield of the same isotope in reactions on air nuclei, being equal to $9 \cdot 10^{-2}$ atom./cm$^2 \cdot$ s, by several orders of magnitude. The estimations of the production rates of the other isotopes in reactions on slow neutrons give even smaller values.

The studies of meteorites falling on the Earth's surface show that they also contain radioactive isotopes such as ^3H, ^{10}Be, ^{22}Na, ^{26}Al, ^{36}Cl, ^{37}Ar, ^{39}Ar, ^{40}K, ^{44}Ti, ^{45}Ca, ^{46}Sc, ^{48}V, ^{49}V, ^{51}Cr, ^{53}Mn, ^{54}Mn, ^{57}Co, ^{58}Co, ^{60}Co and others. Table 10.24 shows data on the flux density of some cosmogenic radioisotopes released into the atmosphere on the burning of between 0.5 to 0.7 of the mass of the meteorite material on the assumption that the total amount of meteorite material amounts to 10^9 kg/year. Table 10.24 also shows the cosmic-ray production rates of the same isotopes in the atmosphere.

It follows from Table 10.24 that the flux densities of the isotopes ^3H, ^{10}Be, ^{14}C, ^{22}Na, ^{36}Cl, ^{37}Ar and ^{39}Ar arriving together with meteorites into the atmosphere are lower by several orders of magnitude than the rates of production in the atmosphere due to the irradiation of the atmospheric nuclei of atoms with cosmic rays. At the same time the ^{26}Al meteorite contribution, for example, is comparable in magnitude to its atmospheric production rate.

Table 10.24 Flux density of radioactive isotopes in meteoritic material falling into the atmosphere and the rate of their production by cosmic rays. (Lujanas 1975)

Isotopes	Flux density due to meteorites (atom/cm^2 · sec)	Production rate by cosmic rays (atom/cm^2 · sec)
^{3}H	$1.5 \cdot 10^{-8}$	0.45
^{14}C	$1 \cdot 10^{-5}$	2.5
^{10}Be	$2 \cdot 10^{-4}$	$4.5 \cdot 10^{-2}$
^{22}Na	$8 \cdot 10^{-10}$	$8.6 \cdot 10^{-5}$
^{26}Al	$1.6 \cdot 10^{-4}$	$1.4 \cdot 10^{-4}$
^{36}Cl	$1 \cdot 10^{-5}$	$1.1 \cdot 10^{-3}$
^{37}Ar	$6 \cdot 10^{-12}$	$1.7 \cdot 10^{-3}$
^{39}Ar	$1 \cdot 10^{-8}$	$6.3 \cdot 10^{-3}$
^{53}Mn	$1 \cdot 10^{-3}$	–
^{54}Mn	$6 \cdot 10^{-3}$	–
^{55}Fe	$1 \cdot 10^{-6}$	–
^{59}Ni	$8 \cdot 10^{-6}$	–
^{60}Co	$2.5 \cdot 10^{-10}$	–

References

Aegerter SK, Loosli HH, Oeschger H (1967) Variation in the production of cosmogenic radionuclides. In: Radioactive dating and methods of low-level counting: proceed symp, IAEA, Vienna, pp 49–55

Afanasenko EA, Morkovkina IK, Romanov VV (1973) Age of groundwater in the Tas-Khayat Ridge and Selennyakh depression. Bull Moscow Univ, Ser Geol 5:105–109

Afanasyev AP (1960) Water balance of Baykal Lake. Proc Baykal Limnol Stn 18:85–95

Allison GB, Hughes MW (1974) Environmental tritium in the unsaturated zone: estimation of recharge to an unconfined aquifer. In: Isotope techniques in groundwater hydrology: proceedings of a symposium, IAEA, Vienna, 11–15 March 1974, pp 57–70

Andersen LJ, Sevel T (1974) Six years' environmental tritium profiles in the unsaturated and saturated zones. In: Isotope techniques in groundwater hydrology: proceeding symp, vol 1, IAEA, Vienna, pp 3–18

Andrews JN, Kay RLE (1982) Natural production of tritium in permeable rocks. Nature 298:361–363

Appa Rao MVK (1962) The ^{3}He/(^{3}He+^{4}He) ratio in primary cosmic radiation. J Geophys Res 67:1289–1392

Atakan YW, Roether W, Münnich KO, Matthess G (1974) The sandhausen shallow groundwater tritium experiment. In: Isotope techniques in groundwater hydrology: proceedings of a symposium, IAEA, Vienna, 11–15 March 1974, vol 1, pp 21–43

Bainbridge AE (1963) Tritium in the Northern Pacific surface water. J Geophys Res 68:3785–3789

Bartels OG (1972) An estimate of volcanic contributions to the atmosphere and volcanic gases and sublimates as the source of the radioisotopes ^{10}B, ^{35}S, ^{32}P and ^{22}Na. Heal Phys 22:387–392

Begemann F (1959) Neubestimmung der natürlichen irdischen Tritiumzerfallstrate und die Frage der Herkunft des natürlichen Tritium. Naturforsch 4a:334–342

Begemann F, Friedman I (1968) Isotopic composition of atmospheric hydrogen. J Geophys Res 73:1139–1147

Begemann F, Libby WF (1957) Continental water balance, groundwater inventory and storage times, surface ocean, mixing rates and world-wide water circulation patterns from cosmic-ray and bomb tritium. Geochim Cosmochim Acta 12:277–296

Berger R (1979) Artificial radiocarbon in the stratosphere. In: Berger R, Suess HE (eds) Radiocarbon dating. University of California, Berkeley, pp 309–321
Bhaudari W, Fruchter J, Evans J (1969) Rates of production of ^{22}Na and ^{28}Mg in the atmosphere by cosmic radiation. Earth Planet Sci Lett 7:89–92
Bien GS, Suess HE (1967) Transfer and exchange of ^{14}C between the atmosphere and the surface water of the Pacific Ocean. In: Radiocarbon Dating and Methods of Low-Level Counting: proc. a symp, IAEA, Vienna, pp 105–115
Bien GS, Rakestrow P, Oldenbourg M, Suess HE (1963) Investigations in marine environments using radioisotopes produced by cosmic rays. In: Radiocarbon dating: proc. symp, IAEA, Vienna, pp 159–174
Bochaler P, Eberhardt P, Geiss J (1971) Tritium in lunar materials. Proc. 2nd Lunar Sci Conf 2:1803–1812
Boella GC, Dilworth M, Panetti M, Scarsi L (1968) The atmospheric and leakage flux of neutrons produced in the atmosphere by cosmic ray interactions. Earth Planet Sci Lett 4:393–398
Bonka H (1979) Production and emission of tritium from nuclear facilities, and the resulting problems. In: Behaviour of tritium in the Environment: proc symp. IAEA, Vienna, pp 105–122
Borevsky BV, Polyakov VA, Subbotina LA (1981) Investigation of regularities in leaching through Neocom-Jurassic strata within the depression funnel of the Bryansk water intake well. In: Isotopes in the Hydrosphere, Abstract Symp, IWP RAN, Moskva, pp 52–53
Bradley W, Stout G (1970) Vertical distribution of tritium in water vapor in the lower troposphere. Tellus 22:699–706
Broder DP, Golubev LI, Ilyasov VM (1979) Tritium distribution in the technology scheme of the New-Voronezh atomic power station. At Energy 47:120–122
Broecker WS, Olson EA (1961) Lamont radiocarbon measurements. Radioscarbon 21:199–216
Broecker WS, Gerard R, Erwing M, Heezen BC (1960) Natural radiocarbon in the Atlantic ocean. J Geophys Res 65:2903–2909
Brown RM (1961) Hydrology of tritium in the Ottawa Valley. Geochim Cosmochim Acta 21:199–216
Brown RM (1970) Distribution of hydrogen isotopes in Canada waters. In: Isotope Hydrology: proc. symp, IAEA, Vienna, pp 3–21
Brown R, Grummit WE (1956) The determination of tritium in natural waters. Canad J Chem 34:220–226
Burchuladze AA, Gedevanishvili DD, Pagava SV, Togonidze GI (1977) Variation of radiocarbon content in the atmosphere for 1950–1975 years measured in Georgian vines. In: Low radioactivity measurements and mpplications. Proceedings of a symposium, High Tatras, 1975, Slovenske Pedagog, Nakland, Bratislava, pp 261–263
Burger LL (1979) Distribution and reactions of tritiated hydrogen and methan. In: Behaviour of Tritium in the Environment, proc symp. IAEA, Vienna, pp 47–63
Burkhard W, Fröhlich K (1970) Grundlagen hydrologischer tritium untersuchungen und Ihre anwendung bei der bestimmung der herkunft in grubenwasser einer eisenerzgrube. Bergakademie, Freiberg vol 22, pp 15–30
Buttlar HV, Libby WF (1955) Natural distribution of cosmic ray produced tritium. J Inorg Nucl Chem 1:75–91
Cain WF (1979) ^{14}C in modern American trees. In: Radiocarbon dating. University of California , Berkeley, pp 495–510
Combs F, Doda RY (1979) Large-scale distribution of tritium in a commercial product. In: Behaviour of Tritium in the Environment: proc symp, IAEA, Vienna, pp 93–99
Craig H (1957) Isotopic standards for carbon and oxygen and correction factors for mass-spectrometric analysis of carbon dioxide. Geochim Cosmochim Acta 12:133–149
Daly IC, Manchester AV, Gabay IJ, Sax NI (1968) Tritiated moisture in the atmosphere, surrounding a nuclear fuel reprocessing plant. Radiol Heal Data and Repts 11:217–229
Damon PE (1970) Climatic versus magnetic perturbation of the atmospheric C-14 reservoir. In: Radiocarbon variations and abcolute chronology, XII nobel symp. Wiley, NY, pp 571–593

Deak J (1974) Use of environmental isotopes to investigate the connection between surface waters in the Nagynusad region, Hungary. In: Isotope techniques in groundwater hydrology: proceedings a symp, vol 1, IAEA, Vienna, pp 157–167
Dergachev VA (1975) Variations in solar activity and radiocarbon content in the atmosphere. Izv AN SSSR, Ser Phys 32:325–333
Dergachev VA (1977) Optimal model for residence time determination of exchange reservoir. In: Low-radioaktivity measurements and applications, proc. symp., IAEA, Vienna, pp 269–277
Dergachev VA, Kocharov GE (1977) The ceqular cycles of radiocarbon variation in the Earth atmosphere. In: Low-Radioaktivity Measurements and Applications. Proceedings a symp, IAEA, Vienna, pp 279–286
Devis DH (1970) Geohydrologic interpretations of a volcanic island from environmental isotopes. Water Resour Res 6:652–671
Dinçer T, Payne BR (1971) An environmental isotope study of the south-western karst region of Turkey. J Hydrol 13:233–258
Dockins KO, Bainbridge AE, Houtermans JC, Suess HE (1967) Tritium in the mixed layer of the North Pacific Ocean.In:Radioactive aating and methods of low-level counting, proceedings a symp, IAEA, Venna, pp 120–160
Domanitsky AP (1971) Rivers and lakes of the Soviet Union. Gidrometizdat, Leningrad
Dubinchuk VT (1979) What is the groundwater age? MOIP, Geol Sect 54:70–79
Dudey ND, Malewski RL, Rymas SL (1972) Tritium yield from fast-neutron fission of ^{235}U. Trans Amer Nucl Soc 15:483
Ehhalt DN (1966) Tritium and deuterium in the atmospheric hydrogen. Tellus 18:249–255
Ehhalt DN (1971) Vertical profiles and transport HTO in the troposphere. J Geophys Res 76:7351–7367
Ehhalt DN (1974) The atmospheric cycle of methane. Tellus 26:58–63
Eisenbund M, Bennett D, Blanco RE et al (1979) Tritium in the environment-NCRP report No 62. In: Behaviour of tritium in the environment: proceedings symp, IAEA, Vienna, pp 585–587
Ekdahl CA, Keeling CD (1973) Atmospheric CO_2 in the natural carbon cycle: 1. Quantitative reduction from records at Mouna Loa Observatory and at the South Pole. In: Carbon and biosphere: 24th Brukhaven symp biol, Springfield, pp 51–85
Eriksson E (1963) Atmospheric tritium as a tool for the study of certain hydrologic aspects of river basins. Tellus 15:303–308
Eriksson E (1965a) Account of the major pulses of tritium and their effects in the atmosphere. Tellus 17:118–130
Eriksson E (1965b) Deuterium and oxygen-18 in precipitation and other natural waters. Tellus 17:498–512
Evans GV, Otlet RL, Downing RA et al (1979) Some problems in the interpretation of isotope measurements in United Kingdom aquifers. In: Isotope Hydrology: proceedings symp, vol 2, IAEA, Vienna, pp 679–706
Fairhall AW (1971) Radiocarbon in the Seas, Rep.No RLO-225-T20-3, US AEC
Fairhall AW, Young YA (1970) Radiocarbon in the environment. In: Radionuclides in the environment. Adv Chem Ser.No 9, Am Chem Soc, pp 401–418
Fairhall AW, Buddemeir RW, Yang IA, Young YA (1969) Radiocarbon from nuclear testing and air-sea exchange of CO_2. Antarctic J 4:14–18
Faltings V, Harteck P (1950) Der Tritium Gehalt der Atmosphere. Ztschr Naturforsch 8:438–439
Fergussen GY (1963) Upper tropospheric carbon-14 levels during spring 1961. J Geophys Res 68:3933–3941
Ferronsky VI, Polyakov VA (2012) Isotopes in the Earth's hydrosphere. Springer, Dordrecht
Ferronsky VI, Danilin AI, Dubinchuk VT et al (1968) Radioisotope methods of investigation in ingeneering geology and hydrogeology. Atomizdat, Moskva
Ferronsky VI, Dubinchuk VT, Polyakov VA et al (1975) Environmental isotopes of the hydrosphere. Nedra, Moskva
Ferronsky VI, Danilin AI, Dubinchuk VT et al (1977) Radioisotope methods of investigation in ingeneering geology and hydrogeology. Atomizdat, Moskva

Fireman EL (1967) Radioactivities in meteorites and cosmic-ray variation. Geochim Cosmochim Acta 31:1197–1206
Fireman EL, Stoenner RW (1982) Carbon and carbon-14 in lunar soil 14163. Proc 12 Lunar and Planet Sci Conf NY 12:559–565
Fluss MJ, Dudey ND (1971) Tritium and helium yields in fast fission of ^{235}U. Trans Amer Nucl Soc 14:809–812
Fonselius S, Östlund HG (1959) Natural radiocarbon measurements on surface water from the North Atlantic and the Arctic sea. Tellus 11:77–82
Fontes JC (1976) Les isotopes du milieu dans les laux naturells. Le Houille Blanche 3/4:205–221
Fröhlich K, Jordan H, Hebert D (1977) Radioactive Umveltisotope in der Hydrologie. Grundstoffindustrie, Leipzig
Galimov EM (1968) Geochemistry of stable carbon isotopes. Nedra, Moskva
Gillespie R, Polach YA (1979) The suitability of marine shells for radiocarbon dating of Australian prehistory. In: Radiocarbon dating. University of Calif. Press, Berkeley, pp 404–421
Gonfiantini R, Panichi C (1982) Geothermal water studies. In: Guidebook on nuclear techniques in Hydrology. IAEA, Vienna, pp 151–162
Gray DC, Damon PE (1970) Sunspots and radiocarbon dating in the middle ages. In: Scientific methods in medieval archeology. University of California Press, Berkley, pp 167–182
Gribbin J, Lem GG (1980) Climate change in hystorical period. In: Climate change. Gidrometeoisdat, Leningrad, pp 122–140 (transl. from Engl.)
Hagemann F, Grey J, Machta L, Turkevich A (1959) Stratospheric carbon-14, carbon dioxide, tritiumю. Science 130:542–552
Harteck P (1954) Relative abundance of HT and HTO in the atmosphere. J Chem Phys 22:1746–1751
Houtermans J, Suess HE, Munk W (1967) Effect of industrial fuel combustion on the carbon− 14 level of atmospheric CO_2. In: Radioactive dating and methods of low-level counting: proceedings of symp, IAEA, Vienna, pp 57–68
International Atomic Energy Agency (1973) Bulletin No 4. IAEA, Vienna, pp 10–16
International Atomic Energy Agency (1983) Guidebook on nuclear techniques in hydrology (1983 Edition), IAEA, Vienna
International Atomic Energy Agency (1969, 1970, 1971, 1973, 1975, 1979, 1983, 1986, 1990, 1994) Environmental isotope data: world survey of isotope concentrations in precipitation, No 1–10, IAEA, Vienna
International Atomic Energy Agency (1996) Manual on the mathematical models in isotope hydrology. Tecdoc no 910. IAEA, Vienna
Jouzel J, Pourchet M, Lorius C, Merlivat L (1979) Artificial tritium fall-out at the South Pole. In: Behaviour of tritium in the environment: proceedings of symp, IAEA, Vienna, pp 31–45
Karasev BV, Sokolovsky LG, Kuznetsova LA (1981) Application of carbon isotopes for identification of break zones gassing by carbon dioxide. In: Ferronsky VI (ed) Investigation of natural waters by isotope methods. Nauka, Moskva, pp 155–157
Katrich IYu (1990) Tritium in natural waters after the Chernobyl atomic power accident. Meteorol and Hydrol 5:92–97
Kaufman S, Libby WF (1954) The natural distribution of tritium. Phys Rev 93:1337–1344
Keeling CD (1972) Carbon dioxide cycle: reservoir models to depict the exchange of atmospheric carbon dioxide with oceans and land plants. In: Chemistry of the lower atmosphere. Plenum , NY, pp 251–329
Kellog WW (1980) Global influence on human activity on climate'. In: Climate change. Hydrometeoizdat, Leningrad, pp. 273–302 (transl. from English)
Kinman TD (1956) An attempt to detect deuterium in the solar atmosphere. Month Not Roy Astrophys Soc 116:77
König LA (1979) Impact of the environment of tritium releases from the Karlsruhe Nuclear Research Center. In: Behaviour of tritium in the environment: proc of symp, IAEA, Vienna, pp 591–610

Krejči K, Zeller A (1979) Tritium pollution in the Swiss luminous compound industry. Behaviour of tritium in the environment: proc of symp, IAEA, Vienna, pp 66–77
Lal D (1963) Study of long and short-term geophysical processes using natural radioactivity. In: Radioactive dating: proc of symp, IAEA, Vienna, pp 149–157
Lal D, Peters B (1962) Cosmic-ray-produced isotopes and their application to problems in geophysics. Progr Elem Part Cosm Ray Phys 6:1–74
Lal D, Peters B (1967) Cosmic-ray-produced radioactivity on the Earth. Encycl Phys 46:551–612
Lal D, Venkatavaradan VS (1967) Activation of cosmic dust by cosmic-ray particles. Earth Planet Sci Lett 3:293–310
Lal D, Rajan RS, Venkatavaradan VS (1967) Nuclear effects of solar and "galactic" cosmic-ray particles in near-surface regions of meteorites. Geochim Cosmochim Acta 31:1859–1869
Libby WF (1955) Radiocarbon dating. Chicago University Press, Chicago
Libby WF (1963) Moratorium tritium geophysics. J Geophys Res 68:4485–4494
Libby WF (1967) History of radiocarbon dating. In: Radiocarbon dating and methods of low-level counting: proc symp, IAEA, Vienna, pp 3–25
Libby LM, Pandolfi LJ (1979) Isotopic tree thermometers: anticorrelation with radiocarbon. In: Radiocarbon dating. Univ Calif Press, Berkeley, pp 661–669
Locante J (1971) Tritium in pressurized water reactor. Trans Am Nucl Soc 14:161–162
Lopes JS, Pinte RE, Almendra M, Machado JA (1977) Variation of ^{14}C activity in portuguese wines from 1940 to 1974. In: Low-radioactivity measurements and applications. Proceedings of a symposium in High Tatras. IAEA, Vienna, pp 265–268
Lujanas VYu (1975) On the rate of cosmogenic radionuclides production. Cosmogenic Radioact Isotopes 3:17–25 (Vilnius)
Lujanas V Yu (1979) Cosmogenic radionuclides in the atmosphere. Mokslas, Vilnius
Maloszewski P, Zuber A (1996) Lanped parameter models for the interpretation of environmental tracer data. In: Manual on the Mathematical Models inIsotope Hydrology. Tecdoc No 910, IAEA, Vienna, pp 9–58
Martell EA (1963) On the inventory of artificial tritium and its occurrence in atmospheric methane. J Geophys Res 68:3759–3769
Martin ID, Hackett IP (1974) Tritium in atmospheric hydrogen. Tellus 26:603–607
Martinec J, Siegenthaler U, Oeschger H et al (1974) A new insights into the run-off mechanism by environmental isotopes. In: Isotope techniques in groundwater hydrology: proc symp, vol. 1, IAEA, Vienna, pp 129–142
Mason AS, Öslund HG (1979) Atmospheric HT and HTO: V. Distribution and large-scale circulation. In: Behaviour of tritium in the environment: proc symp, IAEA, Vienna, pp 3–15
Michel RL, Suess HE (1975) Bomb tritium in the Pacific ocean. J Geophys Res 40:4139–4152
Miskel JA (1973) Production of tritium by nuclear weapons'. In: Moghissi F, Carter M (eds) *Tritium*, messenger graphics. Las Vegas, Phoenix, pp 79–85
Miyake Y (1969) Fundamentals of geochemistry. Nedra, Moskva (translation from English)
Mook WG (1977) The radiocarbon time scale. In: Low radioact meas appl: proc symp. High Tatras, Bratislava, pp 193–298
Morkovkina IK (1978) Tritium application in study of groundwater recharge. In: Frronsky VI (ed) Isotopy of natural waters. Nauka, Moskva, pp 165–179
Morkovkina IK (1979) Tritium use in hydrogeological studies. In: Frronsky VI (ed) Isotope investigation of natural waters. Nauka, Moskva, pp 75–84
Münnich KO (1968) Isotopen datierung von Grundwasser. Naturwissenschaften 55:158–163
Münnich KO, Roether W (1967) Transfer of bomb ^{14}C and tritium from the atmosphere to the ocean on the basis of tritium and ^{14}C profiles. In: Radiocarbon dating and methods of low-level counting: proc symp, IAEA, Vienna, pp 93–104
Münnich KO, Vogel JC (1963) Investigation of meridional transport in the troposphere by means of carbon-14 measurement. Radiocarbon dating. Proceedings of a symp, IAEA, Vienna, pp 189–197
Münnich KO, Roether W, Thilo L (1967) Dating of groundwater with tritium and ^{14}C. In: Isotope hydrology: proc. symp., IAEA., Vienna, pp 305–319

Nir A (1964) On the interpretation of tritium age measurements of groundwater. J Geophys Res 69:423–431
Nydal R, Lövseth K, Gulliksen S (1979) A survey of radiocarbon variation in nature since the Test Ban Treaty. In: Radiocarbon dating. University of California, Berkely, pp 313–323
Oeschger H, Siegenthaller U (1979) Prognosis for expected CO_2 increase to fossil fuel combustion. In: Radiocarbon dating. University of California , Berkely, pp 633–642
Östlund HG, Berry E (1970) Modification of atmospheric tritium and water vapour by Lake Tahoe. Tellus 22:463–468
Östlund HG, Fine RA (1979) Oceanic distribution and transport of tritium. In: Behaviour of tritium in the environment. Proceedings of a symposium, IAEA, Vienna, pp 303–312
Östlund HG, Mason AS (1974) Atmospheric HT and HTO: Experimental procedures and tropospheric data 1968–1972. Tellus 26:91–102
Pinneker EV, Romanov VV, Dzyuba AA (1978) The peculiarities of tritium distribution in the near-Baykal Lake natural waters. In: Regional hydrogeology and engineering geology of the Eastern Siberia. Nauka, Novosibirsk, pp 86–92
Plummer LN (2005) Dating of young groundwater. In: Aggarwal P, Gat J, Froehlich K (eds) Isotopes in the water cycle. Springer, Dordrechht, pp 193–218
Polyakov VA, Golubkova EV (2007) Protection study ogf grounwaters by isotopic and hydrochemical data. Prospect Prot of Miner Resour 5:48–52
Polyakov VA, Seletsky YuB (1978) Radiocarbon and tritium study of groundwater dynamics in the Assel-Kliasinan aquifer at Sudogda River region. Geokhimiya 8:1230–1238
Radnell CL, Aitken MJ, Otlet RL (1979) In situ ^{14}C production in wood. In: Berger R, Suess HE (eds) Radiocarbon dating. University of California Press, Berkely, pp 643–650
Rafter TA, O'Brien BJ (1972) C-14 measurements in the atmosphere and in the South Pacific Ocean. In: Proceedings of the 8th international conf. radiocarbon dating, Lower Hutt, Wellington, p 241
Ralf EK (1972) A cyclic solution for the relationship between magnetic and atmospheric C-14 changes. In: Proc. 8th Intern conf. radiocarbon dating. Lower Hutt, Wellington, pp 76–84
Ralf EK, Klein J (1979) Composite computer plots of ^{14}C dates for treering-dated Bristlecone Pine and Sequoies. In: Radiocarbon dating. University of California Press, Berkely, pp 545–553
Ravoire I, Lorius C, Robert J, Roth E (1970) Tritium content in a firn core from Antarctica. J Geophys Res 75:2331–2336
Roether W, Münnich KO, Östlund HE (1970) Tritium profile at the North Pacific (1969) Geosecs intercalibration station. J Geophys Res 75:7672–7675
Roether W, Münnich KO, Ribbat B, Sarmiento JL (1980) A transatlantic ^{14}C section near 40 °N of F/S Meteor. Ergebnisse A 21:57–69
Romanov VV (1978) Regularities in tritium distribution for natural waters. In: Ferronsky VI (ed) Isotopy of natural waters. Nauka, Moskva, pp 46–89
Romanov VV (1982) Tritium use in study of marine and river water mixing. Water Res 5:22–26
Romanov VV, Kikichev HG (1979) Tririum in atmospheric hydrogen. In: Ferronsky VI (ed) Isotope studies of natural waters. Nauka, Moskva, pp 85–92
Romanov VV, Salnova LV, Seryegina LA (1979) Tritium use in studying dynamics of the Baykal Lake waters. In: Ferronsky VI (ed) Isotope sdudies of natural waters. Nauka, Moskva, pp 46–54
Rooth CG, Östlund HE (1972) Penetration of tritium into the Atlantic thermocline. Deep-sea res 19:481–492
Rowland FS (1959) Ratio of HT/HTO in the atmosphere. J Chem Phys 30:1098–1099
Schell WR (1970) Investigation and comparison of radiogenic argon, tritium and C-14 in atmospheric reservoir. In: Radiocarbon variations and absolute chronology, XII nobel symp. Wiley, NY, pp 447–466
Schell WR, Sauzay G (1970) Global sampling and analysis of tritium and stable isotopes. In: Report to panel on procedures for establisching limits for radionuclides in the sea, IAEA, Vienna
Schell WR, Sauzay G, Payne B (1970) Tritium injections and concentration distribution in the atmosphere. J Geophy Res 75:2251–2266
Schmidt U (1974) Molecular hydrogen in the atmosphere. Tellus 26:78–90

Schlosser P, Stute M, Sonntag C, Münnich KO (1988) Tritium/^{3}He dating of shallow groundwater. Earth Planet Sci Latt 89:353–368

Schlosser P, Shapiro SD, Stute M (2000) Tritium/^{3}He measurements in young groundwater: progress in applications to complex hydrological systems. In: Tracers and modelling in hydrogeology: proc intern conf, IASH Liege, pp 481–486

Scholz TG, Ehhalt DH, Heidt LE, Martell EA (1970) Water vapour, molecular hydrogen, methane and tritium concentrations near the stratopause. J Geophys Res 75:3049–3054

Sehgal BR, Remport HH (1971) Tritium production in fast reactors, containing B_4C. Trans Amer Nucl Soc 14:779–780

Seletsky Yu B, Nechaev VI, Polyakov VA (1979) Radiocarbon as an indicator of groundwater recharge and discharge location. In. In: Ferronsky VI (ed) Isotope studies of natural waters. Nauka, Moskva, pp 111–121

Singer SF (1958) The primery cosmic radiation and its time variations. Prog Cosm Ray Phys 4:205–335

Sobotovich EV, Bondarenko GN, Vetshtein VE et al (1977) Isotope and geochemical estimates of a degree of surface and groundwater interconnection. Naukova Dumka, Kiev

Sokolovsky LG, Polyakov VA, Golubkova EV (2007) Light isotopes of waters of the Asdov-Kuban artesian basin: Conditions of formation and balneological significance. Prospect Protect Miner Resour 5:44–47

Sorokhtin OG (2002) Green house effect: myth and reality. Inf Analit Vest, Rus Center, No 1, Moskva, pp 27–28

Stenhause MJ, Baxter MS (1979) The uptake of bomb ^{14}C in humans. In: Radiocarbon dating. University. California Press, Berkely, pp 324–341

Sternberg RS, Damon PE (1979) Sensitivity of radiocarbon fluctuations and inventory to geomagnetic and reservoir parameters. In: Radiocarbon dating. University of California Press, Berkely, p 691

Stewart GL (1965) Experinces using tritium in scientific hydrology. In: Radiocarbon and tritium dating: proceedings of the 6th intern. conf., USAEC, Washington, pp 645–658

Stiel G, Haendel D, Runge A et al (1979) Isotopenverhältnisse und hydrogeologischen Praxis sowie in der Umwelt. Zeits Ang Geol **2**5:9–14

Stuiver M (1965) Carbon-14 content of 18th and 19th century wood: variations correlated with sunshot activity. Science 149:533–535

Stuiver M (1980) ^{14}C distribution in the Atlantic ocean. J Geophys Res 85:2711–2718

Stuiver M, Quay PD (1981) Atmospheric ^{14}C change resulting from fossil fuel CO_2 release and cosmic ray flux variability. Earth Planet Sci Lett 53:349–362

Suess HE (1969) Tritium geophysics as an international research project. Science 163:1705–1410

Suess HE (1970) The three causes of the secular C-14 fluctuations, their amplitudes and time constants. In: Radiocarbon variations and absolute chronology, XII nobel symp. Wiley, New York, pp 595–605

Suess HE (1979) A calibration table for conventional radiocarbon dates. In: Radiocarbon dating. University of California, Berkely, pp 777–784

Sulerzhitsky LD, Forova VS (1966) Radiocarbon in woods from the modern volcanous areas. Dokl. AN UzbSSR 6:1421–1423

Taylor CR (1968) A comparison of tritium and strontium-90 in fallout in the Southern hemisphere. Tellus 20:559–576

Taylor JR, Pefers FE (1972) Tritium transport in LMFBR's. Trans. Am Nucl Soc 15:431–432

Thatcher LL, Payne BR (1965) The distribution of tritium in precipitation over continents and its significance to groundwater dating. In: Radiocarbon and t6ritium dating. Proceedings of the 6th intern conf, USAEC, Washington, pp 604–629

Theodorsson P (1967) Natural tritium in groundwater studies. In: Isotope hydrology: proceedings of a symp, IAEA, Vienna, pp 371–380

Tokarev I, Zubkov AA, Rumynin VG et al (2005) Origin of high $^{234}U/^{238}U$ ratio in post-permafrost aquifer. In: Merkel BJ, Hasche-Berger A (eds) Uranium in the environment, mining impact and consequences. Springer, New York, pp 854–863

Tolstikhin IN, Kamensky IL (1969) Determination of of groundwater age by the T-^{3}He method. Geochen Int 6:810–811

Van Hook WA (1968) Condensed Phase Isotope Effects. Isotopenpraxis 5:161–169

Verhagen BTh, Smith PE, McGregore I et al (1979) Tritium profiles in Kalachari sands as a measure of rain-water recharge. In: Isotope hydrology 1978: proceedings of a symp, vol 2, IAEA, Vienna, pp 733–749

Vlasova LS, Brezgunov VS (1978) The distribution of hydrogen and oxygen isotopic composition in natural brines by model calculations. In: Ferronsky VI (ed) Isotope study of natural waters. Nauka, Moskva, pp 119–139

Webber W (1967) The spectrum and charge composition of the primary cosmic radiation. Encycl Phys 46:181

Weiss W, Roether W (1975) Der Tritium abfluss des Rheins 1961–1973. Dt. Gewasser Kd Mitt 19:1–10

Weiss W, Bullacher J, Roether W (1979) Evidence of pulsed discharge of tritium from nuclear energy installations in Central European precipitation. In: Behaviour of tritium in the environment: proceedings of a symp, IAEA, Vienna, pp 17–30

Wendland WM, Donley DL (1971) Radiocarbon calendar age relationship. Earth Plane Sci Lett 11:135–139

Yang A, Fairhall AW (1972) Variations of natural radiocarbon during the last 2000 years and geophysical mechanism for producing them. In: Proceedings of the 8th intern conf on radiocarbon datin. Lower Hutt, Wellington, pp A44–A54

Young JA, Wogman NA, Thomas CW, Perkins R (1970) Short lived cosmic ray produced radionuclides as tracers of atmospheric processes. In: Radionuclides in the environment. Adv Chem Ser No 93, Am Chem Soc, Washington, pp 506–521

Zavelsky FS (1968) One more clarification to radiocarbon method Dokl. AN SSSR 180:1189–1192

Zlobina VL, Kovalevsky VS, Morkovkina IK et al (1980) On the use of helium and tritium mapping for groundwater recharge study. Water Res 1:166–170

Zuber A (1994) On calibration and validation of mathematical models for the interpretation of environmental tracer data in aquifer. In: Mathematical models and their application to isotope studies in groundwater hydrology, IAEA, Vienna, pp 11–41